



Doctoral Thesis

Integrated Modeling and Optimization of Multi-Carrier Energy Systems

Author(s):

Geidl, Martin

Publication Date:

2007

Permanent Link:

<https://doi.org/10.3929/ethz-a-005377890> →

Rights / License:

[In Copyright - Non-Commercial Use Permitted](#) →

This page was generated automatically upon download from the [ETH Zurich Research Collection](#). For more information please consult the [Terms of use](#).

Diss. ETH No. 17141

Integrated Modeling and Optimization of Multi-Carrier Energy Systems

A dissertation submitted to
ETH Zurich

for the degree of
Doctor of Sciences

presented by
Martin Geidl
Dipl.-Ing. (TU Graz)
born June 28, 1977
citizen of Austria

accepted on the recommendation of
Prof. Dr. Göran Andersson, examiner
Prof. Dr. Olav B. Fosso, co-examiner

2007

Acknowledgements

This dissertation is the result of my research activity at the Power Systems Laboratory of ETH Zurich, where I spent almost four years. Numerous people have supported me during this time. In particular, I would like to express my sincere thanks to:

- Prof. Göran Andersson, head of the Power Systems Laboratory, for giving me the opportunity to work in an excellent scientific environment. I appreciated the liberal and self-responsible way of working under his supervision, as well as the pleasant atmosphere in the group.
- Prof. Olav B. Fosso from NTNU Trondheim, who kindly accepted to co-referee this thesis.
- Prof. Kas Hemmes from TU Delft, for open-minded discussions and fruitful collaborations, which resulted in a joint publication.
- Prof. Claudio A. Cañizares from the University of Waterloo, for reproducing and confirming some of the results presented in this thesis.
- “My students” Benjamin Marti and Minan Zhu, which I supervised during their Master theses, for their valuable work which delivered important inputs for this dissertation.
- All my colleagues and friends from the PSHVL group for having a good time.

Finally, I would like to thank my parents Maria and Franz Geidl, for their great support and encouragement.

Abstract

In the past, common energy infrastructures such as electricity and natural gas systems were mostly planned and operated independently. Motivated by different reasons, a number of recent publications suggests an integrated view of energy systems including multiple energy carriers, instead of focusing on a single energy carrier. One incentive for that is given by the increasing utilization of gas-fired distributed generation, especially co- and trigeneration. The conversion of energy between different carriers establishes a coupling of the corresponding power flows resulting in system interactions. The investigation of such phenomena requires the development of tools for an integrated analysis of multiple energy carrier systems, which has become a recent field of research.

This thesis presents a generic framework for steady-state modeling and optimization of energy systems including multiple energy carriers. The general system model includes conversion, storage, and transmission of various energy carriers. The couplings between the different infrastructures are explicitly taken into account based on the concept of “energy hubs”. Using this model, various integrated optimization problems are defined. For determining the optimal system operation, multi-carrier optimal dispatch and optimal power flow approaches are developed. A general optimality condition for optimal dispatch of multiple energy carriers is derived and compared with the standard approach for electricity networks. Besides operational optimization, two approaches for the structural optimization of multi-carrier energy systems are presented, which enable to estimate the optimal coupling of energy infrastructures. The models are demonstrated in a number of application examples, showing their basic characteristics and usefulness.

Kurzfassung

In der herkömmlichen Betrachtung von Energiesystemen werden Lastflüsse unterschiedlicher Energieträger, wie z. B. Strom und Erdgas, als nahezu unabhängig voneinander angenommen. Der zunehmende Einsatz von gasgefeuerten, dezentralen Erzeugungsanlagen, vor allem sog. Kraft-Wärme-(Kälte-)Kopplungsanlagen, sowie andere aktuelle Entwicklungen im Bereich der Energiewirtschaft legen allerdings eine integrierte Betrachtung der verschiedenen Energieträger nahe. Die Umwandlung von Energie, z. B. Gas in Strom, hat eine Verkopplung der zugehörigen Lastflüsse zur Folge. Dies führt zu technischen und ökonomischen Wechselwirkungen zwischen den betroffenen Infrastrukturen. Die Untersuchung derartiger Phänomene verlangt nach integrierten Modellen, deren Entwicklung sich die Forschung in den letzten Jahren vermehrt angenommen hat.

In dieser Arbeit wird ein Modell zur stationären Analyse von integrierten Energiesystemen entwickelt. Der allgemeine Ansatz, der auf dem „Energy Hub“-Konzept beruht, erlaubt eine konsistente und kongruente Beschreibung von Umwandlung, Speicherung und Übertragung beliebiger Energieträger. Dieses statische Systemmodell bildet die Grundlage für diverse Optimierungsprobleme, die in der Folge definiert werden. Für die betriebliche Optimierung des Systems wird zunächst ein Ansatz zur optimalen Umwandlung der Energieträger an einem Knoten vorgestellt, der dem klassischen Verfahren zur Bestimmung des optimalen Kraftwerkseinsatzes ähnlich ist. Wie beim klassischen Ansatz kann eine allgemein gültige Optimalitätsbedingung abgeleitet werden, die sich auf die inkrementellen Kosten der Energieträger bezieht. Unter Einbezug der Netzgleichungen kann der optimale Lastfluss aller Energieträger im System bestimmt werden. Neben der betrieblichen Optimierung werden auch zwei Verfahren zur strukturellen Systemopti-

mierung vorgeschlagen. Im ersten Ansatz geht es um die Bestimmung eines theoretischen, mathematischen Optimums, welches als Grundlage für einen Systementwurf dienen kann. Im zweiten Ansatz wird aus einer gegebenen Menge von Energiekonvertoren und -speichern eine konkrete, optimale Struktur gebildet. Einige Anwendungsbeispiele zeigen grundlegende Eigenschaften sowie mögliche Einsatzgebiete der verschiedenen Modelle.

Contents

Acknowledgements	ii
Abstract	iii
Kurzfassung	v
Notation	xii
1 Introduction	1
1.1 Background and Motivation	1
1.2 Previous and Related Work	3
1.3 Main Contributions	3
1.4 List of Publications	5
1.5 Thesis Outline	6
2 Energy Hubs	7
2.1 Basic Concept	7
2.2 Hub Elements	9
2.3 Applications	9
2.4 Potential Benefits	10
2.5 Energy Hub Systems	12
3 Modeling	15
3.1 Basic Modeling Concept	15

3.2	Energy Conversion	17
3.2.1	Single Input and Single Output	18
3.2.2	Multiple Inputs and Multiple Outputs	19
3.3	Energy Storage	23
3.3.1	Storage Element	24
3.3.2	Storage in Energy Hubs	25
3.4	Energy Transmission	29
3.4.1	Network Flow Models	30
3.4.2	Power Flow Models	31
3.5	System of Interconnected Energy Hubs	35
4	Optimization	37
4.1	Problem Outline	37
4.2	Assumptions and Definitions	38
4.3	Optimization Objectives	39
4.3.1	Energy Cost	39
4.3.2	Emissions	39
4.3.3	Composite Objectives	40
4.3.4	Marginal Objectives	40
4.4	Mathematical Problem Formulation	40
4.4.1	Continuous Nonlinear Problems	41
4.4.2	Mixed-Integer Nonlinear Problems	41
4.4.3	Multi-Period Problems	42
4.5	Multi-Carrier Optimal Dispatch	43
4.5.1	Objective	43
4.5.2	Constraints	43
4.5.3	Problem Statement	44
4.5.4	Type of Problem and Solution	44
4.5.5	Convex Case	45
4.6	Multi-Carrier Optimal Power Flow	47
4.6.1	Objective	47

4.6.2	Constraints	47
4.6.3	Problem Statement	48
4.6.4	Type of Problem and Solution	48
4.6.5	Inclusion of Storage	49
4.7	Optimal Hub Coupling	51
4.7.1	Single Energy Hub	52
4.7.2	System of Interconnected Energy Hubs	54
4.8	Optimal Hub Layout	55
4.8.1	Objective	56
4.8.2	Constraints	57
4.8.3	Problem Statement	57
4.8.4	Type of Problem and Solution	59
5	Application	61
5.1	Multi-Carrier Optimal Dispatch	61
5.1.1	Convex Dispatch	61
5.1.2	Nonconvex Dispatch	65
5.1.3	Cost-Emission Dispatch	68
5.1.4	Multi-Period Dispatch	72
5.2	Multi-Carrier Optimal Power Flow	79
5.2.1	Assumptions	79
5.2.2	Cost Reduction and CHP Rating	82
5.2.3	Coupled versus Decoupled Systems	83
5.2.4	Operation of Hubs	85
5.2.5	Marginal Cost and Hub Elasticity	85
5.3	OPF-Based Investment Evaluation	88
5.4	Optimal Hub Coupling	93
5.4.1	Single Hub	94
5.4.2	Multiple Hubs	96
5.5	Optimal Hub Layout	100

6	Closure	105
6.1	Summary	105
6.2	Conclusions	106
6.3	Future Work	107
A	Flow Constant	109
B	Optimality Conditions	111
B.1	Multi-Carrier Optimal Dispatch	112
B.2	Multi-Carrier Optimal Power Flow	112
	Bibliography	113
	Curriculum Vitae	125

Notation

Some of the symbols and acronyms that occur frequently in this thesis are listed below.

Scalars

$N_{\mathcal{H}}$	Number of hubs
$N_{\mathcal{N}}$	Number of nodes
$N_{\mathcal{C}}$	Number of converters
L	Hub output power
P	Hub input power
c	Converter coupling factor
ν	Dispatch factor
η	Energy efficiency
Q	Storage power exchange
\tilde{Q}	Internal storage power
e	Storage energy efficiency
E	Storage energy
\dot{E}	Storage energy derivative
t	Time (continuous or discrete)
\tilde{L}	Modified hub output power
\tilde{P}	Modified hub input power
Q	Input-side storage power
M	Output-side storage power

M^{eq}	Equivalent output-side storage power
s	Storage coupling factor
F	Link power flow
ΔF	Link power losses
V	Nodal voltage (complex)
Z	Series impedance
\tilde{Z}	Short circuit impedance
Y	Shunt reactance
k	Flow constant
δ	Direction of flow
p	Hydraulic pressure
k_{com}	Compressor constant
F_{com}	Compressor power consumption
x	Optimization variable (continuous, real number)
y	Optimization variable (discrete, integer)
Ψ	System marginal objective
Λ	Hub marginal objective
λ	Marginal cost of electricity generator
a, b, c	Function coefficients
u	Number of optimization variables
v	Number of equality constraints
w	Number of inequality constraints
I	Decision variable for converter element
J	Decision variable for storage element

Vectors and Matrices

P	Powers input vector
L	Power output vector
C	Converter coupling matrix
E	Vector of storage energies

\mathbf{E}^{stb}	Vector of storage standby energy losses
$\dot{\mathbf{E}}$	Vector of storage energy derivatives
\mathbf{Q}	Power exchange vector of input-side storage
\mathbf{M}	Power exchange vector of output-side storage
\mathbf{M}^{eq}	Equivalent storage power exchange vector
$\tilde{\mathbf{P}}$	Modified powers input vector
$\tilde{\mathbf{L}}$	Modified power output vector
\mathbf{S}	Storage coupling matrix
\mathbf{F}	Link power flow
\mathbf{x}	Vector of continuous optimization variables
\mathbf{y}	Vector of integer optimization variables
Ψ	System marginal objective vector
Λ	Hub marginal objective vector

The notation does not distinguish between row and column vectors.

Sets

\mathcal{A}	Network arcs
\mathcal{C}	Converter elements
\mathcal{D}	Storage elements
\mathcal{E}	Energy carriers
\mathcal{H}	Energy hubs
\mathcal{N}	Network nodes
\mathcal{S}	Energy sources
\mathbb{I}	Non-negative integers
\mathbb{R}	Real numbers

Functions and Operators

f	General function
\mathcal{F}	Objective function
g, \mathbf{g}	Equality constraint functions

h, \mathbf{h}	Inequality constraint functions
\mathbf{G}	Set of network equations
tr	Trace of matrix
$*$	Conjugation of complex number
\mathbf{T}	Transposition of vector/matrix

Miscellaneous

The following indices are used for the above quantities:

$i, j \in \mathcal{H}$	Energy hubs
$m, n \in \mathcal{N}$	Network nodes
$\alpha, \beta, \omega \in \mathcal{E}$	Energy carriers
$k \in \mathcal{C}$	Converter elements
$h \in \mathcal{D}$	Storage elements

The symbol “ \diamond ” is used to indicate the end of examples, remarks, and definitions.

Acronyms

AC	Alternating current
CHP	Combined heat and power
ED	Economic dispatch
GT	Gas turbine
HMC	Hub marginal cost
KKT	Karush, Kuhn, and Tucker
LMC	Locational marginal cost
MC	Multi-carrier
MCOPF	Multi-carrier optimal power flow
MINLP	Mixed-integer nonlinear programming
MP	Multi-period
NLP	Nonlinear programming
OPF	Optimal power flow

SNG Synthetic natural gas

UC Unit commitment

mu Monetary units

pu Per unit

Chapter 1

Introduction

1.1 Background and Motivation

Over the past decade, two major developments could be observed in most of the industrialized countries' utility industries:

- a) Restructuring of monopolistic frameworks towards liberalized markets providing open access for various (new) participants [1].
- b) Increasing utilization of small distributed energy resources for generation of electricity and heat [2].

In this respect, a transition from “vertically” to “horizontally” integrated energy systems is discussed intensively. However, at the same time energy utilities are faced with other critical issues:

- c) Steadily increasing demand of energy [3].
- d) Dependability on aging and congested infrastructures whose replacement and/or expansion is, due to various reasons, difficult and capital intensive [4].
- e) The global political aims of reducing greenhouse gas emissions and exploiting more environmentally-friendly and sustainable energy sources [5].

Besides these challenges, promising developments can be observed in the area of energy technologies. Power plants are nowadays more efficient and no longer subjected to strong economies of scale. Small-scaled co- and trigeneration plants, for example, show total efficiencies up to 85%, and their investment costs are competitive compared with large units [6–9]. Furthermore, modern information technology is now available which can be utilized to improve the system operation. Advanced supervisory control and data acquisition systems and wide area protection and control technology are examples for that [10, 11].

Against this background, the following conclusions seem to be reasonable for the future:

1. Existing infrastructures should be used as much and as long as possible.
2. New technologies should be introduced taking advantage of their technical, economic, and environmental characteristics.

Ad 1. One way of utilizing the existing infrastructures more efficiently is to consider them as one integrated system in planning and operation. If the infrastructures are integrated properly, i.e., if energy can be exchanged among them, integrated operation, in particular congestion management, could be implemented. For example, burden on a specific congested transmission path could be reduced by shifting part of the energy flow to another network and re-injecting it at less critical points in the system. But this would require appropriate tools incorporating all energy carriers.

Ad 2. Customer-side co- and trigeneration technology enables flexible utilization of electricity, natural gas, and other energy carriers. Thereby a diversity of supply is established which shows a number of potential benefits compared with conventional supply. However, the conversion of power between different energy carriers establishes a coupling of the corresponding power flows resulting in technical and economic system interactions. For example, a gas turbine can be used for simultaneous production of electricity and heat from natural gas; such a device would then affect natural gas and electricity power flow as well as the heat supply of the load. Related energy cost and prices would be influenced as well. Therefore investigations concerning technical and economic system implications of co- and trigeneration should cover all involved energy carriers.

A variety of modeling and analysis tools is available for energy infrastructures commonly installed in the industrialized part of the world, in particular for electricity, natural gas, and district heating systems. Economic and physical performances of these systems are well understood, but global features of integrated systems have not been investigated intensively yet, and there are only a few established tools available for this kind of analysis. Therefore the development of an integrated modeling and analysis framework for multi-carrier energy systems represents an essential need for future research. The questions of optimal system structure and operation are of particular interest.

1.2 Previous and Related Work

In the past, optimization efforts focused on systems employing only one form of energy. Methods have been developed in particular for electricity [12–15], natural gas [16–18], and district heating [19–21] networks.

More recently, the combined modeling and analysis of energy systems including multiple energy carriers have been addressed in a number of publications, e.g., [22–33]. In particular, system interactions and the integrated planning of natural gas, electricity, and other networks have been investigated, see, e.g., [34–39]. Different approaches have been developed and used for different purposes. While approximate flow models are used for instance in [26] for optimizing the flows through an energy supply chain, [28] and others employ detailed steady-state power flow equations for natural gas and electricity, appropriate for dispatching a real system. Also the couplings between the energy carriers are described in different ways.

The terms “multiple energy carrier systems” [24] and “hybrid energy systems” [40] have become accepted when referring to systems including various forms of energy, and they will be used throughout this thesis, as well as the slightly shorter term “multi-carrier systems”.

1.3 Main Contributions

This dissertation introduces a general steady-state modeling and optimization framework for energy systems including multiple energy carriers. The main contributions can be summarized as follows:

- A model for describing steady-state power flow couplings between different energy infrastructures and/or network participants is developed.
- Using this model, an approach for optimizing energy flows through converters and storage elements is formulated.
- A general marginal cost based optimality condition for optimal operation of energy converters is derived and discussed.
- An integrated optimal power flow problem is formulated including transmission, conversion, and storage of multiple energy carriers.
- Two approaches for determining the optimal coupling between energy infrastructures and network participants are developed. The first approach enables to find a theoretical optimum, whereas in the second approach the best-fitting converter and storage elements are selected from a given set of elements by means of optimization.
- Several basic examples are conducted in order to demonstrate the use of the presented optimization approaches. Implementation of the problems as well as some experiences with numerical solvers are reported and discussed.
- Based on the optimization approaches, a method for evaluating investment in converter and storage technologies is proposed.

The approaches presented in this thesis differ from other published material in the following way:

- The proposed modeling framework enables integration of an arbitrary number of energy carriers as well as chemical reactants and products.
- Any technology for transmission, conversion, and storage of energy can be considered.
- The general formulation ensures high flexibility in terms of modeling detail and accuracy. More approximate flow models can be used as well as detailed steady-state power flow equations.

1.4 List of Publications

The work reported in this thesis is basically covered by the following publications:

1. M. Geidl and G. Andersson. Optimal power dispatch and conversion in systems with multiple energy carriers. In *Proc. of 15th Power Systems Computation Conference*, Liege, Belgium, 2005.
2. M. Geidl and G. Andersson. A modeling and optimization approach for multiple energy carrier power flow. In *Proc. of IEEE PES PowerTech*, St. Petersburg, Russian Federation, 2005.
3. M. Geidl and G. Andersson. Operational and structural optimization of multi-carrier energy systems. *European Transactions on Electrical Power*, 16(5):463–477, 2006.
4. M. Geidl, P. Favre-Perrod, B. Klöckl, and G. Koeppel. A green-field approach for future power systems. In *Proc. of Cigre General Session 41*, Paris, France, 2006.
5. M. Geidl, G. Koeppel, P. Favre-Perrod, B. Klöckl, G. Andersson, and K. Fröhlich. Energy hubs for the future. *IEEE Power and Energy Magazine*, 5(1):24–30, 2007.
6. M. Geidl and G. Andersson. Optimal power flow of multiple energy carriers. *IEEE Transactions on Power Systems*, 22(1):145–155, 2007.
7. M. Geidl and G. Andersson. Optimal coupling of energy infrastructures. In *Proc. of IEEE PES PowerTech*, Lausanne, Switzerland, 2007.

Besides that, some other publications related to this dissertation are available:

8. P. Favre-Perrod, M. Geidl, B. Klöckl, and G. Koeppel. A vision of future energy networks. In *Proc. of IEEE PES Inaugural Conference and Exposition in Africa*, Durban, South Africa, 2005.
9. G. Koeppel, P. Favre-Perrod, M. Geidl, and B. Klöckl. Die Vision eines zukünftigen Energieversorgungsnetzwerkes. *Bulletin SEV/VSE*, 19(5):22–26, 2005 (in German).

10. K. Hemmes, J. L. Zachariah-Wolff, M. Geidl, and G. Andersson. Towards multi-source multi-product energy systems. *International Journal of Hydrogen Energy*, to appear.

1.5 Thesis Outline

The remainder of this thesis is organized as follows.

Chapter 2: Energy Hubs presents the conceptual approach of hybrid energy hubs. After the basic concept is introduced, some applications and potential benefits are discussed. System considerations conclude this chapter.

Chapter 3: Modeling deals with steady-state models for conversion, storage, and transmission of multiple energy carriers based on the energy hub concept. The models are merged yielding an integrated system description including all energy carriers.

Chapter 4: Optimization formulates various optimization problems related to multi-carrier energy systems. Optimization of the system structure is addressed as well as the optimal utilization of given structures. Some fundamental properties of the approaches and general results are discussed.

Chapter 5: Application elaborates various application examples in order to demonstrate possible applications and basic features of the optimization approaches. Specific implementation issues and some experience with numerical solvers are discussed.

Chapter 6: Closure concludes the thesis by summarizing and discussing the most important achievements, and suggesting possible future work.

Chapter 2

Energy Hubs

Several conceptual approaches for an integrated view of transmission and distribution systems with distributed energy resources have been published. Besides “energy-services supply systems” [23], “basic units” [26], and “micro grids” [41], so-called “hybrid energy hubs” [42] are proposed, where the term “hybrid” indicates the use of multiple energy carriers. In the following sections, the concept is elaborated on a qualitative level focusing on system aspects.

2.1 Basic Concept

Reference [42] introduces hybrid energy hubs as interfaces between energy producers, consumers, and the transportation infrastructure. From a system point of view, an energy hub can be identified as a unit that provides the basic features

- in- and output,
- conversion, and
- storage

of multiple energy carriers. Energy hubs can serve as interfaces between energy infrastructures and network participants (producers, consumers),

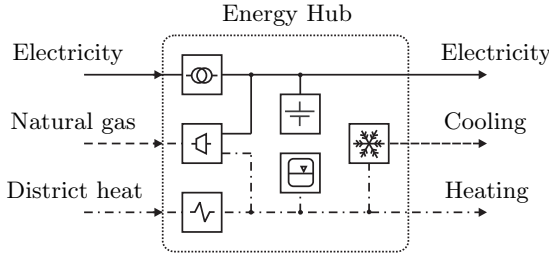


Figure 2.1: Example of a hybrid energy hub that contains typical elements: electrical transformer, gas turbine, heat exchanger, battery storage, hot water storage, absorption chiller.

or between different energy infrastructures, coupling for example electricity and natural gas systems without connecting sources and/or loads. Thus the energy hub represents a generalization or extension of a network node in an electrical system. Figure 2.1 shows a simple example of a hybrid energy hub.

An energy hub exchanges energy with the surrounding systems via hybrid ports. A hybrid port is established by a bundle of single carrier ports. The example hub shown in Figure 2.1 has two hybrid ports. At the input port, electricity, natural gas, and district heat are demanded from the corresponding infrastructures. The output port provides (transformed) electricity, heating, and cooling.

Typically, energy hubs consume common grid-bound energy carriers such as electricity, natural gas, and district heat which are converted and/or conditioned within the hub. Also other fossil fuels, e.g., coal and petroleum products, can be inputs. Hydrogen (or hydrogen-based products, respectively), biomass/biogas, geothermal heat, municipal waste, landfill gas, and other carriers could be an option in the future. Different energy carriers are also provided at the output. Basically, all mentioned input carriers can be transmitted to the output without converting them into other forms. In addition, energy can be converted for the purpose of cooling, production of compressed air, or steam. Besides the mentioned energy carriers one could also consider in- and output of chemical reactants and products such as water, air, emissions, lubricants, and waste.

The energy hub approach is not restricted to any size of the modeled system. It enables the integration of an arbitrary number of energy carriers and products, and thus provides high flexibility in system modeling.

2.2 Hub Elements

In terms of functionality, energy hubs contain three basic elements:

- direct connections,
- converters, and
- storage.

Direct connections are used to deliver an input carrier to the output without converting it into another form or significantly changing its quality (e.g., electric voltage, hydraulic pressure). Electric cables, overhead lines, and pipelines are examples for this type of element. Besides that, converter elements are used to transform power into other forms or qualities. Examples are steam and gas turbines, reciprocating internal combustion engines, Stirling engines, electric machines, fuel cells, electrolyzers, thermoelectric converters, etc. Compressors, pumps, pressure control valves, transformers, power-electronic inverters, filters, heat exchangers and other devices are commonly used for conditioning, i.e., converting power into desirable quantities and/or qualities to be consumed by loads. The third type of element, energy storage, can also be realized with different technologies. Solid, liquid, and gaseous energy carriers can be stored in tanks and containers employing comparably simple technology. Note that gaseous energy carriers can also be stored in the network itself (i.e., in the pipelines) by increasing the pressure in the system; this technique is commonly referred to as “line packing” [43]. Electricity can be stored directly (e.g., supercaps, superconducting devices) or indirectly (e.g., batteries, hydro reservoirs, flywheels, compressed air storage, reversible fuel cells).

2.3 Applications

Figure 2.1 outlines a simple example of an energy hub. There are a number of real facilities that can be modeled as energy hubs, for instance

- power plants (co- and trigeneration),
- industrial plants (steel works, paper mills, refineries),

- big buildings (airports, hospitals, shopping malls),
- bounded geographical areas (rural and urban districts, towns, cities), and
- island power systems (trains, ships, aircrafts).

Originally, the energy hub approach was developed for greenfield design studies [44, 45]. However, in the meantime the concept has been taken over for other purposes. Corresponding to the first item in the above list, application of the energy hub concept for the characterization of trigeneration devices is reported in [46]. Another application example is the conception of fuel cell systems, which is exemplified in [47]. Models for integrated analysis of energy and transportation systems employing the energy hub concept are presented in [48].

The energy hub idea was also picked up by a municipal utility in Switzerland, the Regionalwerke AG Baden, which plans to build an energy hub containing wood chip gasification and methanation, and a cogeneration plant [49]. Figure 2.2 sketches the basic layout of this hub. The idea is to generate synthetic natural gas (SNG) and heat from wood chips, a resource which is available in the company's supply region. The produced SNG can then either be directly injected in the utility's natural gas system, or converted into electricity via a cogeneration unit and fed into the electric distribution network. Waste heat, which accrues in both cases, can be absorbed by the local district heating network. The whole system can be seen as an energy hub processing different energy carriers—wood chips, electricity, heat, and SNG. In addition to these energy carriers, the gasification process requires nitrogen and steam, which have to be provided at the hub input. Figure 6 gives an overview of the hub layout. Not the technology used, but its integrated planning and operation, which is believed to enable better overall system performance, represents an innovation.

2.4 Potential Benefits

From a system point of view, combining and coupling different energy carriers in energy hubs keeps a number of potential advantages over conventional, decoupled energy supply. The diversity of supply results in the following potential benefits.

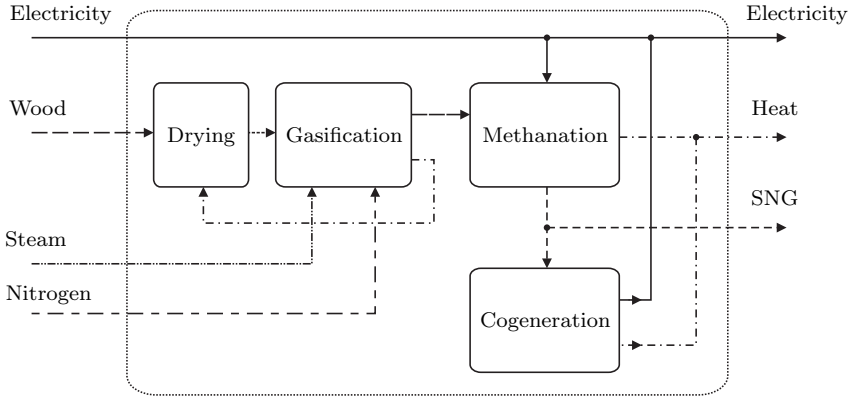


Figure 2.2: Sketch of the energy hub to be realized by Regionalwerke AG Baden, Switzerland.

Increased Reliability: Considering multiple inputs of an energy hub which can be used to meet the output demand makes clear that the hub generally increases availability of energy for the load, because it is no longer dependent on a single infrastructure [50,51]. In practice, this effect is slightly limited since certain infrastructures are dependent on others, i.e., the different hub inputs are not completely redundant. Besides that, almost all modern infrastructures are dependent on certain information technology, for example supervisory control and data acquisition systems, which are in turn dependent on electricity supply.

Increased Load Flexibility: Redundant paths within the hub offer a certain degree of freedom in supplying the loads. Consider for example the electricity load in Figure 2.1. It can be supplied by consuming electricity directly from the corresponding input or by generating part (or all) of the load power using the gas turbine. The hub can thereby substitute for an unattractive energy carrier, for example high-tariff electricity. Thus, from a system point of view, the load appears to be more elastic in terms of its price and demand behavior, even if the actual load at the hub output remains constant.

Optimization Potential: The fact that various inputs and different combinations of them can be used to meet the output requirement

yields to the question of optimal supply. The different inputs can be characterized by different cost, related emissions, availability, and other criteria. Then the input of the hub can be optimized using the additional degree of freedom established by redundant connections.

Synergy Effects: The energy hub processes different energy carriers, each of which showing specific characteristics. Electricity, for example, can be transmitted over long distances with comparably low losses. Chemical energy carriers can be stored employing relatively simple and cheap technology. Gaseous energy carriers can—to some extent—be stored in the network by using line pack capabilities. Transmission and storage characteristics as well as other specific virtues of the different energy carriers can be combined synergetically.

2.5 Energy Hub Systems

In the context of energy hubs, the whole energy supply infrastructure can be considered as a system of interconnected energy hubs. Figure 2.3 shows three energy hubs interconnected by electricity and natural gas networks. This is an example for the supply of a town that is roughly divided into three areas: industrial, commercial, and private/residential. Each area is interfaced with natural gas and electricity distribution networks via an energy hub. The internal layout of the hubs is adapted to the specific load requirements. The system is supplied via adjacent networks, a photovoltaic plant connected to hub H3, and wind and hydro plants connected to the electricity network via node N4. This node could represent a more remote station outside the town where hydro reservoirs are available.

Concerning energy transmission between the hubs, it should be noted that the combination of different energy carriers in integrated transmission devices is subject to research [52, 53].

This general system view—hubs interconnected by networks—is also reflected in the system model derived in Chapter 3.

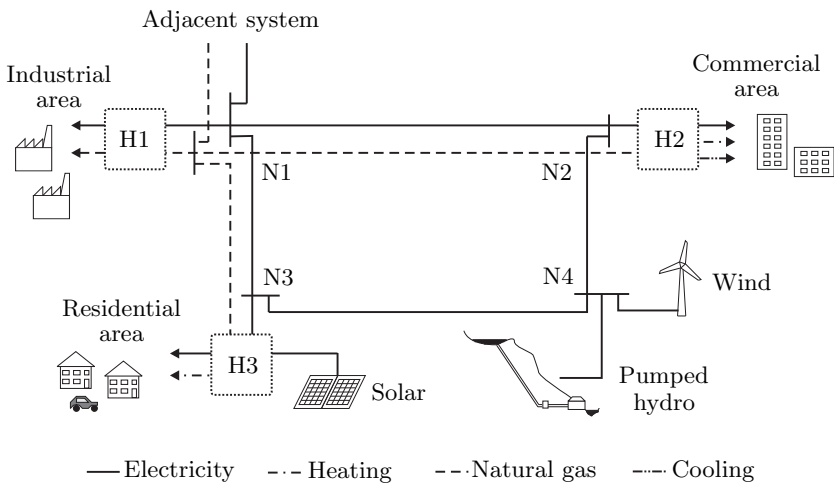


Figure 2.3: Sketch of a system of interconnected energy hubs.

Chapter 3

Modeling

In this chapter, models are elaborated for describing steady-state flows in multiple energy carrier systems. First, a model for conversion of multiple energy carriers is developed based on the energy hub concept. Then energy storage is included in the equations. After that, models for energy transmission are discussed focusing on two of the most common energy infrastructures—electricity and pipeline systems. Finally, it is outlined how the flows in a system of interconnected energy hubs can be described.

3.1 Basic Modeling Concept

The multi-carrier energy system is considered as a system of energy hubs interconnected by different networks. Energy is transmitted via the networks and converted and stored within the energy hubs. Accordingly, the system model is stated in two parts: power flow *within* and *between* hubs. The model is based on the following assumptions and simplifications:

- The system is considered to be in steady-state, which is reached after all transients or fluctuating conditions have damped out, and all quantities remain essentially constant, or oscillate uniformly.

- Within energy hubs, losses occur only in converter and storage elements.
- If not mentioned explicitly, unidirectional power flow from the inputs to the outputs of the converters is assumed.
- Power flow through converter devices is characterized through power and energy efficiency only, no other quantities are used.

The following definitions and notations will be used in the development of the model:

- A set of energy carriers \mathcal{E} is considered whose members are denoted by small Greek letters:

$$\alpha, \beta, \dots, \omega \in \mathcal{E} = \{\text{electricity, natural gas, hydrogen, } \dots\}$$

- Furthermore, a set of hubs \mathcal{H} is introduced; small Roman letters are used to denote its members:

$$i, j \in \mathcal{H} = \{1, 2, \dots, N_{\mathcal{H}}\}$$

where $N_{\mathcal{H}}$ is the number of energy hubs considered.

- Each hub i contains a set of converters \mathcal{C}_i ; the subset $\mathcal{C}_{i\alpha} \subseteq \mathcal{C}_i$ contains all elements of hub i which convert α into another carrier:

$$k \in \mathcal{C}_{i\alpha} = \{1, 2, \dots, N_{\mathcal{C}_{i\alpha}}\}$$

where $N_{\mathcal{C}_{i\alpha}}$ is the number of converters in hub i , and $N_{\mathcal{C}_i}$ is the number of converters in hub i processing α .

- Besides converters, the hubs contain storage elements summarized in a set \mathcal{D}_i :

$$h \in \mathcal{D}_i = \{1, 2, \dots, N_{\mathcal{D}_i}\}$$

where $N_{\mathcal{D}_i}$ is the number of storage elements in hub i .

- All network nodes are collected in a set \mathcal{N} :

$$m, n \in \mathcal{N} = \{1, 2, \dots, N_{\mathcal{N}}\}$$

where $N_{\mathcal{N}}$ is the number of network nodes in the system. The subset $\mathcal{N}_{\alpha} \subseteq \mathcal{N}$ includes all nodes of the α -system.

- All network branches (arcs, links) are collected in a set \mathcal{A} :

$$(m, n) \in \mathcal{A} = \{(1, 2), (1, 3), \dots, (N_{\mathcal{N}} - 1, N_{\mathcal{N}})\}$$

The subset $\mathcal{A}_{\alpha} \subseteq \mathcal{A}$ contains all branches transmitting the energy carrier α .

- The symbols P and L refer to the hubs' steady-state power in- and outputs, respectively. Flows on links between the hubs are generally denoted with F , storage power is denoted Q and M .

3.2 Energy Conversion

A generic model for energy converters can be developed focusing on their in- and output power flows while considering the device as a black box characterized by its energy efficiency. Converter elements or combinations of different converters (converter clusters) may have multiple in- and outputs. Four types of conversions can be classified according to the number of in- and outputs:

- single input and single output (e.g., gas furnace converting natural gas to heat);
- single input and multiple outputs (e.g., trigeneration plant converting natural gas in order to provide heating, cooling, and electricity);
- multiple inputs and single output (e.g., heat pump, converting low temperature heat and electricity into high temperature heat);
- multiple inputs and multiple outputs (e.g., reversible fuel cell system with hydrogen and water input, electricity and heat output).

The converter model is developed in two steps. First, a converter with single input and single output is considered. This model is then generalized for conversions with multiple in- and outputs.

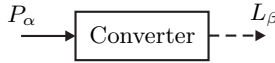


Figure 3.1: Converter with single input and output. Steady-state input power P_α , output power L_β .

Table 3.1: Conversion Types.

Type of coupling	Coupling factor	Energy carriers
Lossless transmission	$c_{\alpha\beta} = 1$	$\alpha = \beta$
Lossy transmission	$0 < c_{\alpha\beta} \leq 1$	$\alpha = \beta$
Lossless conversion	$c_{\alpha\beta} = 1$	$\alpha \neq \beta$
Lossy conversion	$0 < c_{\alpha\beta} \leq 1$	$\alpha \neq \beta$
No coupling	$c_{\alpha\beta} = 0$	any α, β

3.2.1 Single Input and Single Output

Consider a converter device as indicated in Figure 3.1 that converts an input energy carrier α into β , where $\alpha, \beta \in \mathcal{E}$. Input and output power flows are not independent, we consider them to be coupled:

$$L_\beta = c_{\alpha\beta} P_\alpha \quad (3.1)$$

where P_α and L_β are the steady-state input and output powers, respectively. The *coupling factor* $c_{\alpha\beta}$ defines the coupling between input and output power flow. For a simple converter device with one input and one output, the coupling factor corresponds to the converter's steady-state energy efficiency.

Due to conservation of power, the output of the converter device must be lower than or equal to the input. Accordingly, the coupling factor is limited:

$$L_\beta \leq P_\alpha \quad \Rightarrow \quad 0 \leq c_{\alpha\beta} \leq 1 \quad (3.2)$$

Common converter devices show non-constant efficiencies varying with the converted power level. The dependency can be included in (3.1) by expressing the coupling factor as a function of the converted power, i.e., $c_{\alpha\beta} = f_\beta(P_\alpha)$.

Table 3.1 outlines the meaning of coupling factors with respect to physical processes.

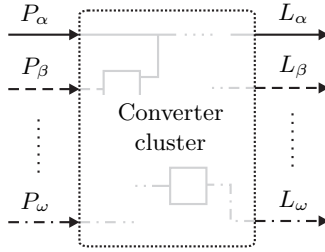


Figure 3.2: Converter arrangement with inputs $P_\alpha, P_\beta, \dots, P_\omega$ and outputs $L_\alpha, L_\beta, \dots, L_\omega$.

Remark 3.1 This general modeling concept enables the description of power transmission in the same way as conversion. As shown in Table 3.1, transmission of power can be seen as a special case of a conversion. \diamond

3.2.2 Multiple Inputs and Multiple Outputs

A general model covering couplings with multiple in- and outputs can be created according to Figure 3.2. We consider a unit where multiple inputs are converted into multiple outputs. This conversion can either be established by a single device or by a combination of multiple converters. However, we consider this as one unit with dedicated inputs and outputs, i.e., as an energy hub. Since only one hub is considered in the following derivations, the hub index i is omitted.

Stating all power inputs $P_\alpha, P_\beta, \dots, P_\omega$ and outputs $L_\alpha, L_\beta, \dots, L_\omega$ in vectors \mathbf{P} and \mathbf{L} , respectively, enables the formulation of multi-input multi-output power conversion analogous to (3.1):

$$\underbrace{\begin{bmatrix} L_\alpha \\ L_\beta \\ \vdots \\ L_\omega \end{bmatrix}}_{\mathbf{L}} = \underbrace{\begin{bmatrix} c_{\alpha\alpha} & c_{\beta\alpha} & \cdots & c_{\omega\alpha} \\ c_{\alpha\beta} & c_{\beta\beta} & \cdots & c_{\omega\beta} \\ \vdots & \vdots & \ddots & \vdots \\ c_{\alpha\omega} & c_{\beta\omega} & \cdots & c_{\omega\omega} \end{bmatrix}}_{\mathbf{C}} \underbrace{\begin{bmatrix} P_\alpha \\ P_\beta \\ \vdots \\ P_\omega \end{bmatrix}}_{\mathbf{P}} \quad (3.3)$$

The matrix \mathbf{C} is called *converter coupling matrix*. Mathematically speaking, this matrix describes the mapping of the powers from the input to

the output of the converter arrangement. The entries of the converter coupling matrix are coupling factors as defined in (3.1). Each coupling factor relates one particular input to a certain output.

Remark 3.2 As long as coupling factors are assumed constant, (3.1) and (3.3) represent linear transformations. Including power dependencies such as $c_{\alpha\beta} = f_{\beta}(P_{\alpha})$ or $\mathbf{C} = f(\mathbf{P})$ yields nonlinear relations. \diamond

Remark 3.3 Note that \mathbf{C} is generally not invertible, i.e., (3.3) represents an underdetermined system of equations. This is an important property of many realistic coupling matrices. It reflects the degrees of freedom in supply which can be used for optimization. If \mathbf{C} is regular, then (3.3) describes a one-to-one mapping and there is only one solution \mathbf{P} for given loads \mathbf{L} , hence no potential for optimization, unless \mathbf{C} is not constant. \diamond

Remark 3.4 As indicated in Figures 3.1 and 3.2, the underlying causality for (3.1) and (3.3) is that power flows from the input to the output of the converters, i.e., $P_{\alpha}, L_{\beta} \geq 0$ and $\mathbf{P}, \mathbf{L} \geq \mathbf{0}$. Nevertheless, reverse power flow is possible as long as the corresponding coupling is realized by technology which enables bidirectional flows. An electrical transformer for instance allows power flow in both directions, whereas a gas turbine does not provide this feature. Reverse power flow has to be considered in the converter coupling matrix whenever the corresponding coupling factor differs from one. \diamond

Two important characteristics of the converter coupling matrix are obvious:

- Since no power can be gained by converting one form of energy into another one, all matrix entries are limited according to minimal and maximal energy efficiency, respectively:

$$0 \leq c_{\alpha\beta} \leq 1 \quad \forall \alpha, \beta \in \mathcal{E} \quad (3.4)$$

- The sum of all outputs converted from a single input has to be lower than or equal to the input. Thus each column-sum is limited:

$$0 \leq \sum_{\beta \in \mathcal{E}} c_{\alpha\beta} \leq 1 \quad \forall \alpha \in \mathcal{E} \quad (3.5)$$

In contrast to converters with one input and one output, the coupling factors are in general no longer equal to converter efficiencies when

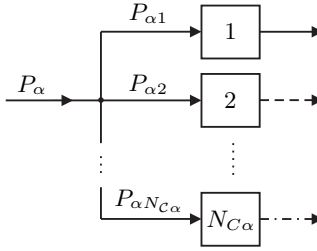


Figure 3.3: Dispatch of total input power P_α at an input junction. Converter elements $1, 2, \dots, N_{C_\alpha}$, corresponding power inputs $P_{\alpha 1}, P_{\alpha 2}, \dots, P_{\alpha N_{C_\alpha}}$.

considering multiple inputs and outputs. Since the total input of one energy carrier may split up to several converters (at input junctions), so-called *dispatch factors* have to be introduced that define the dispatch of the total input to the devices converting this carrier.

Figure 3.3 outlines this concept. The total input flow P_α splits up to N_{C_α} converters. The dispatch factors $\nu_{\alpha k}$ specify how much of the total input power P_α flows into converter k :

$$P_{\alpha k} = \nu_{\alpha k} P_\alpha \quad (3.6)$$

where $k \in C_\alpha = \{1, 2, \dots, N_{C_\alpha}\}$. Considering conservation of power at the input junction yields two straightforward requirements for the dispatch factors:

- Since every branch carries only a part of the total input flow, all dispatch factors must be lower than or equal to one:

$$0 \leq \nu_{\alpha k} \leq 1 \quad \forall \alpha \in \mathcal{E}, \forall k \in C_\alpha \quad (3.7)$$

- The sum of all dispatch factors related to a junction is equal to one:

$$\sum_{k \in C_\alpha} \nu_{\alpha k} = 1 \quad \forall \alpha \in \mathcal{E} \quad (3.8)$$

From this property it can be seen that for a junction where the total input splits up to N_{C_α} branches, $(N_{C_\alpha} - 1)$ dispatch factors have to be introduced.

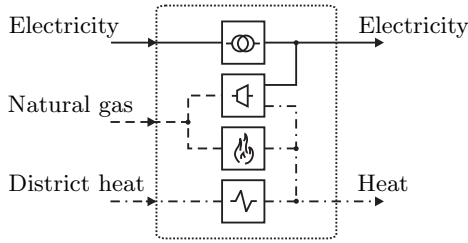


Figure 3.4: Example hub that contains an electrical transformer, a gas turbine, a gas furnace, and a heat exchanger.

Junctions may also appear at the output side of the converters. The total output of a certain energy carrier is then equal to the sum of all individual converter outputs. Output junctions do not require to introduce additional variables such as dispatch factors.

Remark 3.5 An alternative way of dealing with input junctions is to treat each converter input as a separate hub input by including the individual power inputs $P_{\alpha k}$ in the hub's power input vector \mathbf{P} . \diamond

For a given converter arrangement, the converter coupling matrix can be derived in the following manner:

1. Define input and output power vectors.
2. Introduce dispatch factors at junctions where converter inputs are connected.
3. Express converter outputs as functions of the inputs.
4. State nodal power balance at converter output junctions.
5. Formulate the results according to (3.3).

The procedure is demonstrated in the following example.

Example 3.1 We will now derive the converter coupling matrix for the energy hub shown in Figure 3.4, which consumes electricity, natural gas, and district heat, and delivers transformed electricity and heat. We assign the electricity, natural gas, and district heat input powers as P_e , P_g , and P_h , and the electricity and heat output powers as L_e

and L_h , respectively. These are the entries of input and output vectors. According to the second item in the aforementioned procedure, we have to introduce a dispatch factor ν at the natural gas input junction:

- $P_{g1} = \nu P_g$ is fed into the gas turbine, and
- $P_{g2} = (1 - \nu)P_g$ flows into the furnace,

where $0 \leq \nu \leq 1$. Next we have to express all converter outputs as the products of their inputs and efficiencies. For the sake of simplicity, we assume constant efficiencies of the converter devices: η_{ee}^T for the transformer, η_{ge}^{GT} and η_{gh}^{GT} for the gas turbine, η_{gh}^F for the furnace and η_{hh}^{HE} for the heat exchanger. The power output of the hub results in

$$L_e = \eta_{ee}^T P_e + \nu \eta_{ge}^{GT} P_g \quad (3.9a)$$

$$L_h = \nu \eta_{gh}^{GT} P_g + (1 - \nu) \eta_{gh}^F P_g + \eta_{hh}^{HE} P_h \quad (3.9b)$$

Finally, we can write (3.9) in matrix notation:

$$\begin{bmatrix} L_e \\ L_h \end{bmatrix} = \begin{bmatrix} \eta_{ee}^T & \nu \eta_{ge}^{GT} & 0 \\ 0 & \nu \eta_{gh}^{GT} + (1 - \nu) \eta_{gh}^F & \eta_{hh}^{HE} \end{bmatrix} \begin{bmatrix} P_e \\ P_g \\ P_h \end{bmatrix} \quad (3.10)$$

According to Remark 3.5, an alternative formulation without dispatch factors can be achieved by considering the individual converter inputs P_{g1} and P_{g2} as separate hub inputs:

$$\begin{bmatrix} L_e \\ L_h \end{bmatrix} = \begin{bmatrix} \eta_{ee}^T & \eta_{ge}^{GT} & 0 & 0 \\ 0 & \eta_{gh}^{GT} & \eta_{gh}^F & \eta_{hh}^{HE} \end{bmatrix} \begin{bmatrix} P_e \\ P_{g1} \\ P_{g2} \\ P_h \end{bmatrix} \quad (3.11)$$

Clearly, (3.10) and (3.11) are underdetermined, hence several input vectors can be found that satisfy (3.10) for given loads. \diamond

3.3 Energy Storage

In this section, a generic model for energy storage is developed. First, a single storage device is considered and equations describing its energy

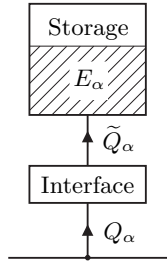


Figure 3.5: Model of an energy storage device. Stored energy E_α , internal power \tilde{Q}_α , power exchange Q_α .

exchange are stated. These relations are then merged with the converter model from the preceding sections resulting in a complete energy hub model including conversion and storage.

3.3.1 Storage Element

A general model for energy storage devices is developed based on Figure 3.5. The storage devices is considered to consist of an interface and an internal (ideal) storage. Through the interface, power may be conditioned and/or converted into another energy carrier, which is then stored. For example, pressurized air storage plants exchange electrical power, but internally pressurized air is stored. However, when a storage device exchanges an energy carrier α , then it is reasonable to consider it as a storage of α , even if $\beta \neq \alpha$ is stored internally. Therefore, in the following considerations, storage content and power exchanged are considered to be of the same form.

The storage interface can be modeled similar to a converter device. The steady-state input and output power values can be related to each other by

$$\tilde{Q}_\alpha = e_\alpha Q_\alpha \quad (3.12)$$

where e_α describes how much the power exchanged with the system affects the energy stored. This factor generally depends on the direction of power flow, i.e., if the storage is charged or discharged:

$$e_\alpha = \begin{cases} e_\alpha^+ & \text{if } Q_\alpha \geq 0 \quad (\text{charging/standby}) \\ 1/e_\alpha^- & \text{else} \quad (\text{discharging}) \end{cases} \quad (3.13)$$

Here e_{α}^{+} and e_{α}^{-} can be understood as forward and reverse energy efficiencies of the interface, respectively. These values can also be considered as the storage's charging and discharging efficiencies, respectively.

Remark 3.6 Taking a closer look on storage technology makes clear that storage performance, such as charging and discharging efficiencies, generally depends on the energy stored and its time derivative [55]. Power and energy dependent efficiencies $e_{\alpha}^{+}, e_{\alpha}^{-} = f(Q_{\alpha}, E_{\alpha})$ can be included in the equations above, but in order to keep the complexity of the optimization problems reasonably low, they are assumed to be constant throughout this thesis. \diamond

The stored energy after a certain operating period T equals the initial storage content plus the time integral of the power:

$$E_{\alpha}(T) = E_{\alpha}(0) + \int_0^T \tilde{Q}_{\alpha}(t) dt \quad (3.14)$$

The internal power flow \tilde{Q}_{α} corresponds to the time derivative of the stored energy. For steady-state considerations, power is approximated by the change in energy ΔE during a time period Δt ; the slope dE_{α}/dt is assumed to be constant during Δt , what corresponds to constant power \tilde{Q}_{α} :

$$\tilde{Q}_{\alpha} = \frac{dE_{\alpha}}{dt} \approx \frac{\Delta E_{\alpha}}{\Delta t} \triangleq \dot{E}_{\alpha} \quad (3.15)$$

3.3.2 Storage in Energy Hubs

Energy hubs may contain multiple storage elements. In principle, storage can be connected to the hub inputs, the hub outputs, or between converters connecting inputs and outputs. It will be shown that the corresponding storage power flow can be transformed to either side of the hub, independently where the storage device is connected physically.

Consider the energy hub in Figure 3.6 which contains storage at the input and output side. The power flowing into the converter equals the total hub input minus the storage power:

$$\tilde{P}_{\alpha} = P_{\alpha} - Q_{\alpha} \quad (3.16)$$

The corresponding equation for output side storage is

$$\tilde{L}_{\beta} = L_{\beta} + M_{\beta} \quad (3.17)$$

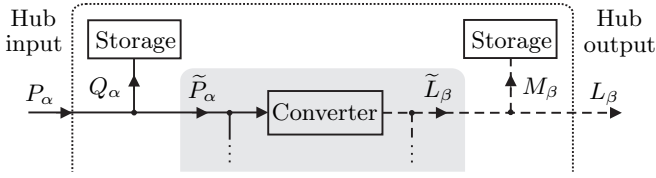


Figure 3.6: Storage elements in energy hubs. Hub input and output powers P_α and L_β , respectively; input and output side storage flows Q_α and M_β , respectively; converter input and output flows \tilde{P}_α and \tilde{L}_β , respectively.

The shaded area in Figure 3.6 represents a converter cluster without storage elements. For this part of the hub, power transformation can be expressed according to (3.3). Stating all inputs and outputs of this converter cluster in vectors $\tilde{\mathbf{P}}$ and $\tilde{\mathbf{L}}$, respectively, yields

$$\tilde{\mathbf{L}} = \mathbf{C} \tilde{\mathbf{P}} \quad (3.18)$$

With (3.16) and (3.17) the storage flows can be included explicitly:

$$\mathbf{L} + \mathbf{M} = \mathbf{C} \left[\mathbf{P} - \mathbf{Q} \right] \quad (3.19)$$

where \mathbf{M} keeps all output side storage powers, and \mathbf{Q} contains the input side storage flows. All storage influence can be summarized in an equivalent storage flow vector \mathbf{M}^{eq} :

$$\mathbf{L} = \mathbf{C} \left[\mathbf{P} - \mathbf{Q} \right] - \mathbf{M} = \mathbf{C} \mathbf{P} - \mathbf{M}^{\text{eq}} \quad (3.20)$$

Assuming a constant coupling matrix \mathbf{C} , superposition can be applied and the equivalent storage flows can be stated as

$$\mathbf{M}^{\text{eq}} = \mathbf{C} \mathbf{Q} + \mathbf{M} \quad (3.21)$$

In general, each element of \mathbf{M}^{eq} has two components:

$$M_\beta^{\text{eq}} = c_{\alpha\beta} Q_\alpha + M_\beta = \frac{c_{\alpha\beta}}{e_\alpha} \dot{E}_\alpha + \frac{1}{e_\beta} \dot{E}_\beta \quad (3.22)$$

The term $c_{\alpha\beta} Q_\alpha$ corresponds to the input-side storage power apparent at the hub output, and M_β corresponds to the output-side storage power. Equation (3.22) enables the transformation of storage power

flows between inputs and outputs of converters. If a storage device is connected between two converters connecting hub inputs and outputs (i.e., not directly at an input or output), the corresponding power exchange can be transformed either to the input or to the output side of the hub. Equation (3.22) can be written in matrix form:

$$\underbrace{\begin{bmatrix} M_{\alpha}^{\text{eq}} \\ M_{\beta}^{\text{eq}} \\ \vdots \\ M_{\omega}^{\text{eq}} \end{bmatrix}}_{\mathbf{M}^{\text{eq}}} = \underbrace{\begin{bmatrix} s_{\alpha\alpha} & s_{\beta\alpha} & \cdots & s_{\omega\alpha} \\ s_{\alpha\beta} & s_{\beta\beta} & \cdots & s_{\omega\beta} \\ \vdots & \vdots & \ddots & \vdots \\ s_{\alpha\omega} & s_{\beta\omega} & \cdots & s_{\omega\omega} \end{bmatrix}}_{\mathbf{S}} \underbrace{\begin{bmatrix} \dot{E}_{\alpha} \\ \dot{E}_{\beta} \\ \vdots \\ \dot{E}_{\omega} \end{bmatrix}}_{\dot{\mathbf{E}}} \quad (3.23)$$

The matrix \mathbf{S} is denoted *storage coupling matrix*. It describes how changes of the storage energies affect the hub output flows. In other words, it maps all storage energy derivatives into equivalent output-side flows. The entries $s_{\alpha\beta}$ are derived according to (3.22). Finally, a relation including hub input and output flows as well as the storage energy derivatives can be achieved by including (3.23) in (3.20):

$$\mathbf{L} = \mathbf{C}\mathbf{P} - \mathbf{S}\dot{\mathbf{E}} = \begin{bmatrix} \mathbf{C} & -\mathbf{S} \end{bmatrix} \begin{bmatrix} \mathbf{P} \\ \dot{\mathbf{E}} \end{bmatrix} \quad (3.24)$$

This relation represents a complete model of an energy hub including converter and storage elements. The following example outlines the derivation of (3.24) for a given hub layout.

Example 3.2 In this example, derivation of (3.18) and (3.24) is outlined using a simple energy hub. Consider the hub shown in Figure 3.7 which contains two converters and two storage devices: gas turbine and heat exchanger, and gas tank and hot water storage, respectively. The gas turbine is characterized by its gas-electric and gas-heat efficiencies $\eta_{\text{ge}}^{\text{GT}}$ and $\eta_{\text{gh}}^{\text{GT}}$, respectively. The heat exchanger operates with an efficiency $\eta_{\text{hh}}^{\text{HE}}$. Efficiencies of the storage devices are e_{g} and e_{h} , for the gas tank and the heat storage, respectively. The electrical connection between input and output is assumed to be lossless. The converters are described by the following coupling matrix:

$$\mathbf{C} = \begin{bmatrix} 1 & \eta_{\text{ge}}^{\text{GT}} & 0 \\ 0 & \eta_{\text{gh}}^{\text{GT}} & \eta_{\text{hh}}^{\text{HE}} \end{bmatrix} \quad (3.25)$$

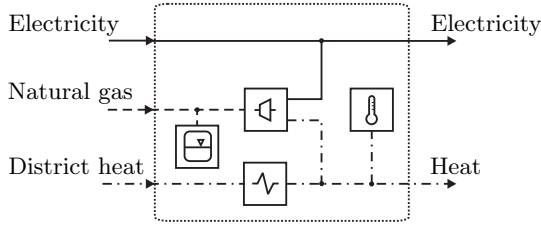


Figure 3.7: Example hub with gas turbine, heat exchanger, gas tank, and heat storage.

The storage devices exchange the powers

$$Q_g = \frac{1}{e_g} \cdot \dot{E}_g \quad (3.26a)$$

$$M_h = \frac{1}{e_h} \cdot \dot{E}_h \quad (3.26b)$$

Now (3.18) can be formulated:

$$\begin{bmatrix} L_e \\ L_h + \frac{1}{e_h} \cdot \dot{E}_h \end{bmatrix} = \begin{bmatrix} 1 & \eta_{ge}^{GT} & 0 \\ 0 & \eta_{gh}^{GT} & \eta_{hh}^{HE} \end{bmatrix} \begin{bmatrix} P_e \\ P_g - \frac{1}{e_g} \cdot \dot{E}_g \\ P_h \end{bmatrix} \quad (3.27)$$

Alternatively, the hub can be described according to (3.24). Therefore input-side and output-side storage flow have to be transformed to equivalent output-side flows:

$$M_e^{eq} = \frac{\eta_{ge}^{GT}}{e_g} \dot{E}_g \quad (3.28a)$$

$$M_h^{eq} = \frac{\eta_{gh}^{GT}}{e_g} \dot{E}_g + \frac{1}{e_h} \dot{E}_h \quad (3.28b)$$

From these equations, the storage coupling matrix can be extracted:

$$\mathbf{S} = \begin{bmatrix} \frac{\eta_{ge}^{GT}}{e_g} & 0 \\ \frac{\eta_{gh}^{GT}}{e_g} & \frac{1}{e_h} \end{bmatrix} \quad (3.29)$$

Finally, the flows through the energy hub can be formulated as (3.24):

$$\begin{bmatrix} L_e \\ L_h \end{bmatrix} = \begin{bmatrix} 1 & \eta_{ge}^{GT} & 0 & -\frac{\eta_{ge}^{GT}}{e_g} & 0 \\ 0 & \eta_{gh}^{GT} & \eta_{hh}^{HE} & -\frac{\eta_{gh}^{GT}}{e_g} & -\frac{1}{e_h} \end{bmatrix} \begin{bmatrix} P_e \\ P_g \\ P_h \\ \dot{E}_g \\ \dot{E}_h \end{bmatrix} \quad (3.30)$$

From this formulation it is obvious that energy storage present in the hub results in additional degrees of freedom in its operation. \diamond

3.4 Energy Transmission

In this section, models for energy transmission via networks are elaborated. Different levels of abstraction are considered according to the following classification.

Network Flow Models (Type I): Energy flows in the networks are described by conservation laws only, physical losses are usually not considered in the equations. Commonly, the network links are characterized by specific transmission costs (e.g., € per transmitted MWh) in order to get a criterion for optimization. This value includes all transmission-related efforts, such as maintenance cost, operating cost, and losses. Such models are commonly used for more general investigations in the system behavior as reported in [30, 56].

Network Flow Models (Type II): In contrast to Type I network flow models, link losses are directly incorporated in the equations by expressing them as functions of the corresponding flow. Compared with the aforementioned models, these models represent the network flows more accurately. Applications can be found in [26, 57].

Power Flow Models: Besides conservation of flow, these models are based on constitutional laws linking for example electrical voltage and current, hydraulic pressure and mass flow etc. These models

deliver the most accurate results for steady-state analysis. Steady-state power flow models for electricity and natural gas networks are used for example in [28, 58].

Networks are generally modeled as graphs consisting of a set of nodes \mathcal{N} and a set of branches (arcs, links) \mathcal{A} which connect the nodes [59]. An individual network transporting $\alpha \in \mathcal{E}$ is defined by a set of nodes $\mathcal{N}_\alpha \subseteq \mathcal{N}$ and branches $\mathcal{A}_\alpha \subseteq \mathcal{A}$. In the following considerations, the index α is omitted in order to improve legibility.

3.4.1 Network Flow Models

Network flow models are generally based on conservation laws. For any node $m \in \mathcal{N}$ in the network, the sum of all branch flows must be equal to the power injection:

$$F_m - \sum_{n \in \mathcal{N}_m} F_{mn} = 0 \quad (3.31)$$

where $\mathcal{N}_m \subseteq \mathcal{N} \setminus m$ is the set of nodes connected node m , and F_m is the net power injection¹ at m . Describing a system of $N_{\mathcal{N}}$ nodes requires $N_{\mathcal{N}}$ nodal equations of the form (3.31).

Type I

When network links are assumed to transmit energy without losses, flows are equal on either side (see Figure 3.8):

$$F_{mn} = -F_{nm} \quad (3.32)$$

For optimization purposes, links can be characterized by penalties expressed as functions of the flows. For example, each link can be characterized by its transportation cost including cost of investment, capital, maintenance, operation, etc.

¹Multiple sources and sinks may be connected to a node. The net power injection is the total difference between infeeds and loads.

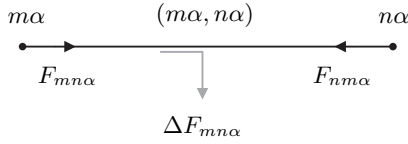


Figure 3.8: General model of a branch $(m\alpha, n\alpha)$ connecting nodes $m\alpha$ and $n\alpha$. Terminal power flows $F_{mn\alpha}$ and $F_{nm\alpha}$, losses $\Delta F_{mn\alpha}$.

Type II

Losses on links can be considered as the difference between input and output power flow (see Figure 3.8):

$$F_{mn} = -F_{nm} + \Delta F_{mn} \quad (3.33)$$

The losses ΔF_{mn} can be derived as functions of the corresponding flows. Losses on an electricity line, for example, can be modeled as quadratic functions of the transmitted power. Pipeline losses can be approximated with cubic functions of the flow [26].

3.4.2 Power Flow Models

In contrast to network flow models, classical steady-state power flow models incorporate constitutional physical laws, such as the relation between electric voltage and current, hydraulic pressure and flow, etc. Since these relations are specific for the individual systems, no general model covering all types of energy flow is available. In the following paragraphs, steady-state power flow models for two of the most common energy infrastructures—AC electricity and pipeline networks—are shortly reviewed based on References [60–64].

AC Electricity Networks

Power flow in an electricity network can be formulated based on nodal power balance and line equations. The power balance at node m in an AC electricity network can be stated according to (3.31). For alternating current, nodal injections and branch flows are complex quantities. Each node m is characterized by four real variables: voltage magnitude $|V_m|$

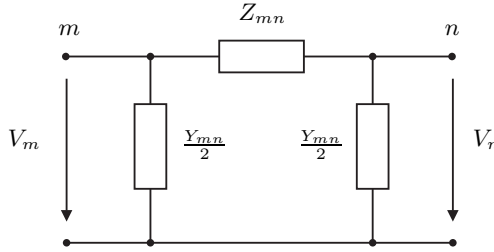


Figure 3.9: Pi-section equivalent of an AC transmission line. Series impedance Z_{mn} , shunt admittance Y_{mn} , nodal voltages V_m and V_n at nodes m and n , respectively.

and phase angle θ_m ,² and net power injections P_m (active) and Q_m (reactive).³ Two of these variables are specified, the remaining two have to be determined. Depending upon which variables are specified and which are unknown, the nodes can be divided into three groups.

- *PQ node*: active and reactive net power injections P_m and Q_m , respectively, are specified, voltage magnitude $|V_m|$ and angle θ_m have to be determined.
- *PV node*: active power injection P_m and voltage magnitude $|V_m|$ are specified, the voltage angle θ_m and the reactive net injection Q_m are unknown.
- *Vθ/slack node*: voltage magnitude $|V_m|$ and angle θ_m are defined, net power injections P_m and Q_m are unknown.

Besides nodal power injection, Equation (3.31) includes also branch flows to other nodes. The complex branch power flows F_{mn} are functions of the complex nodal voltages V_m and V_n , respectively, and parameters of the connecting lines:

$$F_{mn} = \frac{|V_m|^2}{\tilde{Z}_{mn}^*} - \frac{V_m V_n^*}{Z_{mn}^*} \quad (3.34)$$

where

$$\tilde{Z}_{mn} = \left(\frac{1}{Z_{mn}} + \frac{Y_{mn}}{2} \right)^{-1} \quad (3.35)$$

² $V_m = |V_m| e^{j\theta_m}$

³In this notation, the net injection at node m is $F_m = P_m + jQ_m$.

As shown in Figure 3.9, Z_{mn} is the series impedance and Y_{mn} is the shunt admittance of the section's Pi-equivalent, with $Y_{mn}/2$ at each end. The determination of the lumped circuit elements from the distributed line parameters (or the line's geometry and materials, respectively) is outlined in [60]. Active and reactive link flows can be calculated as the real and imaginary parts of the complex flows, respectively. Depending on the purpose of the investigation, certain approximations of (3.34) and (3.35) can be used, e.g., $Y_{mn} \approx 0$ for short overhead lines.

Pipeline Networks

Power flow through a pipeline network can also be described by stating nodal power balance and line equations. The flow balance for an arbitrary node m can be stated as (3.31). This equation includes the net injection F_m and flows to other nodes F_{mn} . Each node is characterized by its nodal pressure p_m and net injection F_m . According to which quantity is specified and which one is to be determined, the nodes can be categorized into:

- *Known-injection node*: the net injection F_m is known, the pressure p_m is to be determined.
- *Known-pressure/slack node*: the nodal pressure p_m is specified, the net injection F_m is unknown.

Flows between nodes can be expressed as functions of the upstream and downstream pressures p_m and p_n , respectively, and properties of the pipeline and the fluid represented by the flow constant k_{mn} :

$$F_{mn} = k_{mn} \delta_{mn} \sqrt{\delta_{mn} (p_m^2 - p_n^2)} \quad (3.36)$$

where

$$\delta_{mn} = \begin{cases} +1 & \text{if } p_m \geq p_n \\ -1 & \text{else} \end{cases} \quad (3.37)$$

Appendix A gives details on the flow constant k_{mn} . The pipeline flow equation (3.36) is generally valid for all types of isothermal pipeline flow (liquid and gaseous). However, a number of modified equations are available delivering more precise results for specific fluids and flow conditions. An additional term accounting for elevation can be included in (3.36), see [61–63].

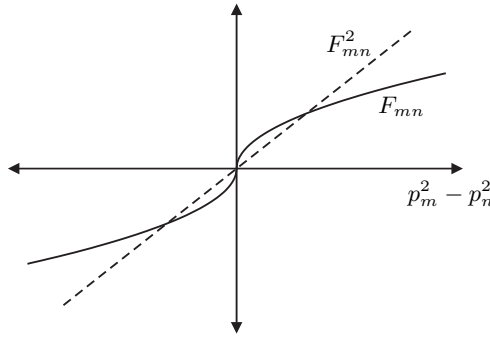


Figure 3.10: Pipeline flow function.

Remark 3.7 Note that (3.36) is a continuous function even if (3.37) is discontinuous (see Figure 3.10). An important but unfavorable characteristic of (3.36) is that the slope of F_{mn} goes to infinity at the origin, since $\lim_{x \rightarrow 0} \frac{d}{dx} \sqrt{x} = \infty$. Besides infinite derivatives, the case $p_m = p_n$ represents a problem, because then $\sqrt{0}$ has to be solved, and computer programs may malfunction. However, using (3.36) for numerical computation, particularly optimization, may cause problems. Therefore it is recommended to use the quadratic form $F_{mn}^2 = k_{mn}^2 (p_m^2 - p_n^2)$, which is constantly sloped. After this equation is solved for F_{mn}^2 , an appropriate function may be used to calculate F_{mn} . Formulations such as $\delta_{mn} = \frac{p_m - p_n}{|p_m - p_n|}$ should be avoided since they may cause divisions by zero if $p_m = p_n$. \diamond

In contrast to electricity networks, where theoretically no active power is necessary to maintain a certain voltage, generation of pressure via compressors or pumps needs power. If the compressor is driven by a gas turbine, the corresponding power consumption can be considered as additional power flowing into the pipeline section, as shown in Figure 3.11. The amount of power consumed by a compressor basically depends on the pressure added to the fluid and the volume flow rate through it. Using the nomenclature of Figure 3.11, the compressor demand can be approximated with

$$F_{\text{com}} = k_{\text{com}} F_{mn} (p_m - p_k) \quad (3.38)$$

where k_{com} is a constant characterizing the compressor unit; p_k and p_m are the suction and discharge pressures, respectively. More advanced

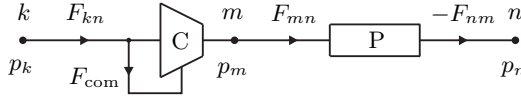


Figure 3.11: Model of a transmission link with compressor (C) and pipeline (P) connecting nodes k and n via m . Nodal pressures p_k , p_m , and p_n , terminal flows F_{kn} and F_{nm} , compressor demand F_{com} , pipeline input F_{mn} .

compressor equations that take into account changing fluid properties are given in [63].

3.5 System of Interconnected Energy Hubs

The equations derived in the preceding sections can be used to model transmission, conversion, and storage of energy in a system of interconnected energy hubs. Figure 3.12 outlines the basic model.

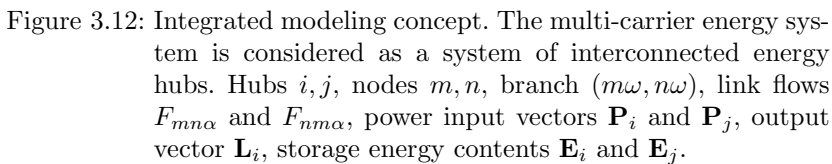
Energy conversion and storage is defined by the converter and storage coupling matrices \mathbf{C}_i and \mathbf{S}_i of all hubs $i \in \mathcal{H}$, respectively. All hub flows are then described according to (3.24):

$$\mathbf{L}_i = \begin{bmatrix} \mathbf{C}_i & -\mathbf{S}_i \end{bmatrix} \begin{bmatrix} \mathbf{P}_i \\ \dot{\mathbf{E}}_i \end{bmatrix} \quad \forall i \in \mathcal{H} \quad (3.39)$$

The network flows are covered by nodal equations such as (3.31) and line equations such as (3.32), (3.33), (3.34), (3.36), and others. Nodal and line equations generally represent a system of nonlinear equations which will be denoted $\mathbf{G}_\alpha(\mathbf{F}_\alpha, \mathbf{P}_i)$ for further investigations. All network flows are then described by

$$\mathbf{G}_\alpha(\mathbf{F}_\alpha, \mathbf{P}_i) = \mathbf{0} \quad \forall \alpha \in \mathcal{E} \quad (3.40)$$

The connection between energy hubs and networks is established by considering hub in- and outputs as nodal injections. Hence, the information how energy hubs are connected with the networks is included in \mathbf{G}_α .



Chapter 4

Optimization

Based on the models presented in the preceding chapter, several integrated optimization problems are formulated in this chapter addressing optimal conversion, storage, and transportation of energy in multi-carrier systems as well as the optimal system structure and layout. Some of the problems correspond in their nature to standard problems known from electrical and chemical process engineering, such as “economic dispatch” (ED), “optimal power flow” (OPF), “hydrothermal scheduling”, and “optimal plant layout” [65–67].

4.1 Problem Outline

Considering systems of interconnected energy hubs as shown in Figure 2.3 raises questions of optimal system structure and operation. With different energy carriers available at the hub inputs and the possibility of internal conversion and storage, the hubs get more flexible in supply. Also the power flows through the interconnecting networks can be controlled with a certain degree of freedom. In the planning phase, the following questions might be of interest:

- To which infrastructures should the hubs be connected?
- Which elements should the hubs contain?

For operating an existing, given structure, questions to be answered are:

- How much of which energy carriers should the hubs consume?
- How should the energy carriers be converted within the hubs?
- How should power flow between the hubs be controlled?

After some general assumptions and definitions are made, possible optimization objectives and general mathematical problem classes are discussed in the next sections. This is the basis for different types of multi-carrier optimization problems addressed in this thesis. Firstly, optimization of the flows through a single energy hub is addressed. We call this problem *multi-carrier optimal dispatch*. Secondly, power flow optimization in a system of interconnected energy hubs is investigated. Since this approach generally covers power demand, conversion, and transmission, it is denoted *multi-carrier optimal power flow* problem. Thirdly, approaches are presented which enable the determination of optimal hub structures defined as *optimal hub coupling* and *optimal hub layout*.

4.2 Assumptions and Definitions

If not mentioned otherwise, the optimization problems are based on the following assumptions and simplifications:

- The loads at the hub outputs are inelastic, i.e., they consume constant power within the considered time period.
- Penalties, such as cost, related to the individual energy carriers and/or system components, are independent of and separable from each other.
- Optimization is generally performed for a single snapshot of the system. An extended approach for multi-period optimization is discussed in Section 4.6.5.
- Storage elements are not included at first, since it is pointless to consider storage operation at a single time instant. The inclusion of storage devices in a multi-period approach is discussed in Section 4.6.5.

- All problems are formulated as minimization problems. Maximization problems can be simply transformed into minimization problems [68]: $\max_x f(x) = -\min_x -f(x)$.

Throughout this thesis, \mathcal{F} generally refers to a scalar-valued objective function.

4.3 Optimization Objectives

There are a number of reasonable objectives that can be used for optimizing energy systems. This work mainly focuses on minimization of operational energy cost and gaseous emissions.

4.3.1 Energy Cost

Energy cost is probably the most common criterion employed in the operational optimization of energy systems. The classical approach for optimal dispatch of thermal units, for example, targets minimal fuel cost for the plants, which are modeled as quadratic functions of the plants' power outputs [65]. The cost of energy consumed at a certain node in a network can be modeled in a similar way, although they involve certain transmission-related premiums besides generation cost [69]. In this work, the cost of energy are generally stated as polynomial functions of the average power provided by the source during a unit of time.

4.3.2 Emissions

Besides cost, minimization of gaseous plant emissions accruing in the operation of energy systems is a reasonable objective. Analog to economic dispatch and optimal power flow, "minimum emission dispatch" [70] and "minimum emission power flow" [71] have been developed. Emission models and typical numbers, in particular for thermal power plants, are collected in [72,73]. The common approach is to model gaseous emissions as polynomial or exponential functions of the source's power output.

4.3.3 Composite Objectives

Optimization with multiple objectives can be performed by stating a composite objective function as a weighted linear combination of individual objectives. An example for bi-objective optimization is “economic-environmental dispatch” [74] of electricity generators. An overview of multi-criteria optimization approaches applied to energy planning is provided by [75].

4.3.4 Marginal Objectives

When optimization is performed, the sensitivity of the objective function with respect to the optimization candidates is of interest. When energy cost is minimized, this sensitivity is commonly denoted “incremental cost” or “marginal cost” [65, 76, 77]. For a general objective reflected by a function \mathcal{F} , the marginal objective can be calculated as the partial derivative of the objective function with respect to the optimization variable:

$$\frac{\partial \mathcal{F}}{\partial x_i} \quad (4.1)$$

where x_i is an optimization variable. Accordingly, it will be referred to as marginal cost, marginal emissions, etc. throughout this thesis.

If x_i is the quantity exchanged at node i of a network and \mathcal{F} reflects the related cost, then the derivative in (4.1) is commonly termed “bus incremental cost” or “locational marginal cost” (LMC) at node i .

4.4 Mathematical Problem Formulation

In the following, different classes of mathematical optimization problems are shortly reviewed based on References [66, 68, 78]. The general problem structures will then be used for formulating applied problems related to multi-carrier energy systems.

In this thesis, optimization problems generally aim at minimizing a nonlinear objective function while fulfilling various nonlinear constraints. Thus, nonlinear constrained optimization is the basic mathematical issue to be addressed.

4.4.1 Continuous Nonlinear Problems

Nonlinear programming (NLP) problems with continuous optimization variables $x_i \in \mathbb{R}$ are mathematically stated in the following way:

$$\text{Minimize } \mathcal{F}(\mathbf{x}) \quad (4.2a)$$

$$\text{subject to } \mathbf{g}(\mathbf{x}) = \mathbf{0} \quad (4.2b)$$

$$\mathbf{h}(\mathbf{x}) \leq \mathbf{0} \quad (4.2c)$$

where

- $\mathbf{x} \in \mathbb{R}^u$ is the $u \times 1$ vector of continuous optimization variables;
- $\mathcal{F}(\mathbf{x}) : \mathbb{R}^u \mapsto \mathbb{R}$ is a scalar-valued objective function;
- $\mathbf{g}(\mathbf{x}) : \mathbb{R}^u \mapsto \mathbb{R}^v$ is the $v \times 1$ vector of equality constraints;
- $\mathbf{h}(\mathbf{x}) : \mathbb{R}^u \mapsto \mathbb{R}^w$ is the $w \times 1$ vector if inequality constraints.

A typical power system application of continuous NLP is economic dispatch of thermal power plants [65]. For this problem, the objective function in (4.2a) reflects the cost of the generators in the system (commonly modeled as quadratic polynomials of the power outputs). Conservation of power results in an equality constraint (4.2b); power limitations of the generators are covered by an inequality constraint of the form (4.2c).

4.4.2 Mixed-Integer Nonlinear Problems

Besides continuous variables $x_i \in \mathbb{R}$, mixed-integer nonlinear programming (MINLP) problems include also integer variables $y_i \in \mathbb{I}$, where $\mathbb{I} = \{0, 1, 2, \dots\}$ is the set of non-negative integers. Similar to (4.2), the problem is formulated as:

$$\text{Minimize } \mathcal{F}(\mathbf{x}, \mathbf{y}) \quad (4.3a)$$

$$\text{subject to } \mathbf{g}(\mathbf{x}, \mathbf{y}) = \mathbf{0} \quad (4.3b)$$

$$\mathbf{h}(\mathbf{x}, \mathbf{y}) \leq \mathbf{0} \quad (4.3c)$$

where

- $\mathbf{x} \in \mathbb{R}^{u_{\mathbb{R}}}$ is the $u_{\mathbb{R}} \times 1$ vector of continuous optimization variables;

- $\mathbf{y} \in \mathbb{I}^{u_i}$ is the $u_i \times 1$ vector of integer optimization variables;
- $\mathcal{F}(\mathbf{x}, \mathbf{y}) : \{\mathbb{R}^{u_R}, \mathbb{I}^{u_i}\} \mapsto \mathbb{R}$ is a scalar-valued objective function;
- $\mathbf{g}(\mathbf{x}, \mathbf{y}) : \{\mathbb{R}^{u_R}, \mathbb{I}^{u_i}\} \mapsto \mathbb{R}^v$ is the $v \times 1$ vector of equality constraints;
- $\mathbf{h}(\mathbf{x}, \mathbf{y}) : \{\mathbb{R}^{u_R}, \mathbb{I}^{u_i}\} \mapsto \mathbb{R}^w$ is the $w \times 1$ vector if inequality constraints.

Unit commitment (UC) problems are common MINLP problems in the area of power system optimization [65]. From a mathematical point of view, the basic difference between UC and ED is that UC involves on/off-type variables besides continuous quantities.

4.4.3 Multi-Period Problems

Considering not only a single snapshot of the system but multiple time periods $t \in \{1, 2, \dots, N_t\}$ results in multi-period (MP) optimization problems, which can be continuous or mixed-integer problems. However, in the continuous case, multi-period problems are generally stated as:

$$\text{Minimize} \quad \sum_{t=1}^{N_t} \mathcal{F}^t(\mathbf{x}) \quad (4.4a)$$

$$\text{subject to} \quad \mathbf{g}^t(\mathbf{x}) = \mathbf{0} \quad \forall t \quad (4.4b)$$

$$\mathbf{h}^t(\mathbf{x}) \leq \mathbf{0} \quad \forall t \quad (4.4c)$$

where

- $\mathbf{x} \in \mathbb{R}^{(N_t \cdot u)}$ is the $(N_t \cdot u) \times 1$ vector of continuous optimization variables, i.e., the total number of variables is $N_t \cdot u$;
- $t \in \{1, 2, \dots, N_t\}$ is the time period;
- $\mathcal{F}^t(\mathbf{x}) : \mathbb{R}^{(N_t \cdot u)} \mapsto \mathbb{R}$ is a scalar-valued objective function reflecting the penalty for time period t ;
- $\mathbf{g}^t(\mathbf{x}) : \mathbb{R}^{(N_t \cdot u)} \mapsto \mathbb{R}^v$ is the $v \times 1$ vector of equality constraints at period t ;
- $\mathbf{h}^t(\mathbf{x}) : \mathbb{R}^{(N_t \cdot u)} \mapsto \mathbb{R}^w$ is the $w \times 1$ vector if inequality constraints at period t .

Note that MP formulations allow to consider couplings between different time periods. For example, the change of a certain quantity between two time periods can be limited and/or penalized. This is commonly done when introducing e.g. power ramping limits and/or minimum up-/down-times of thermal units [79].

A classical application of MP optimization is the hydrothermal scheduling problem [65]. Other typical applications in the field of power systems are model predictive control applications and multi-period auctioning in electricity markets [80, 81].

4.5 Multi-Carrier Optimal Dispatch

In this section, an optimization problem related to the power flows through a single energy hub is stated and discussed. Verbally, the problem is defined as follows.

Definition 1 *Multi-carrier optimal dispatch* is the determination of an optimal operation policy for a number of converter units processing multiple energy carriers. \diamond

The converters processing multiple energy carriers are considered as an energy hub, which is characterized by a coupling matrix \mathbf{C} . For specified hub loads \mathbf{L} , the optimal input power vector \mathbf{P} and dispatch factors $\nu_{\alpha k}$ can be determined according to a certain objective.

4.5.1 Objective

Considering a single energy hub, the objectives discussed in Section 4.3 may depend on the input powers as well as on the hub-internal power dispatch on the individual elements. Therefore the objective function is stated as a function of the input power vector \mathbf{P} and the dispatch factors $\nu_{\alpha k}$.

4.5.2 Constraints

The feasible region of the optimization problem is defined by different constraints. An equality constraint is given by the equation which describes the power flow through the hub (3.3). Inequalities arise from

limitations of the hub's input power vector \mathbf{P} and the power inputs to the individual converters $P_{\alpha k}$. Lower and upper limits of \mathbf{P} and $P_{\alpha k}$ are defined in vectors $\underline{\mathbf{P}}$, $\overline{\mathbf{P}}$, $\underline{P}_{\alpha k}$, and $\overline{P}_{\alpha k}$, respectively. Limitation of the dispatch factors $\nu_{\alpha k}$ by zero and one has to be regarded as well.

4.5.3 Problem Statement

According to the general form (4.2), multi-carrier optimal dispatch is formulated in the following way:

$$\text{Minimize } \mathcal{F}(\mathbf{P}, \nu_{\alpha k}) \quad (4.5a)$$

$$\text{subject to } \mathbf{L} - \mathbf{C}\mathbf{P} = \mathbf{0} \quad (4.5b)$$

$$\underline{\mathbf{P}} \leq \mathbf{P} \leq \overline{\mathbf{P}} \quad (4.5c)$$

$$\underline{P}_{\alpha k} \leq \nu_{\alpha k} P_{\alpha} \leq \overline{P}_{\alpha k} \quad \forall \alpha \in \mathcal{E}, \forall k \in \mathcal{C}_{\alpha} \quad (4.5d)$$

$$0 \leq \nu_{\alpha k} \leq 1 \quad \forall \alpha \in \mathcal{E}, \forall k \in \mathcal{C}_{\alpha} \quad (4.5e)$$

Remark 4.1 Note that the constraints (4.5c)–(4.5e) can be written in the form (4.2c):

$$\underline{h} \leq h(x) \leq \overline{h} \quad \Leftrightarrow \quad \begin{cases} h(x) - \overline{h} \leq 0 \\ \underline{h} - h(x) \leq 0 \end{cases} \quad (4.6)$$

where h is a function of the optimization variable x . This form is more suitable when investigating the Lagrange function and optimality conditions. \diamond

Remark 4.2 The requirement (3.8) does not have to be included in (4.5) explicitly if one of the dispatch factors is expressed by the others, which is generally assumed: $\nu_{\alpha h} = 1 - \sum_{k \in \mathcal{C}_{\alpha} \setminus h} \nu_{\alpha k}$. \diamond

4.5.4 Type of Problem and Solution

In general, the problem (4.5) represents a nonlinear constrained optimization problem [68]. With nonlinear constraints (4.5b)–(4.5d), the solution space is not convex, thus finding the global optimum cannot be ensured by using numerical methods.

Using a convex objective function (4.5a) and linear(ized) constraints (4.5b)–(4.5d) yields a convex solution space, and the global optimum

can be determined using numerical methods. This latter case should be discussed more extensively in the following section.

4.5.5 Convex Case

We now consider optimal dispatch of an energy hub characterized by a constant coupling matrix \mathbf{C} , what results in a linear transformation of power, thus a linear constraint (4.5b). Accordingly, we denote such a hub *linear energy hub*. Furthermore, we assume the objective function \mathcal{F} in (4.5a) to be convex. Under these conditions, (4.5e) can be ignored because the dispatch factors $\nu_{\alpha k}$ are constant and predefined. Also (4.5d) drops out since it is redundantly covered by (4.5c). The remaining equations (4.5a), (4.5b), and (4.5c) form a problem with convex solution space.

For this type of problem, optimality conditions due to Karush, Kuhn, and Tucker (KKT) are both necessary and sufficient for a global solution point [68,78]. The derivation of these conditions for convex multi-carrier optimal dispatch is given in Appendix B.1. As a result, a general optimality condition for linear hubs can be written as

$$\mathbf{\Psi} = \mathbf{\Lambda} \mathbf{C} \quad (4.7)$$

where $\mathbf{\Psi}$ and $\mathbf{\Lambda}$ are vectors that contain the marginal objectives at the input and the output side of the hub, respectively. Accordingly, we denote

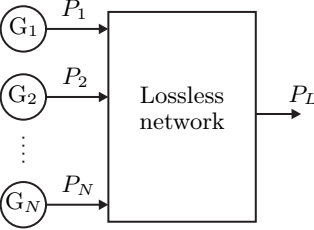
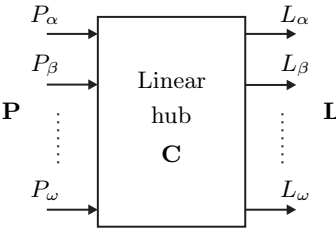
- $\mathbf{\Psi}$ the vector of *system marginal objectives* and
- $\mathbf{\Lambda}$ the vector of *hub marginal objectives*.

\mathbf{C} is the constant coupling matrix of the hub as defined in (3.3).

Equations (3.3) and (4.7) show that conversion of power in an energy hub results in a conversion of marginal cost. If the input power is just passed through the hub without being changed, then the coupling is described by a unity matrix. In this case power as well as marginal costs are equal on all sides of the hub. If conversion takes place in the hub, then the coupling matrix differs from a unity matrix, and power as well as marginal costs are related in a similar way:

$$\begin{aligned} \text{no conversion: } \mathbf{L} &= \mathbf{P} & \Leftrightarrow \mathbf{\Psi} &= \mathbf{\Lambda} \\ \text{conversion: } \mathbf{L} &= \mathbf{C} \mathbf{P} & \Leftrightarrow \mathbf{\Psi} &= \mathbf{\Lambda} \mathbf{C} \end{aligned} \quad (4.8)$$

Table 4.1: Electricity and Multi-Carrier Optimal Dispatch.

Electricity optimal dispatch	Multi-carrier optimal dispatch
 <p>Constraint:</p> $P_1 + P_2 + \dots + P_N = P_L$ <p>Optimality condition:</p> $\lambda_1 = \lambda_2 = \dots = \lambda_N = \lambda_L$	 <p>Constraint:</p> $\mathbf{L} = \mathbf{C} \mathbf{P}$ <p>Optimality condition:</p> $\mathbf{\Psi} = \mathbf{\Lambda} \mathbf{C}$

Similar to the well-known economic dispatch rule for generators in an electrical system, the “equal incremental cost” rule [60, 65], Equation (4.7) represents a general condition for optimally dispatching the supply of linear energy hubs. Table 4.1 compares the classical approach for electricity with the multi-carrier approach. In the simplest case, only conservation of power has to be regarded as a constraint. The resulting optimality condition concerns the marginal cost of generators $(\lambda_1, \lambda_2, \dots, \lambda_N)$, or, in the multi-carrier approach, the marginal cost of the energy carriers at the hub inputs and outputs ($\mathbf{\Psi}$ and $\mathbf{\Lambda}$, respectively).

Equation (4.7) represents also a new principle for optimally dispatching co- and trigeneration systems. In contrast to other models such as presented in [82], (4.7) provides a general marginal cost based optimization rule which can be applied to any converter configuration described by $\mathbf{L} = \mathbf{C} \mathbf{P}$, independent of technological details. However, restrictions arising from technological characteristics can be considered if wanted. The application of the dispatch rule (4.7) for determining the optimal operation of a cogeneration plant is demonstrated in Section 5.1.1.

4.6 Multi-Carrier Optimal Power Flow

In this section optimization of energy flows in a system of interconnected energy hubs is investigated. Since the problem covers power transmission and conversion, it comes down to an optimal power flow problem. Carpentier defined electricity optimal power flow as “the determination of the complete state of a power system corresponding to the best operation within security constraints” [14]. This definition is slightly modified for the multi-carrier case.

Definition 2 *Multi-carrier optimal power flow* is the determination of an optimal operating policy of an energy system and its complete state, including transmission and conversion of multiple energy carriers within security constraints. \diamond

The energy system is characterized by the hubs’ coupling matrices \mathbf{C}_i and network parameters and topologies. For specified hub loads \mathbf{L}_i , the optimal hub inputs \mathbf{P}_i , dispatch factors $\nu_{i\alpha k}$, and network power flows \mathbf{F}_α can be determined. Here i indicates the hub, α the energy carrier, and k the converter, respectively.

Mathematically, multi-carrier optimal power flow is stated as a nonlinear constrained optimization problem according to the general form (4.2). Therefore an objective and constraint functions have to be formulated.

4.6.1 Objective

Considering a system of interconnected energy hubs, an objective function as discussed in Section 4.3 may depend the consumption of the energy hubs \mathbf{P}_i , the dispatch factors $\nu_{i\alpha k}$, and the network flows \mathbf{F}_α , where $i \in \mathcal{H}$, $\alpha \in \mathcal{E}$, and $k \in \mathcal{C}_{i\alpha}$.

4.6.2 Constraints

The feasible region of the optimization problem is defined by a number of constraint functions. Equality constraints are given by the power flow equations of the hubs (3.39) and the networks (3.40). Inequality constraints arise from power limitations of the hub inputs \mathbf{P}_i and network flows \mathbf{F}_α . The corresponding lower and upper limits are defined in

vectors $\underline{\mathbf{P}}_i$, $\overline{\mathbf{P}}_i$, $\underline{\mathbf{F}}_\alpha$, and $\overline{\mathbf{F}}_\alpha$, respectively. Not only the hub inputs but also the individual converter inputs $P_{i\alpha k}$ can be limited (i indicates the hub, α the energy carrier, and k the converter, respectively). Lower and upper limits of $P_{i\alpha k}$ are defined as $\underline{P}_{i\alpha k}$ and $\overline{P}_{i\alpha k}$, respectively. Finally it has to be regarded that all dispatch factors $\nu_{i\alpha k}$ are limited by zero and one.

Other restrictions specific for certain system components are not considered in the following general problem statement, but can be included in a straightforward manner. Examples of further constraints which are commonly taken into account are

- voltage and pressure limits,
- real and reactive power limits of generators, and
- compression ratio and flow limits of gas compressors.

Such limits are considered in the example in Section 5.2.

4.6.3 Problem Statement

The multi-carrier optimal power flow problem is formulated according to the general NLP structure (4.2):

$$\text{Minimize } \mathcal{F}(\mathbf{P}_i, \nu_{i\alpha k}, \mathbf{F}_\alpha) \quad (4.9a)$$

$$\text{subject to } \mathbf{L}_i - \mathbf{C}_i \mathbf{P}_i = \mathbf{0} \quad \forall i \in \mathcal{H} \quad (4.9b)$$

$$\mathbf{G}_\alpha = \mathbf{0} \quad \forall \alpha \in \mathcal{E} \quad (4.9c)$$

$$\underline{\mathbf{P}}_i \leq \mathbf{P}_i \leq \overline{\mathbf{P}}_i \quad \forall i \in \mathcal{H} \quad (4.9d)$$

$$\underline{\mathbf{F}}_\alpha \leq \mathbf{F}_\alpha \leq \overline{\mathbf{F}}_\alpha \quad \forall \alpha \in \mathcal{E} \quad (4.9e)$$

$$\underline{P}_{i\alpha k} \leq \nu_{i\alpha k} P_{i\alpha} \leq \overline{P}_{i\alpha k} \quad \forall i \in \mathcal{H}, \forall \alpha \in \mathcal{E}, \forall k \in \mathcal{C}_{i\alpha} \quad (4.9f)$$

$$0 \leq \nu_{i\alpha k} \leq 1 \quad \forall i \in \mathcal{H}, \forall \alpha \in \mathcal{E}, \forall k \in \mathcal{C}_{i\alpha} \quad (4.9g)$$

Note that the remarks from Section 4.5.3 apply here as well.

4.6.4 Type of Problem and Solution

In general, the problem (4.9) represents a nonlinear constrained optimization problem. The solvability of this problem depends on the actual

system description used. When the objective function is convex and all constraints are expressed as linear equations, then the solution space is convex and the global optimum can be determined using numerical methods. In this case, the KKT optimality conditions apply, which are derived in Appendix B.2.

With a concave objective function and/or nonlinear constraints such as (3.34), the solution space is no longer convex [83]. Numerical methods can be used in this case as well, but it cannot be ensured that the global optimum is achieved.

When an overall penalty such as total energy cost is minimized, the resulting marginal objectives related to the optimization variables are of interest. Considering not only a single hub but a system of interconnected energy hubs, we end up with different marginal objective vectors Ψ_i and Λ_i at different hubs i . Then Ψ_i is a vector of locational marginal objectives (e.g., locational marginal prices), i.e., marginal objectives related to the nodes which connect hub i with the networks [69]. The vector Λ_i contains hub marginal objectives related to the outputs of hub i .

In Section 5.2, the multi-carrier optimal power flow approach is applied to a system of three energy hubs interconnected by electricity and natural gas networks.

4.6.5 Inclusion of Storage

It was mentioned before that investigating optimal storage utilization requires to consider multiple time periods. Multi-period multi-carrier optimal dispatch and power flow can be stated based on the problem definitions (4.5) and (4.9), respectively, which can be extended to multi-period approaches according to (4.4). Besides the multi-period extension, a few other modifications have to be carried out in order to account for characteristics of the storage elements. The storage elements are modeled as outlined in Section 3.3.

When storage elements are present in the system, the objective function may also depend on the stored energies \mathbf{E}_i^t , where i indicates the hub, and t denotes the time period. Equivalent storage power flow vectors \mathbf{M}_i^{eq} have to be considered in the hub flow equations, as done in (3.20). Standby losses can be included in this equation as additional energy to

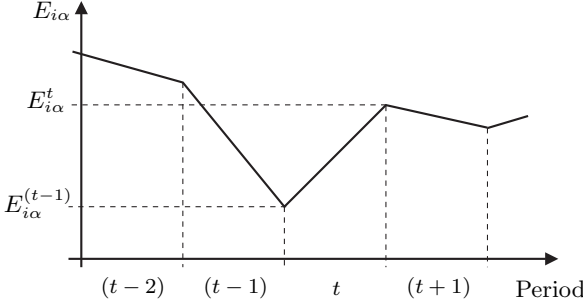


Figure 4.1: Storage energy $E_{i\alpha}$ at different time periods. $E_{i\alpha}^t$ refers to the energy stored at the end of period t .

be recharged in each period:

$$\mathbf{M}_i^{\text{eq } t} = \mathbf{S}_i^t \dot{\mathbf{E}}_i^t = \mathbf{S}^t \left[\mathbf{E}_i^t - \mathbf{E}_i^{(t-1)} + \mathbf{E}_i^{\text{stb}} \right] \quad (4.10)$$

As indicated in Figure 4.1, the vector \mathbf{E}_i^t denotes the stored energies at the end of period t ; $\mathbf{E}_i^{\text{stb}}$ represents the standby energy losses per period in hub i .

Besides that, additional inequality constraints have to be included in order to account for power and energy limits. Minimal and maximal storage powers have to be regarded. For the sake of simplicity, it is assumed that only one storage element is available in the hub for each energy carrier, which can be connected at any side of the hub. At the input side, where the energy carriers $\rho \in \mathcal{E}$ are stored, lower and upper limits $\underline{Q}_{i\rho}$ and $\overline{Q}_{i\rho}$ have to be regarded, respectively. At the output side of the hub, where the energy carriers $\sigma \in \mathcal{E}$ are stored, the corresponding limits $\underline{M}_{i\sigma}$ and $\overline{M}_{i\sigma}$ apply. The power limits corresponds to energy ramping limits, since they determine how much the storage energy can change within one period. Besides power (or energy ramping), the storage energies have to be limited. The limits are stated in vectors $\underline{\mathbf{E}}_i$ and $\overline{\mathbf{E}}_i$. In order to obtain sustainable storage utilization, the storage contents at the end of the last period $\mathbf{E}_i^{N_t}$ should be equal to the contents before the first period, which is denoted \mathbf{E}_i^0 .¹

¹This is an intuitive assumption which could be reconsidered against the background of a liberalized market environment. Under certain circumstances, it could be reasonable to exploit the storage more or less, ending up with lower or higher storage energy at the end of the last period.

With these extensions, multi-period multi-carrier optimal power flow can be stated as follows:

$$\text{Minimize } \mathcal{F} = \sum_{t=1}^{N_t} \mathcal{F}^t(\mathbf{P}_i^t, \nu_{i\alpha k}^t, \mathbf{E}_i^t, \mathbf{F}_\alpha^t) \quad (4.11a)$$

$$\text{subject to } \mathbf{L}_i^t - \mathbf{C}_i^t \mathbf{P}_i^t + \mathbf{M}_i^{\text{eq}t} = \mathbf{0} \quad \forall t, \forall i \quad (4.11b)$$

$$\mathbf{G}_\alpha^t = \mathbf{0} \quad \forall t, \forall \alpha \quad (4.11c)$$

$$\underline{\mathbf{P}}_i \leq \mathbf{P}_i^t \leq \overline{\mathbf{P}}_i \quad \forall t, \forall i \quad (4.11d)$$

$$\underline{Q}_{i\rho} \leq Q_{i\rho}^t \leq \overline{Q}_{i\rho} \quad \forall t, \forall i, \forall \rho \quad (4.11e)$$

$$\underline{M}_{i\sigma} \leq M_{i\sigma}^t \leq \overline{M}_{i\sigma} \quad \forall t, \forall i, \forall \sigma \quad (4.11f)$$

$$\underline{\mathbf{E}}_i \leq \mathbf{E}_i^t \leq \overline{\mathbf{E}}_i \quad \forall t, \forall i \quad (4.11g)$$

$$\mathbf{E}_i^0 - \mathbf{E}_i^{N_t} = \mathbf{0} \quad \forall i \quad (4.11h)$$

$$\underline{\mathbf{F}}_\alpha \leq \mathbf{F}_\alpha^t \leq \overline{\mathbf{F}}_\alpha \quad \forall t, \forall \alpha \quad (4.11i)$$

$$\underline{P}_{i\alpha k} \leq \nu_{i\alpha k}^t P_{i\alpha}^t \leq \overline{P}_{i\alpha k} \quad \forall t, \forall i, \forall \alpha, \forall k \quad (4.11j)$$

$$0 \leq \nu_{i\alpha k}^t \leq 1 \quad \forall t, \forall i, \forall \alpha, \forall k \quad (4.11k)$$

where $t \in \{1, 2, \dots, N_t\}$; $i \in \mathcal{H}$; $\alpha, \beta \in \mathcal{E}$; $k \in \mathcal{C}_{i\alpha}$. Energy carriers $\rho \in \mathcal{E}$ are stored at the input side of the hub, the carriers $\sigma \in \mathcal{E}$, $\sigma \neq \rho$ are stored at the output side.

Remark 4.3 The constraint (4.11h) may be relieved in order to allow exploiting stored energy. A reasonable problem formulation would then penalize the energy mismatch between $\mathbf{E}_i^{N_t}$ and \mathbf{E}_i^0 . \diamond

Remark 4.4 Removing the network flows \mathbf{F}_α^t from (4.11a) and neglecting (4.11c), (4.11i), and the index i in (4.11) yields the corresponding optimal dispatch approach [84], which is not discussed explicitly. \diamond

4.7 Optimal Hub Coupling

In this section, a rather theoretical approach is developed for determining the optimal coupling matrix of energy hubs. In contrast to the operational optimization problems discussed in the preceding sections, the structure of the hubs, i.e., their coupling matrices, are now subject to optimization. Even if the approach can and will be applied to systems of interconnected energy hubs, it concerns only the structure of the

hubs, not of the networks connecting the hubs. Parameters and topologies of the networks are assumed to be given. The problem is verbally defined as follows.

Definition 3 *Optimal hub coupling* is the determination of optimal coupling matrices describing the conversion of multiple energy carriers in energy hubs. \diamond

Mathematically, the problem is stated as a nonlinear constrained optimization problem according to the general form (4.2). The problem can be formulated for a single energy hub or for a system of multiple, interconnected energy hubs.

4.7.1 Single Energy Hub

Consider a single energy hub with power in- and outputs \mathbf{L} and \mathbf{P} , respectively. For given loads \mathbf{L} , both the optimal input \mathbf{P} as well as the optimal coupling matrix \mathbf{C} can be determined.

For this problem, an objective function may be stated that includes the power supply of the hub \mathbf{P} . Besides that, certain criteria which include characteristics of the coupling matrix \mathbf{C} could be included in the objective function in order to account for desired technological features of the coupling. The objective function is thus a function of the hub's power input \mathbf{P} and the coupling matrix \mathbf{C} .

The problem is constrained by the hub flow equation (3.3) and limitations of the input \mathbf{P} , specified in vectors $\underline{\mathbf{P}}$ and $\overline{\mathbf{P}}$. Additional inequalities are given by the characteristics of the coupling matrix (3.4) and (3.5).

Finally, the problem is mathematically stated according to the general NLP structure (4.2):

$$\text{Minimize } \mathcal{F}(\mathbf{P}, \mathbf{C}) \quad (4.12a)$$

$$\text{subject to } \mathbf{L} - \mathbf{C}\mathbf{P} = \mathbf{0} \quad (4.12b)$$

$$\underline{\mathbf{P}} \leq \mathbf{P} \leq \overline{\mathbf{P}} \quad (4.12c)$$

$$0 \leq c_{\alpha\beta} \leq 1 \quad \forall \alpha \in \mathcal{E}, \forall \beta \in \mathcal{E} \quad (4.12d)$$

$$0 \leq \sum_{\beta \in \mathcal{E}} c_{\alpha\beta} \leq 1 \quad \forall \alpha \in \mathcal{E} \quad (4.12e)$$

The problem (4.12) represents a nonlinear constrained optimization problem. The constraint (4.12b) contains the product of the optimization variables \mathbf{C} and \mathbf{P} , therefore it represents a nonlinear constraint, and convexity of the feasible region cannot be guaranteed. NLP techniques can be employed to find at least a local solution, but again it cannot be ensured that the global optimum is reached. Two major complications can be expected when using numerical solvers:

1. The problem may have an infinite number of (equally optimal) solutions, whereas not all of them are technically reasonable.
2. The obtained solution may depend on the starting point (initial values) given to the solver.

A simple ad hoc solution to overcome the problem of infinite solutions is to include a proper term related to the coupling matrix in the objective function. The second problem can be eliminated by starting the optimization routine at technically reasonable values, what includes the risk that unexpected, unconventional solutions may remain undiscovered. The following example should demonstrate these problems.

Example 4.1 Consider a three-dimensional load vector which contains electricity, gas, and heat load powers, respectively:

$$\mathbf{L} = \begin{bmatrix} 1 & 1 & 1 \end{bmatrix}^T \text{ pu} \quad (4.13)$$

The loads are supplied by three corresponding infrastructures, which connect the loads via an energy hub. The optimal coupling matrix \mathbf{C} and power input \mathbf{P} of the hub can be determined. The objective function to be minimized is stated as the sum of the squared input powers. According to (4.12), the problem is formulated as follows:

$$\text{Minimize } P_e^2 + P_g^2 + P_h^2 \quad (4.14a)$$

$$\text{subject to } \mathbf{L} - \mathbf{C} \mathbf{P} = \mathbf{0} \quad (4.14b)$$

$$\mathbf{P} \geq \mathbf{0} \quad (4.14c)$$

$$0 \leq c_{\alpha\beta} \leq 1 \quad \alpha, \beta = e, g, h \quad (4.14d)$$

$$0 \leq \sum_{\beta=e,g,h} c_{\alpha\beta} \leq 1 \quad \alpha = e, g, h \quad (4.14e)$$

The optimal input yielding a minimal objective is evident:

$$\mathbf{P} = \begin{bmatrix} P_e & P_g & P_h \end{bmatrix}^T = \begin{bmatrix} 1 & 1 & 1 \end{bmatrix}^T \text{ pu} \quad (4.15)$$

It can be achieved with different coupling matrices \mathbf{C} , for example:

$$\begin{bmatrix} 1 & 0 & 0 \\ 0 & 1 & 0 \\ 0 & 0 & 1 \end{bmatrix}; \begin{bmatrix} 0 & 0 & 1 \\ 0 & 1 & 0 \\ 1 & 0 & 0 \end{bmatrix}; \frac{1}{3} \begin{bmatrix} 1 & 1 & 1 \\ 1 & 1 & 1 \\ 1 & 1 & 1 \end{bmatrix}; \frac{1}{2} \begin{bmatrix} 0 & 1 & 1 \\ 1 & 0 & 1 \\ 1 & 1 & 0 \end{bmatrix} \quad (4.16)$$

All matrices result in the same optimum, and there is an infinite number of other optimal solutions for \mathbf{C} . However, in this case the coupling described by the very left matrix is possibly the most reasonable one to implement, since it corresponds to directly connecting inputs and outputs. Realization of the second matrix for instance would require a thermal-electrical conversion which is usually less efficient and more expensive than a transmission line. The fourth matrix establishes the coupling without any direct connections, all input powers are converted into other forms. \diamond

A more extensive application example of this approach is presented in Section 5.4.1.

4.7.2 System of Interconnected Energy Hubs

Optimal coupling matrices can also be determined for multiple energy hubs interconnected by different energy infrastructures. For given loads \mathbf{L}_i , both the optimal inputs \mathbf{P}_i as well as the optimal coupling matrices \mathbf{C}_i can be determined, where $i \in \mathcal{H}$.

For this problem, an objective function may be stated that includes the supply of the hubs \mathbf{P}_i , the coupling matrices \mathbf{C}_i , and the network flows \mathbf{F}_α .

Similar to (4.12), the problem is constrained by the hub flow equations (3.39); also the network flow equations (3.40) have to be included. Hub input limitations specified in vectors $\underline{\mathbf{P}}_i$ and $\overline{\mathbf{P}}_i$ as well as link flow limits defined in $\underline{\mathbf{F}}_\alpha$ and $\overline{\mathbf{F}}_\alpha$ represent inequality constraints. Characteristics of the coupling matrices (3.4) and (3.5) have to be regarded for all hubs.

Mathematically, the problem is formulated in the following way:

$$\text{Minimize } \mathcal{F}(\mathbf{P}_i, \mathbf{C}_i, \mathbf{F}_\alpha) \quad (4.17a)$$

$$\text{subject to } \mathbf{L}_i - \mathbf{C}_i \mathbf{P}_i = \mathbf{0} \quad \forall i \in \mathcal{H} \quad (4.17b)$$

$$\mathbf{G}_\alpha = \mathbf{0} \quad \forall \alpha \in \mathcal{E} \quad (4.17c)$$

$$\underline{\mathbf{P}}_i \leq \mathbf{P}_i \leq \overline{\mathbf{P}}_i \quad \forall i \in \mathcal{H} \quad (4.17d)$$

$$\underline{\mathbf{F}}_\alpha \leq \mathbf{F}_\alpha \leq \overline{\mathbf{F}}_\alpha \quad \forall \alpha \in \mathcal{E} \quad (4.17e)$$

$$0 \leq \sum_{\beta \in \mathcal{E}} c_{i\alpha\beta} \leq 1 \quad \forall i \in \mathcal{H}, \forall \alpha \in \mathcal{E} \quad (4.17f)$$

$$0 \leq c_{i\alpha\beta} \leq 1 \quad \forall i \in \mathcal{H}, \forall \alpha \in \mathcal{E}, \forall \beta \in \mathcal{E} \quad (4.17g)$$

Similar to (4.12), the problem (4.17) generally represents a nonlinear and nonconvex constrained optimization problem. However, due to additional nonlinear constraints (4.17c), the discussed issues might even be more severe.

In Section 5.4.2, this approach is applied to a system of two energy hubs interconnected by electricity and natural gas networks.

4.8 Optimal Hub Layout

In contrast to the previous section, where mathematical optima are determined, this section investigates the structural problem in a more practical manner.

When designing energy hubs, a limited number of hub elements (converters and storage devices) are available, which may show different technical, environmental, and economic characteristics. Different combinations of the available elements will result in different hub characteristics. In order to obtain the desired performance, optimization can be employed; the corresponding problem is defined as follows.²

Definition 4 *Optimal hub layout* is the selection of elements to be placed in an energy hub from a given set of converter and storage elements in order to achieve best overall performance. \diamond

²A similar problem is known in process/manufacturing industry—the “optimal plant layout” problem. Reference [67] defines an optimal plant layout as “the arrangement of machinery and flow of materials from one facility to another, which minimizes material-handling costs while considering any physical restrictions on such arrangements.”

All elements from a given set of converter and storage devices can be characterized consistently by technical, environmental, and economic parameters, for example power and energy ratings, energy efficiencies, standby losses, emissions, operation cost, maintenance cost, and installation cost. The performance of the hub may depend not only on the elements but also on the situation outside of the hub, i.e., the supplying infrastructures and the loads. For example, certain elements will perform well in low load situations, while others may be advantageous when the loads are high. The supply infrastructures may be characterized by (time-dependent) energy prices and availability, which is another aspect to consider. For example, utilization of a certain element may be profitable as long as electricity is cheaper than natural gas. Another example which may influence the value of a converter or storage element significantly is the possibility of selling power to the grids. Also the combination of elements is important. Certain devices may perform well only when they are used together with others. For example, operation of an electricity-controlled CHP device may require a thermal storage when no heat is needed at the same time.

These considerations yield the conclusion that the whole system—supply infrastructures, energy hub, and loads—has to be considered when determining the optimal hub layout. Therefore the optimization model integrates the hub in the supply and load environment/situation in which it has to perform. A multi-period optimization is performed for given (or expected) loads and energy prices. The optimization model comprises on/off-type variables assigned to each element from the set of available elements; this integer variable represents the decision whether an element is used in the hub or not.

4.8.1 Objective

For economic optimization, the objective function should penalize the cost for energy, operation, maintenance and installation. The installation costs are fixed costs which occur if the element is used for the hub, i.e., when the corresponding decision variable is equal to one. Maintenance and operation costs are normally dependent on the operation of the device. The cost for energy depend on the operation of the hub as well, which is determined by the loads. It can be concluded that the objective function generally depends on the decision variables as well as on the energy and power quantities related to the hub and its elements.

4.8.2 Constraints

Similar to (4.11), constraints are given by the hub and network models. Restrictions related to the individual elements include the integer variables which decide whether an element is used or not. In the latter case, the element's constraint is multiplied by zero, thereby eliminated. Additional constraints could for example limit the total installation or operating cost for the hub. As mentioned in Section 4.4.3, a multi-period approach could also include constraints related to the change of a quantity between two time periods, such as ramping, minimum up-/down-times, etc. For the sake of simplicity, such limits are not considered, but can be included in the approach. Furthermore, a single hub is considered only, i.e., network constraints are not included.

4.8.3 Problem Statement

For the problem statement, decision variables have to be introduced that keep the information whether an element is used in the optimal layout or not. For an element A, an integer variable I_A is introduced, which is

$$I_A = \begin{cases} 1 & \text{if element A is part of the optimal layout} \\ 0 & \text{else} \end{cases} \quad (4.18)$$

The problem is basically defined as (4.11), but all elements' quantities are multiplied with their corresponding decision variables. If $I_A = 1$, then element A is considered in the model equations; if $I_A = 0$, the related quantities, equations, and constraints vanish. This is shown in the following example.

Example 4.2 Consider the energy hub in Figure 4.2, which converts the input carriers α and β into γ and δ . With decision variables $I_A, I_B, I_C \in \{0, 1\}$ for elements A, B, and C, respectively, the converter coupling matrix can be stated as

$$\mathbf{C} = \begin{bmatrix} I_A \eta_{\alpha\gamma}^A & I_B \nu \eta_{\beta\gamma}^B \\ 0 & I_B \nu \eta_{\beta\delta}^B + I_C (1 - I_B \nu) \eta_{\beta\delta}^C \end{bmatrix} \quad (4.19)$$

The variables I_A , I_B , and I_C can be understood as the states of virtual switches connecting elements A, B, and C with the hub inputs. \diamond

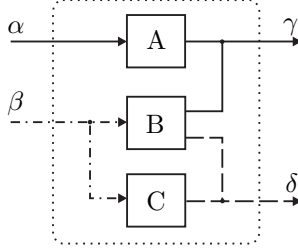


Figure 4.2: Example hub with optional elements A, B, and C.

Mathematically, the problem is stated as follows:

$$\text{Minimize } \mathcal{F} = \sum_{t=1}^{N_t} \mathcal{F}^t(\mathbf{P}^t, \nu_{\alpha k}^t, \mathbf{E}^t, I_{\alpha k}, J_{\alpha}) \quad (4.20a)$$

$$\text{subject to } \mathbf{L}^t - \mathbf{C}^t \mathbf{P}^t + \mathbf{M}^{\text{eq}t} = \mathbf{0} \quad \forall t \quad (4.20b)$$

$$\underline{\mathbf{P}} \leq \mathbf{P}^t \leq \overline{\mathbf{P}} \quad \forall t \quad (4.20c)$$

$$J_{\rho} \underline{Q}_{\rho} \leq J_{\rho} Q_{\rho}^t \leq J_{\rho} \overline{Q}_{\rho} \quad \forall t, \forall \rho \quad (4.20d)$$

$$J_{\sigma} \underline{M}_{\sigma} \leq J_{\sigma} M_{\sigma}^t \leq J_{\sigma} \overline{M}_{\sigma} \quad \forall t, \forall \sigma \quad (4.20e)$$

$$J_{\alpha} \underline{E}_{\alpha} \leq J_{\alpha} E_{\alpha}^t \leq J_{\alpha} \overline{E}_{\alpha} \quad \forall t, \forall \alpha \quad (4.20f)$$

$$J_{\alpha} (E_{\alpha}^0 - E_{\alpha}^{N_t}) = 0 \quad \forall \alpha \quad (4.20g)$$

$$I_{\alpha k} \underline{P}_{\alpha k} \leq I_{\alpha k} \nu_{\alpha k}^t P_{\alpha k}^t \leq I_{\alpha k} \overline{P}_{\alpha k} \quad \forall t, \forall \alpha, \forall k \quad (4.20h)$$

$$0 \leq I_{\alpha k} \nu_{\alpha k}^t \leq 1 \quad \forall t, \forall \alpha, \forall k \quad (4.20i)$$

where $I_{\alpha k}, J_{\alpha} \in \{0, 1\}$; $t \in \{1, 2, \dots, N_t\}$; $\alpha, \beta \in \mathcal{E}$; $k \in \mathcal{C}_{\alpha}$. Energy carriers $\rho \in \mathcal{E}$ are stored at the input side of the hub, the carriers $\sigma \in \mathcal{E}$, $\sigma \neq \rho$ are stored at the output side.

Note that the converter and storage coupling matrices are functions of the decision variables $I_{\alpha k}$ and J_{α} , which is not explicitly visible in (4.20b).

Remark 4.5 Additional constraints related to the decision variables $I_{\alpha k}$ and J_{α} can be simply added to (4.20). For example, the number of converter elements can be limited. \diamond

Remark 4.6 For software implementation, a more appropriate con-

straint formulation can be used similar to (4.6):

$$I_A \underline{h} \leq I_A h(x_A) \leq I_A \bar{h} \quad \Leftrightarrow \quad \begin{cases} I_A [h(x_A) - \bar{h}] \leq 0 \\ I_A [\underline{h} - h(x_A)] \leq 0 \end{cases} \quad (4.21)$$

where x_A is an optimization variable related to element A, and I_A is the decision variable for A. \diamond

4.8.4 Type of Problem and Solution

The problem (4.20) represents a mixed-integer nonlinear constrained problem. Both the objective function as well as the constraints may include nonlinearities and discontinuities, which results in a nonconvex solution space. Numerical solvers can be used to find a solution, but it cannot be ensured that the global optimum has been achieved.

Chapter 5

Application

The intention of this chapter is to demonstrate possible applications and basic features of the developed optimization models. Based on more or less realistic assumptions, various elementary, rather small-scaled application examples are elaborated. Some experience with numerical solvers is reported and application to realistically-sized problems is discussed.

5.1 Multi-Carrier Optimal Dispatch

In this section, optimal dispatch of a single energy hub is exemplified. First, the solution of convex and nonconvex problems is demonstrated, then two possible extensions are shown: bi-objective optimization considering cost and emissions, and multi-period optimization of an energy hub.

5.1.1 Convex Dispatch

In this example, application of the general optimality condition for convex multi-carrier optimal dispatch (4.7) is demonstrated. We consider a linear energy hub as shown in Figure 5.1. The hub contains a direct connection to the electricity network (assumed lossless), a combined heat and power (CHP) plant, and a heat exchanger (HE) which connects the

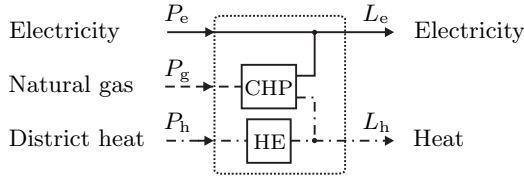


Figure 5.1: Energy hub with combined heat and power (CHP) plant and heat exchanger (HE). Input powers P_e , P_g , and P_h , load powers L_e and L_h .

load with the heating infrastructure. Electricity and heat loads can be met by directly consuming the required power from the corresponding networks or by generating part (or all) of the load power with the CHP.

The power flows through the hub should be optimized for a specific snapshot of the load aiming at minimal energy cost. Required loads are given with $L_e = 2$ pu and $L_h = 5$ pu. The CHP is assumed to operate with constant efficiencies $\eta_{ge}^{CHP} = 0.3$ (gas-electricity) and $\eta_{gh}^{CHP} = 0.4$ (gas-heat). The efficiency of the heat exchanger is $\eta_{hh}^{HE} = 0.9$. We assume a convex objective function that reflects the total energy cost for the hub in the time period considered in monetary units (mu), where costs of the individual energy carriers are modeled as quadratic functions of the corresponding powers in power units (pu):

$$TC = \sum_{\alpha=e,g,h} (a_{\alpha} P_{\alpha} + b_{\alpha} P_{\alpha}^2) \quad (5.1)$$

The coefficients a_{α} and b_{α} assumed for this example are given in Table 5.1. Figure 5.2 plots the total cost TC as functions of the hub's input powers. The minimum of TC can already be identified in the plot, but now application of the general optimality condition should be demonstrated.

The question to be answered is: Which input vector \mathbf{P} minimizes the total energy cost TC? Without considering limitations of the power input, we can formulate a convex problem of the structure (4.5a) and (4.5b). The KKT optimality conditions apply and they are now used to solve the problem.

Therefore we have to state and solve (4.5b) (transformation of power) and (4.7) (marginal cost relation). Both equations include the coupling

Table 5.1: Objective Function Coefficients.

Carrier (α)	a_α in mu/pu	b_α in mu/pu ²
Electricity (e)	12	0.12
Natural gas (g)	5	0.05
Heat (h)	4	0.04

mu ... monetary units; pu ... per unit

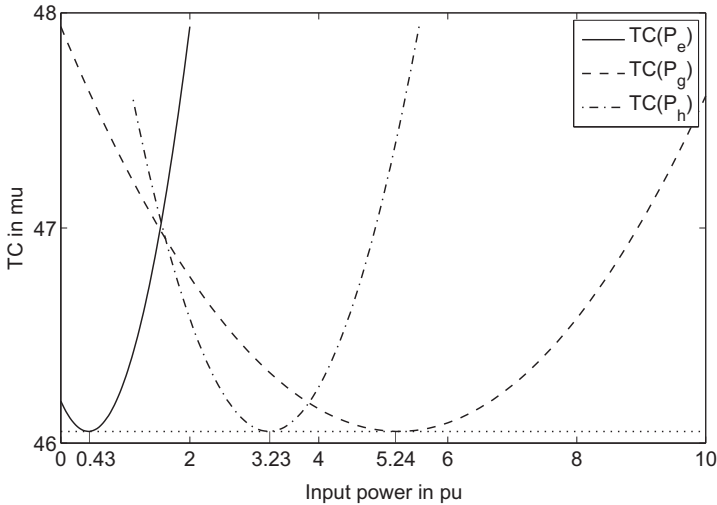


Figure 5.2: Total energy cost TC in monetary units (mu) versus input powers P_e , P_g , and P_h in power units (pu). Note that P_e , P_g , and P_h are related to each other by (5.4).

matrix \mathbf{C} which can be derived from the converter efficiencies and the topology of the hub (as outlined in Section 3.2):

$$\mathbf{C} = \begin{bmatrix} c_{ee} & c_{ge} & c_{he} \\ c_{eh} & c_{gh} & c_{hh} \end{bmatrix} = \begin{bmatrix} 1 & 0.3 & 0 \\ 0 & 0.4 & 0.9 \end{bmatrix} \quad (5.2)$$

The dispatch rule (4.7) includes also the vector of system marginal objectives, in this case system marginal cost (SMC) denoted Ψ . Its elements Ψ_α can be calculated as the partial derivatives of the total cost TC from (5.1) with respect to the input powers P_α :

$$\Psi_\alpha = \frac{\partial \text{TC}}{\partial P_\alpha} = a_\alpha + 2b_\alpha P_\alpha \quad (5.3)$$

where $\alpha = e, g, h$. Now (4.5b) and (4.7) can be formulated for the given problem:

$$\underbrace{\begin{bmatrix} 2 \\ 5 \end{bmatrix}}_{\mathbf{L}} - \underbrace{\begin{bmatrix} 1 & 0.3 & 0 \\ 0 & 0.4 & 0.9 \end{bmatrix}}_{\mathbf{C}} \underbrace{\begin{bmatrix} P_e \\ P_g \\ P_h \end{bmatrix}}_{\mathbf{P}} = \begin{bmatrix} 0 \\ 0 \end{bmatrix} \quad (5.4)$$

$$\underbrace{\begin{bmatrix} a_e + 2b_e P_e \\ a_g + 2b_g P_g \\ a_h + 2b_h P_h \end{bmatrix}}_{\Psi} - \underbrace{\begin{bmatrix} \Lambda_e \\ \Lambda_h \end{bmatrix}}_{\Lambda} \underbrace{\begin{bmatrix} 1 & 0.3 & 0 \\ 0 & 0.4 & 0.9 \end{bmatrix}}_{\mathbf{C}} = \begin{bmatrix} 0 \\ 0 \\ 0 \end{bmatrix}^T \quad (5.5)$$

Note that (5.4) is underdetermined, which indicates the potential for optimization. Together with (5.5), a system of 5 linear (scalar) equations with 5 unknowns (elements of \mathbf{P} and Λ) is achieved, which is straightforward to solve. The unique solution is found at

$$\mathbf{P} = \begin{bmatrix} 0.430 \\ 5.235 \\ 3.229 \end{bmatrix} \text{ pu}; \quad \Lambda = \begin{bmatrix} 12.103 & 4.732 \end{bmatrix} \text{ mu/pu} \quad (5.6)$$

For the given situation, the vector \mathbf{P} yields minimal total energy cost $\text{TC} = 46.054$ mu. In this optimal operation point, the CHP converts

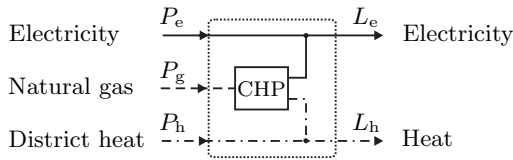


Figure 5.3: Energy hub with combined heat and power (CHP) plant. Input powers P_e , P_g , and P_h , load powers L_e and L_h .

5.235 pu of natural gas into electricity and heat. $\mathbf{\Lambda}$ contains the hub marginal cost (HMC) for electricity and heat appearing at the output side of the hub. The marginal cost at the input side of the hub, the system marginal cost (SMC), can be calculated from the results according to (5.3):

$$\mathbf{\Psi} = \begin{bmatrix} 12.103 & 5.524 & 4.258 \end{bmatrix} \text{ mu/pu} \quad (5.7)$$

It can be observed that the marginal cost of heat increase between the input and the output of the hub from 4.258 to 4.732 mu/pu, which origins from 10% losses in the heat exchanger ($\eta_{hh}^{\text{HE}} = 0.9$). The marginal cost of electricity are equal on both sides of the hub since the connection is assumed to be lossless.

5.1.2 Nonconvex Dispatch

In this example, the flows through a nonlinear energy hub characterized by a variable coupling matrix should be dispatched optimally. Figure 5.3 shows the simple hub which basically consists of a combined heat and power (CHP) unit. The hub is supplied with electricity, natural gas, and district heat, and delivers electricity and heat to the loads.

The conversion efficiencies of the CHP are not constant over its operating range (see, e.g., [9, 85]). Assume that the efficiencies have been determined experimentally at four different operating states. Table 5.2 gives the corresponding data.

For the optimization, the energy efficiencies have to be expressed as continuous functions of the gas input, therefore the measured data are

Table 5.2: Measured CHP Efficiencies.

Gas input P_g in kW	Gas-electricity η_{ge}	Gas-heat η_{gh}
25	0.18	0.38
50	0.32	0.39
75	0.36	0.37
100	0.37	0.40

Table 5.3: Parameters of Polynomial Fit.

Order i	q_{gei}	q_{ghi}
0	$-130 \cdot 10^{-3}$	$260 \cdot 10^{-3}$
1	$167 \cdot 10^{-4}$	$8 \cdot 10^{-3}$
2	$-192 \cdot 10^{-6}$	$-152 \cdot 10^{-6}$
3	$747 \cdot 10^{-9}$	$853 \cdot 10^{-9}$

fitted with the following functions:

$$\eta_{ge}(P_g) = \sum_{i=0}^3 q_{gei} P_g^i \quad (5.8a)$$

$$\eta_{gh}(P_g) = \sum_{i=0}^3 q_{ghi} P_g^i \quad (5.8b)$$

The resulting coefficients q_{gei} and q_{ghi} are given in Table 5.3. Figure 5.4 plots the measured as well as the fitted energy efficiencies of the CHP plant.

For the optimization constraints, the coupling matrix of the hub is needed. It contains the power-dependent efficiencies from (5.8):

$$\mathbf{C}(\mathbf{P}) = \begin{bmatrix} 1 & \eta_{ge}(P_g) & 0 \\ 0 & \eta_{gh}(P_g) & 1 \end{bmatrix} \quad (5.9)$$

The flows through the hub should be optimized for a given required output:

$$\mathbf{L} = \begin{bmatrix} L_e & L_h \end{bmatrix}^T = \begin{bmatrix} 50 & 100 \end{bmatrix}^T \text{ kW} \quad (5.10)$$

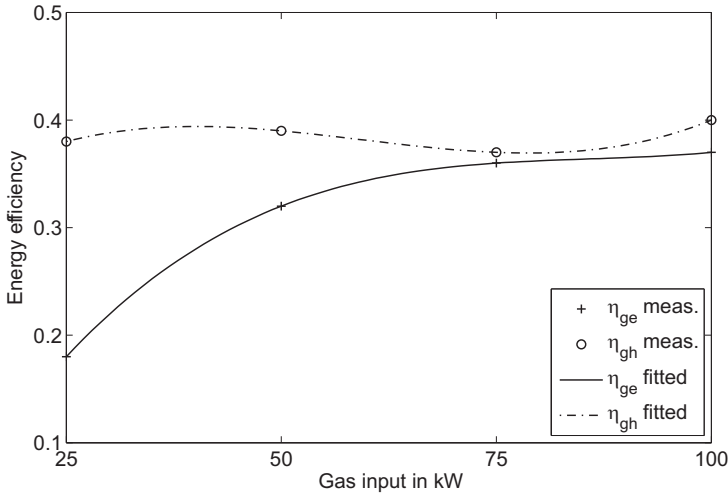


Figure 5.4: Measured and fitted energy efficiencies for gas-electric (η_{ge}) and gas-heat (η_{gh}) conversion, respectively, as functions of the gas input P_g in kW.

Operation of the CHP device is restricted to the range between 25 kW and 100 kW gas input. The other hub inputs have a lower limit of zero (the hub is not allowed to export power), but no upper limit:

$$\begin{bmatrix} 0 \\ 25 \\ 0 \end{bmatrix} \text{ kW} \leq \begin{bmatrix} P_e \\ P_g \\ P_h \end{bmatrix} \leq \begin{bmatrix} \infty \\ 100 \\ \infty \end{bmatrix} \text{ kW} \quad (5.11)$$

The objective to be minimized is again energy cost as stated in (5.1). Cost parameters used in this example are given in Table 5.4. Figure 5.5 plots the objective TC as functions of the different hub input powers. Clearly, these functions are not convex. Note that the same objective function is used as in Section 5.1.1, but due to the nonlinear structure of Equations (5.8), the functions $TC(\cdot)$ are nonconvex.¹ Consider for example $TC(P_g)$, which shows minima at $P_g = 65$ kW and $P_g = 100$ kW.

¹This originates from the nonlinear relations between P_e , P_g , and P_h . Note that these variables are not independent but related to each other by $\mathbf{L} = \mathbf{C}\mathbf{P}$. For a given gas input, electrical and thermal inputs can be calculated.

Table 5.4: Objective Function Coefficients.

Carrier (α)	a_α in €-Cent/kW	b_α in €-Cent/kW ²
Electricity (e)	10	0.01
Natural gas (g)	5	0.02
Heat (h)	5	0.03

The total costs at these points are:

$$\text{TC}(P_g = 65 \text{ kW}) = 12.37 \text{ €} \quad (5.12a)$$

$$\text{TC}(P_g = 100 \text{ kW}) = 12.40 \text{ €} \quad (5.12b)$$

Thus, the hub is operated optimally at $P_g = 65 \text{ kW}$.

This example was implemented using commercial software for convex NLP problems (“fmincon.m” from the Matlab Optimization Toolbox [86]). The numerical solver is able to find an optimum, but depending on the initial value, it either converges to (5.12a) or (5.12b).

5.1.3 Cost-Emission Dispatch

Besides energy cost, operational system emissions are an important criterion in the operation of energy systems. In order to account for both operational energy cost and emissions, bi-objective optimization can be implemented. A composite objective function can be stated that combines cost and emissions. Commonly, cost and emission terms are multiplied by weighting factors. Variation of the weighting factors enables to study the tradeoff between the individual criteria—in this case energy cost and emissions.²

In the previous examples, energy hubs are considered that are supplied with electricity, natural gas, and district heating. Equation (5.1) models energy cost as quadratic functions of the power consumed:

$$\text{TC} = \sum_{\alpha=e,g,h} (a_\alpha P_\alpha + b_\alpha P_\alpha^2)$$

²Alternatively, emissions could be included in the optimization by penalizing related cost, e.g., the cost for emission rights.

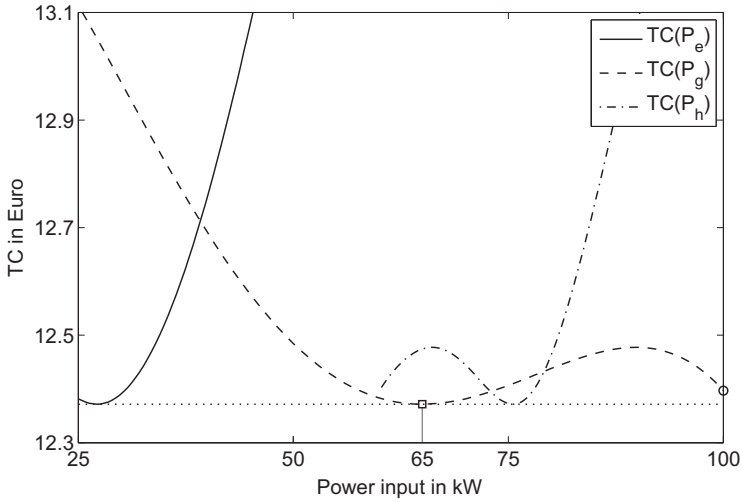


Figure 5.5: Total energy cost TC in € versus input powers P_e , P_g , and P_h in kW. Local minimum at $P_g = 100$ kW (○), global minimum at $P_g = 65$ kW (□).

Emissions dedicated to an energy hub can be stated in a similar way. Basically, the hub causes emissions in two ways:

1. *Pre-hub emissions* are inherent to the energy carriers consumed by the hub. These emissions accrue in generation (e.g., electric power plants) and transportation (e.g., gas compressor stations).
2. *Hub-internal emissions* are resulting from the operation of hub elements (for example gas turbines).

In this simple example, a single CHP-equipped energy hub as shown in Figure 5.3 is considered. Emissions caused by the hub are modeled as linear functions of the power consumption. All energy carriers available at the hub input are characterized by pre-hub CO_2 emissions c_α^{pre} expressed in kg CO_2 per MW consumed. Natural gas is converted within the hub, therefore every MW of gas consumed by the hub causes additional emissions. These hub-internal emissions are reflected by c_α^{int} (in kg CO_2 per MW converted). The total CO_2 emissions of the energy hub

Table 5.5: Objective Function Coefficients.

Energy carrier (α)	a_α in €/MW	b_α in €/MW ²	$c_\alpha^{\text{pre}} + c_\alpha^{\text{int}}$ in kg/MW
Electricity (e)	50	0.05	444 + 0
Natural gas (g)	25	0.25	50 + 168
Heat (h)	25	0.50	50 + 0

are reflected by the following function:

$$\text{TE} = \sum_{\alpha=e,g,h} (c_\alpha^{\text{pre}} + c_\alpha^{\text{int}}) P_\alpha \quad (5.13)$$

Energy cost and emission coefficients assumed for this example are printed in Table 5.5. The coefficient for pre-hub electricity emissions c_e^{pre} is based on the power mix in the European Community [73]. Gas and heat emission coefficients c_g^{pre} and c_h^{pre} , respectively, are assumed according to typical transportation losses in these networks. The value for internal hub emissions resulting from CHP operation is taken from [8], it is typical for a combined cycle gas turbine in the few MW range.

For the optimization, cost and emissions are reflected by the following composite objective function:

$$\mathcal{F} = \xi \cdot \text{TC} + (1 - \xi) \cdot \text{TE} \quad (5.14)$$

where ξ is the cost-emission weighting factor. It can be adjusted between 0 and 1:

- $\xi = 1$ yields minimal energy cost,
- $\xi = 0$ yields minimal emissions.

With other factors $0 < \xi < 1$, so-called Pareto optimal solutions are obtained [87, 88]. Variation of the factor ξ will always result in an increase of one and a decrease of the other objective function component (TC and TE), which means that the criteria are conflicting.

The flows through the energy hub in Figure 5.3 should be optimized for different weighting factors ξ . Equation (5.14) provides the objective

Table 5.6: Results for Cost-Emission Dispatch.

Result	$\xi = 1$ (min. cost)	$\xi = 0$ (min. emissions)
TC in €	234.53	238.83
TE in kg	975.60	786.32
P_e in MW	1.08	0.00
P_g in MW	3.08	6.67
P_h in MW	3.77	2.33

function to be minimized. The equality constraint is given by the hub's power transformation (3.3) which involves the coupling matrix. With gas-electric and gas-heat efficiencies of 30% and 40%, respectively, the coupling matrix results in

$$\mathbf{C} = \begin{bmatrix} 1 & 0.3 & 0 \\ 0 & 0.4 & 1 \end{bmatrix} \quad (5.15)$$

Electricity and heat loads to be met by the hub are assumed as

$$\mathbf{L} = \begin{bmatrix} L_e & L_h \end{bmatrix}^T = \begin{bmatrix} 2 & 5 \end{bmatrix}^T \text{ MW} \quad (5.16)$$

The problem is further constrained by input power limits:

$$\begin{bmatrix} 0 \\ 0 \\ 0 \end{bmatrix} \leq \begin{bmatrix} P_e \\ P_g \\ P_h \end{bmatrix} \quad (5.17)$$

Since the objective function (5.14) is convex and all constraints are linear, global optima can be determined for different ξ with standard NLP solvers. This example is implemented in Matlab using the solver “fmincon.m” [86]. In order to achieve well distributed solutions among the ξ -range, an adaptive algorithm from [89] is employed.

Figure 5.6 shows the result of the optimization for different weighting factors $0 \leq \xi \leq 1$. The plot clearly shows that cost and emissions are conflicting criteria. Decreasing emissions (by decreasing ξ) yields increased cost and vice versa. Table 5.6 prints results for the extreme points of the Pareto curve ($\xi = 0$ and $\xi = 1$).

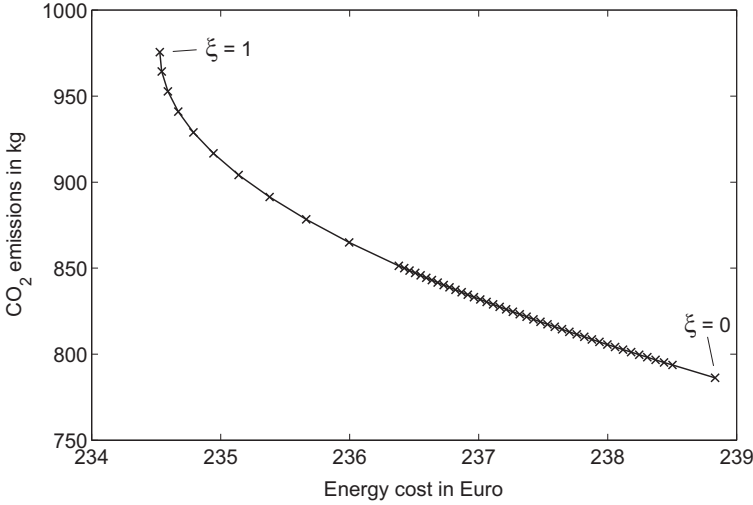


Figure 5.6: Pareto front of multi-carrier cost-emission dispatch. $\xi = 1$ yields minimal cost, $\xi = 0$ results in minimal CO_2 emissions.

The Pareto front demonstrates the tradeoff between conflicting objectives, in this case energy cost and CO_2 emissions. It provides a tool for the decision maker who finally has to find the most suitable solution among the range of ξ .

5.1.4 Multi-Period Dispatch

In the following, the multi-period optimization approach presented in Section 4.6.5 is applied to the example hub shown in Figure 5.7. The hub contains an electrical transformer, a CHP plant, a gas furnace, and a heat storage. The data of these elements are given in Table 5.7. Electricity can be consumed from the grid or generated with the CHP unit. The heat load can be supplied by converting natural gas with the furnace and/or the CHP, and/or exploiting the heat storage.

According to the general model (3.24), the hub can be described by a converter and a storage coupling matrix, respectively:

$$\mathbf{C} = \begin{bmatrix} \eta_{ee}^T & \nu \eta_{ge}^{\text{CHP}} \\ 0 & \nu \eta_{gh}^{\text{CHP}} + (1 - \nu) \eta_{gh}^{\text{F}} \end{bmatrix}; \quad \mathbf{S} = \begin{bmatrix} 0 \\ 1/e_h \end{bmatrix} \quad (5.18)$$

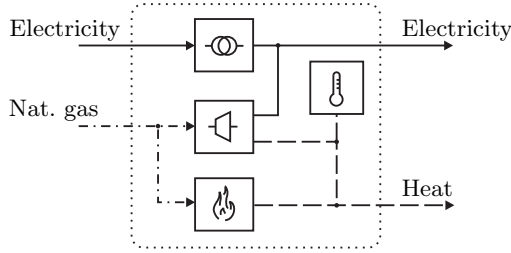


Figure 5.7: Example hub containing a transformer, a CHP unit, a gas furnace, and a heat storage.

where

$$e_h = \begin{cases} e_h^+ & \text{if } M_h \geq 0 \quad (\text{charging/standby}) \\ 1/e_h^- & \text{else} \quad (\text{discharging}) \end{cases} \quad (5.19)$$

The dispatch factor ν in (5.18) describes the dispatch of the total gas input to the CHP and the furnace (see Section 3.2.2).

Figure 5.8 shows the assumed 24×1 hour load curves and energy prices. Electricity and heat loads are aggregated for a number of individual consumers which have to be supplied by the hub. The curves represent a typical mixed commercial/residential load on a summer day in central Europe. The tariff system for electricity includes three different prices, whereas the natural gas price is constant over the day.

Operation of the hub is optimized according to the total energy cost accruing in the 24 periods. The function to be minimized is

$$\text{TC} = \sum_{t=1}^{24} (a_e^t P_e^t + a_g^t P_g^t) \quad (5.20)$$

where P_e^t and P_g^t are the electricity and gas powers consumed by the hub at period t , respectively; a_e^t and a_g^t are the cost coefficients (energy prices) for electricity and gas, respectively (see lower plot in Figure 5.8).

The problem is stated according to the general form (4.11). Since we consider a single energy hub only, the network constraints (4.11c) and (4.11i) drop out. For implementation of this example, the Knitro solver is used within the framework of Tomlab and Matlab [86, 90, 91].

Table 5.7: Data of Hub Elements.

Transformer	
Efficiency	$\eta_{ee}^T = 0.98$
Min./max. power	0/10 pu
Gas turbine	
Electric efficiency	$\eta_{ge}^{CHP} = 0.35$
Thermal efficiency	$\eta_{gh}^{CHP} = 0.45$
Min./max. power	0/5 pu (input)
Gas furnace	
Efficiency	$\eta_{gh}^F = 0.9$
Min./max. power	0/10 pu
Storage	
Charge efficiency	$e_h^+ = 0.9$
Discharge efficiency	$e_h^- = 0.9$
Min./max. power	-3/3 pu
Min./max. energy	0.5/3 pu
Standby losses	0.3 pu

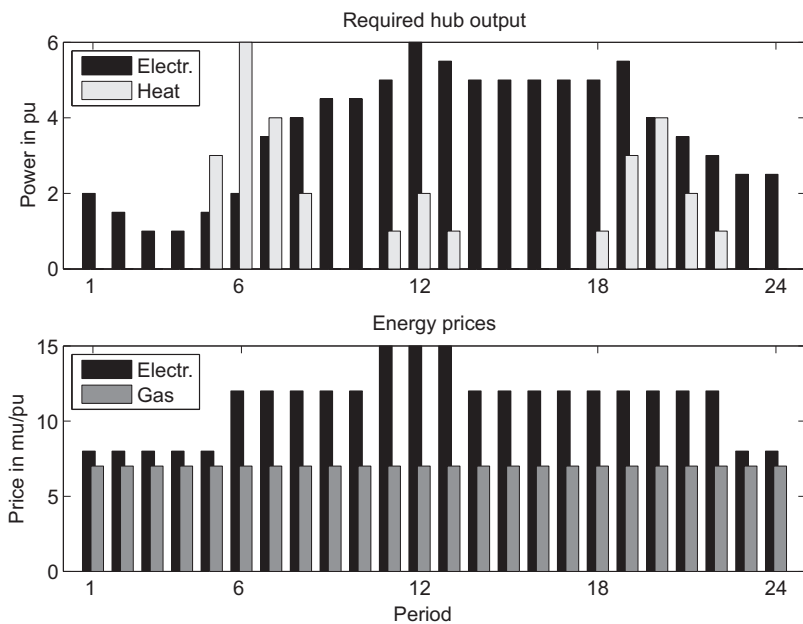


Figure 5.8: Required load powers and energy prices for 24 hours.

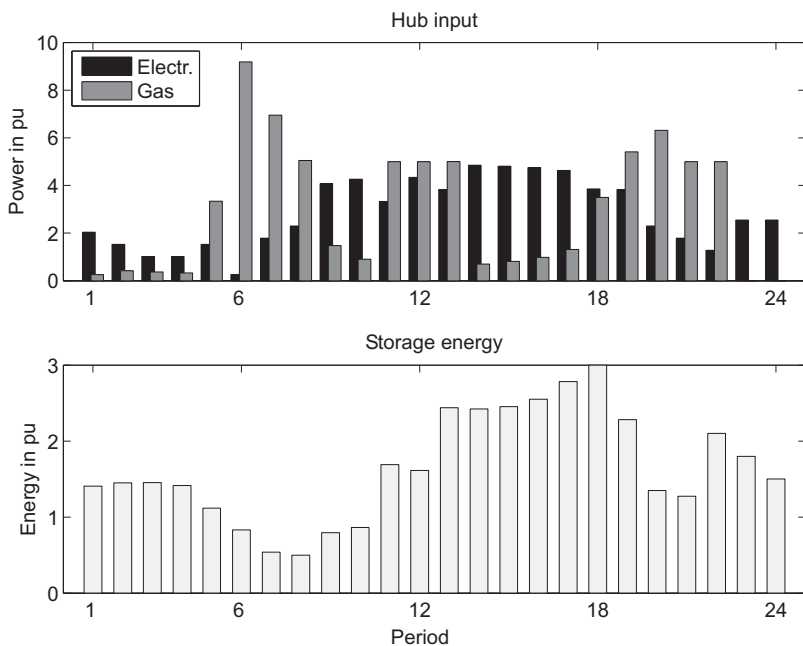


Figure 5.9: Results of multi-period optimal dispatch: hub inputs and storage energy.

The upper plot in Figure 5.9 shows the resulting optimal hub input powers. The hub's electricity consumption shows almost the same pattern as the required electricity load. Note that the load peak around noon (periods 11, 12, 13) is significantly reduced. This is reasonable since electricity is expensive at these periods. The second peak in the evening (period 19) is reduced as well. Considering the gas consumption of the hub, it can be observed that it correlates quite well with the heat demand. But gas is also converted at times where no heat is required. For example, at periods 14...17, heat is produced and stored in the heat storage; the stored heat is used in the following periods 18...22, where heat loads are high.

The lower plot in Figure 5.9 shows the stored heat for all 24 periods. Each bar represents the energy stored at the end of the period. The storage is assumed to be half full at the beginning of period 1. Due to the “sustainability constraint” (4.11h), the storage is again half full after period 24. During the first periods, the storage almost keeps its initial energy. Discharging starts as soon as the heat load increases at period 5. After the morning peak, the storage is charged until the evening peak around period 18, where it is discharged again.

The storage is not only important for the heat supply, but—indirectly—also for electricity generation. It enables the CHP to be used for electricity peak shaving around noon. At periods 11 and 13, the CHP generates 2.25 pu of heat, whereas the heat load requires only 1 pu. The difference is compensated by the storage. At period 12, the heat load is 2 pu, and together with the standby losses of 0.3 pu (which have to be compensated each period), the heat production of the CHP (2.25 pu) is exceeded. Consequently, the storage energy slightly decreases in this period. However, without the heat storage it would not be possible to operate the CHP at full power during the periods 11 and 13.

Figure 5.10 shows the optimal conversion of natural gas by the furnace and the CHP unit. Figure 5.11 shows the corresponding dispatch factor ν according to (5.18), which defines how much of the total gas input is converted by the CHP. The plots show that most of the gas is converted by the CHP. In this example, the CHP is solely utilized when the electricity price is medium or high (periods 6...22). The general pattern reflects both the high load periods in terms of heat (periods 5...8, 18...22) and the high price period in terms of electricity (periods 11, 12, 13).

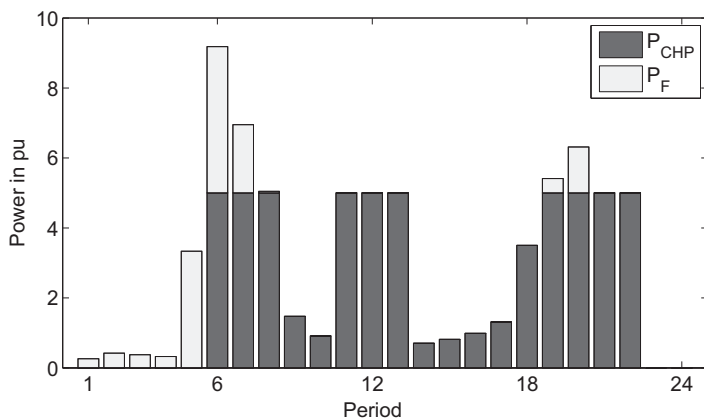


Figure 5.10: Results of multi-period optimal dispatch: conversion of natural gas by the CHP and the furnace. CHP input power P_{CHP} , furnace input power P_{F} .

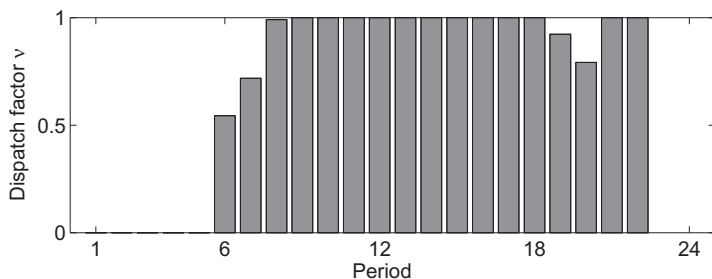


Figure 5.11: Results of multi-period optimal dispatch: dispatch factor ν according to (5.18).

5.2 Multi-Carrier Optimal Power Flow

In this example, optimal power flow and conversion in a system of interconnected energy hubs will be investigated.

5.2.1 Assumptions

Figure 5.12 shows the structure of the networks and the hubs. System parameters are given in Table 5.8. The system comprises three equal energy hubs which consume electricity and natural gas from the interconnections and provide electricity and heat at their outputs. Each hub is equipped with a gas furnace (F) and a combined heat and power (CHP) plant. The latter element establishes redundancy for the supply of both electricity and heat loads. The electricity network connects generators G_1 and G_2 with the hub inputs (P_{1e} , P_{2e} , and P_{3e} ; note that these are complex apparent power quantities). Natural gas is demanded from an adjacent network N and delivered to the hub inputs (P_{1g} , P_{2g} , and P_{3g}). The gas connections (1, 2) and (1, 3) are equipped with compressors C_{12} and C_{13} , respectively.

The energy hubs are characterized by the following coupling matrix:

$$\mathbf{C}_i = \begin{bmatrix} 1 & \nu\eta_{ge}^{\text{CHP}} \\ 0 & \nu\eta_{gh}^{\text{CHP}} + (1 - \nu)\eta_{gh}^{\text{F}} \end{bmatrix} \quad i = 1, 2, 3 \quad (5.21)$$

The objective to be minimized is chosen as the total energy cost in the system, which is modeled as quadratic functions of the powers consumed from the sources:

$$\text{TC} = \sum_{s=G_1, G_2, N} (a_s + b_s P_s + c_s P_s^2) \quad (5.22)$$

The coefficients a_s , b_s , and c_s are assumed according to common energy prices in central Europe and given in Table 5.8.

The optimization problem is constrained by the steady-state power flow equations as discussed in Section 3. Further constraints are given by limitations of the nodal voltage magnitudes and pressures, active, reactive, and apparent power output of G_2 , and compression ratios of C_{12} and

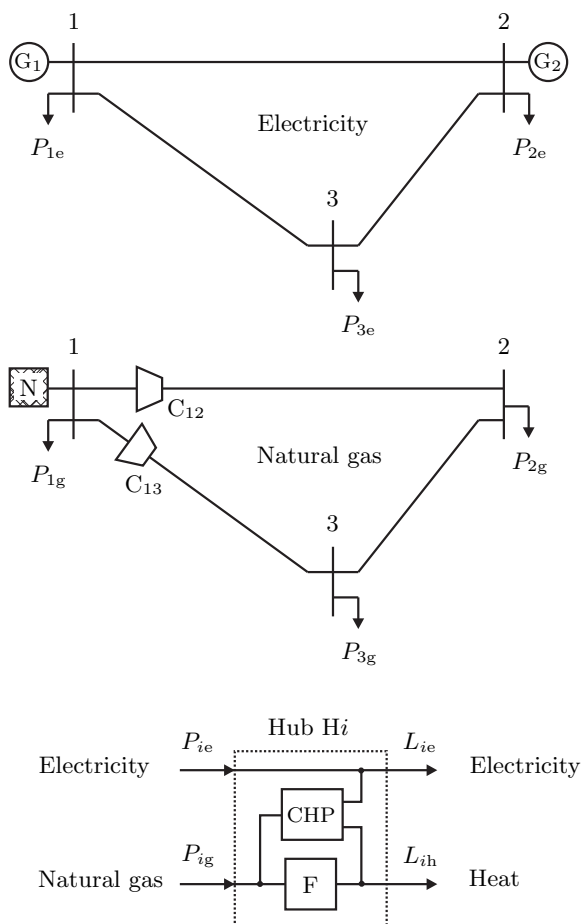


Figure 5.12: Example system of interconnected energy hubs. The network nodes 1, 2, and 3 connect to equal hubs H_1 , H_2 , and H_3 , which contain a combined heat and power (CHP) unit and a gas furnace (F). The system is supplied by the generators G_1 and G_2 , and an adjacent gas network N .

Table 5.8: Parameters of 3-Hub Example System.

Element data	
El. line (1, 2)	$Z_{12} = 0.3 + j0.9 \text{ pu}$, $Y_{12} = j3.5 \cdot 10^{-6} \text{ pu}$
El. line (1, 3)	$Z_{13} = 0.2 + j0.6 \text{ pu}$, $Y_{13} = j2.5 \cdot 10^{-6} \text{ pu}$
El. line (2, 3)	$Z_{23} = 0.1 + j0.4 \text{ pu}$, $Y_{23} = j1.5 \cdot 10^{-6} \text{ pu}$
G_1	slack type, $V_1 = 1\angle 0^\circ \text{ pu}$, $a_{G_1} = 0 \text{ mu}$, $b_{G_1} = 10 \text{ mu/pu}$, $c_{G_1} = 0.0010 \text{ mu/pu}^2$
G_2	PQ type, $a_{G_2} = 0 \text{ mu}$, $b_{G_2} = 12 \text{ mu/pu}$, $c_{G_2} = 0.0012 \text{ mu/pu}^2$
Pipe (1, 2)	$k_{12} = 4.5$
Pipe (1, 3)	$k_{13} = 3.0$
Pipe (2, 3)	$k_{23} = 2.0$
C_{12}, C_{13}	$k_{C_{12}} = k_{C_{13}} = 0.5 \text{ pu}^{-1}$
N	slack type, $p_1 = 1 \text{ pu}$, $a_N = 0 \text{ mu}$, $b_N = 5 \text{ mu/pu}$, $c_N = 0 \text{ mu/pu}^2$
CHP	$\eta_{ge} = 0.30$, $\eta_{gh} = 0.40$
F	$\eta_{gh} = 0.75$
Loads	$L_{ie} = 1 + j0.1 \text{ pu}$, $L_{ih} = 2 \text{ pu}$
Limitations	
Nodes	$0.9 \leq V_m \leq 1.1 \text{ pu}$
$m = 1, 2, 3$	$0.8 \leq p_m \leq 1.2 \text{ pu}$
G_2	$0 \leq P_{G_2} \leq 4 \text{ pu}$, $0 \leq Q_{G_2} \leq 4 \text{ pu}$, $0 \leq P_{G_2} + jQ_{G_2} \leq 5 \text{ pu}$
C_{12}, C_{13}	$1.2 \leq \frac{p_m}{p_k} \leq 1.8$

C_{13} (see Table 5.8). The problem is defined according to the general form (4.9).

It was mentioned above that the feasible region of this problem is not convex and thus finding the global optimum cannot be ensured with numerical methods. Nevertheless this example is implemented using commercial NLP software being aware that the result may differ from the global optimum. The solvers used are

1. “fmincon.m” from the Matlab Optimization Toolbox [86], and
2. Knitro within the Ampl environment [90].

With the same initial values, both solvers deliver practically the same results. However, the Knitro solver performs much better, both in terms of computation time and convergence behavior.

Different investigations can be carried out using the presented combined optimal power flow approach. In this example, we focus on the system performance depending on the utilization of the CHP devices within the energy hubs.

5.2.2 Cost Reduction and CHP Rating

Figure 5.13 shows the sensitivity of the penalty function (total energy cost TC) with respect to the size of the CHP devices, i.e., their maximal natural gas input. In this particular example, total energy cost decrease with increasing CHP size until a certain point is reached (≈ 5 pu). A further increase of the CHP limit does not yield decreased TC since other restrictions (in this case pressure and generator constraints) limit the operation of the devices. From Figure 5.13 it can be seen that with sufficiently rated and optimally controlled CHP devices, the total energy cost can be reduced by almost 10%. The results in Figure 5.13 could be used as a basis for network planning or investment decisions. In a simple approach, the potential savings of energy cost arising from utilization of the CHP unit can be accumulated over a certain period. Future and present values of the cost savings can be calculated and compared with the investment (and other) cost of a CHP device. The investment could be reasonable if the present value of the savings is higher than the actual cost of the plant. An example for an optimization-based investment evaluation is presented in Section 5.3.

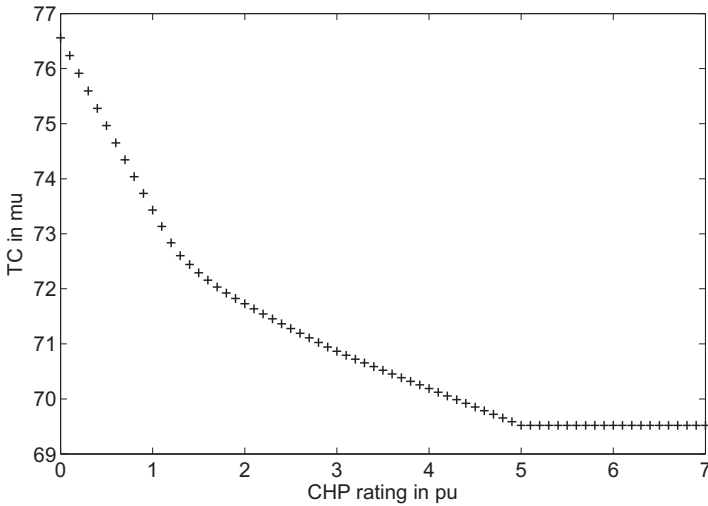


Figure 5.13: Total energy cost TC in monetary units (mu) versus CHP rating (maximal gas input) in power units (pu).

5.2.3 Coupled versus Decoupled Systems

Figure 5.14 compares optimization results with and without CHP devices. In the first case (black bars), no power is converted by the CHP devices, the systems are operated in decoupled mode. Electricity loads are directly supplied from the network interconnections, and all heat is generated by the furnaces. In the second case (grey bars), CHP devices of sufficient rating (6 pu gas input) are installed and the hubs are dispatched optimally. The effects of decentralized CHP generation are obvious:

- Voltages magnitudes are closer to their nominal value (1 pu) without compensating reactive power, and transmission angles are smaller.
- Nodal pressures deviate stronger from their nominal value (1 pu).
- Losses in the electricity system are decreased whereas natural gas losses are increased.

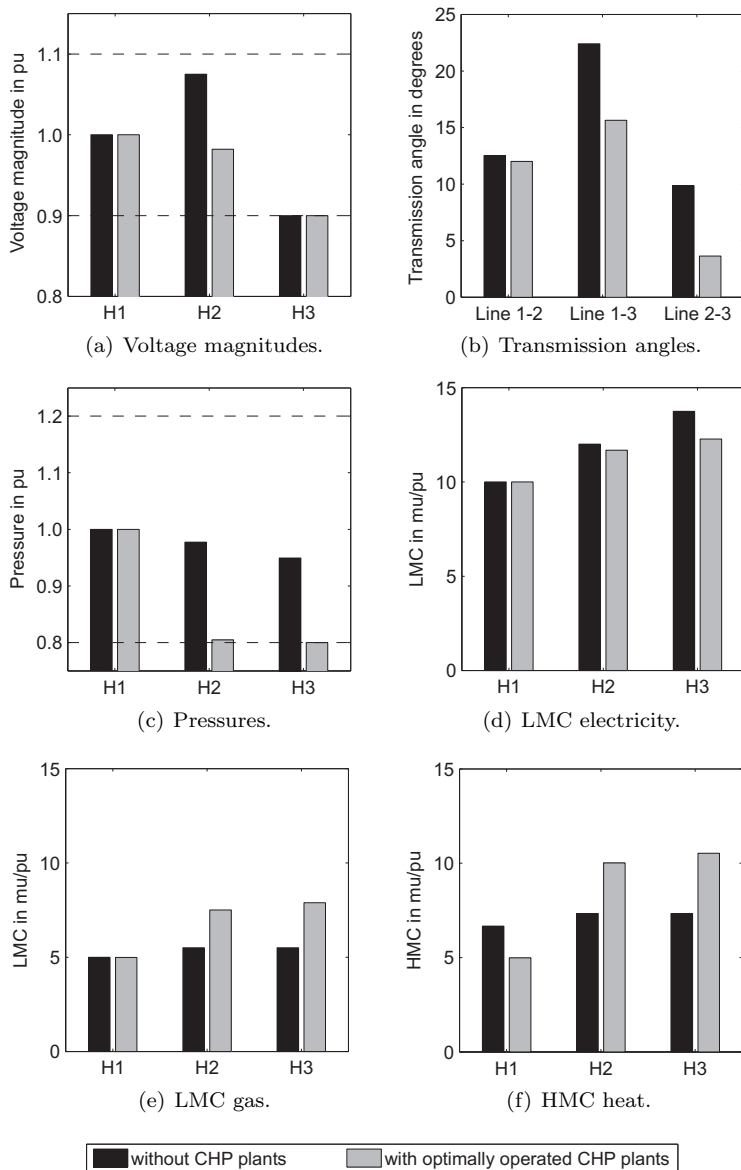


Figure 5.14: Comparison of optimization results.

- Locational marginal cost (LMC) for electricity are decreased, natural gas LMC are increased.³

5.2.4 Operation of Hubs

All hubs are of equal structure, but due to their position in the network, they are dispatched differently. An important factor for the utilization of each CHP unit is the transmission losses caused by the power flow dedicated to the CHP. On the one hand, transmission losses in the gas system and therefore the cost for gas increase with increasing CHP utilization. On the other hand, electricity power flow is reduced when the CHP units are operated, what reduces the electric network losses and electricity cost. Thereby (lower) gas and (higher) electricity marginal cost converge with increasing utilization of the CHP. The optimum depends on the conversion efficiency and the location of the CHP, as well as on constraints such as voltage and pressure limits.

The resulting dispatch factors which specify how much of the total gas input is converted by the CHP are $\nu_1 = 1$, $\nu_2 = 0.778$, and $\nu_3 = 0.425$. The CHP in H1 is fully utilized since the corresponding natural gas input does not cause network losses (directly connected to the slack N). The situation is different for H2 and H3, since related natural gas power flows involve compressor losses. The resulting electricity production in the hubs is 1.5 pu in H1, 0.98 pu in H2, and 0.43 pu in H3. With active power loads of 1 pu, this means that H1 injects 0.5 pu of active power in the electricity network.

5.2.5 Marginal Cost and Hub Elasticity

The final cost per unit of power at inputs and outputs of the hubs are another result of the optimization. Since the system comprises several hubs connected to different network nodes, each hub is subjected to different locational marginal cost (LMC) at the input side, which are transformed into hub marginal cost (HMC) appearing at the output side. For example, LMC at the input of H2 are 11.71 mu/pu for electricity and 7.53 mu/pu for natural gas. Electricity costs are equal at the input and the output since there is a lossless, unlimited connection

³Locational marginal costs are the marginal cost of energy at a certain node in the network (see Section 4.3.4).

in between. The cost for heat at the output side of the hub result in 10.04 mu/pu. Marginal costs are generally slightly higher for H3 since it is located more remote from the slack nodes.

It was mentioned in Chapter 2 that from a system point of view, energy hubs show a certain elastic behavior in terms of price sensitivity due to the possibility of substitution, even if the loads at the output are inelastic. For example, if the electricity LMC are high, an optimally operated hub will substitute with another energy carrier, for example natural gas, if possible. In economics, so-called “elasticity of substitution” is defined as “a measure of the ease with which the varying factor can be substituted for others” [92]. A somewhat different elasticity measure for energy hubs called *hub elasticity* is defined as the relative change in power consumption divided by the relative change in LMC:

$$\sigma_{i\alpha\beta} = \frac{\Delta P_{i\alpha}/P_{i\alpha}}{\Delta \Psi_{i\beta}/\Psi_{i\beta}} \quad (5.23)$$

where $\Delta P_{i\alpha}$ is the absolute change in power consumption due to an absolute change in LMC $\Delta \Psi_{i\beta}$. Note that power and LMC may have different indices α and β , i.e., they can be related to different energy carriers. This is the case when, for example, the influence of the electric power consumption P_{ie} on the natural gas LMC Ψ_{ig} should be investigated.

As an example, elasticity of H2 is now investigated. Therefore LMC are varied and the resulting change in the hub’s electricity consumption is observed. In order to vary the LMC, the cost coefficients a_s , b_s , and c_s of generators G_1 and G_2 are multiplied with a factor between 0.6 and 1.1. The coefficients related to the gas source N are kept constant.

Figure 5.15 plots the electricity and natural gas powers consumed from the grids P_{2e} and P_{2g} , respectively, versus the LMC of electricity at node 2. The figure clearly shows that the hub substitutes for electric power when the electricity LMC increases. For LMC below 8.7 mu/pu, H2 consumes the full electric load power from the electricity grid ($P_{2e} = L_{2e} = 1$ pu). For higher LMC, H2 starts to substitute for expensive electricity with natural gas: P_{2g} increases while P_{2e} decreases.

From the data plotted in Figure 5.15, elasticities can be calculated for H2. For LMC between 8.0 and 8.7 mu/pu, the hub is inelastic, thus

$$\sigma_{2ee} (8.0 \leq \Psi_{2e} \leq 8.7) = \sigma_{2ge} (8.0 \leq \Psi_{2e} \leq 8.7) = 0 \quad (5.24)$$

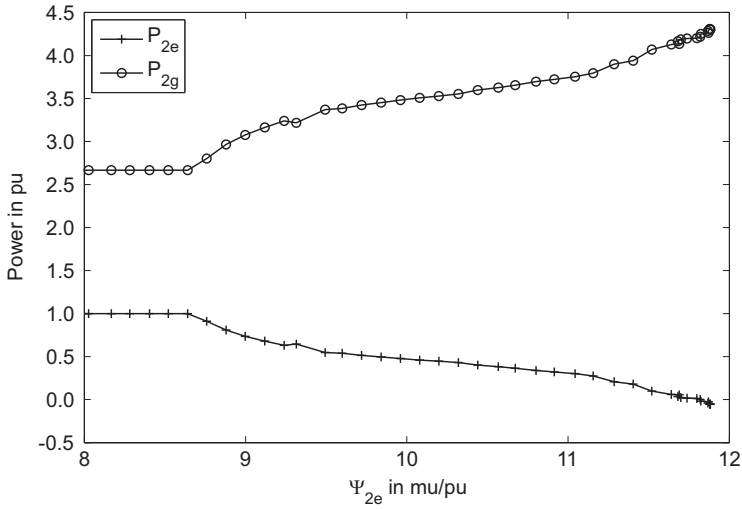


Figure 5.15: Electrical and natural gas power consumption P_{2e} and P_{2g} , respectively, versus electricity LMC Ψ_{2e} at H2.

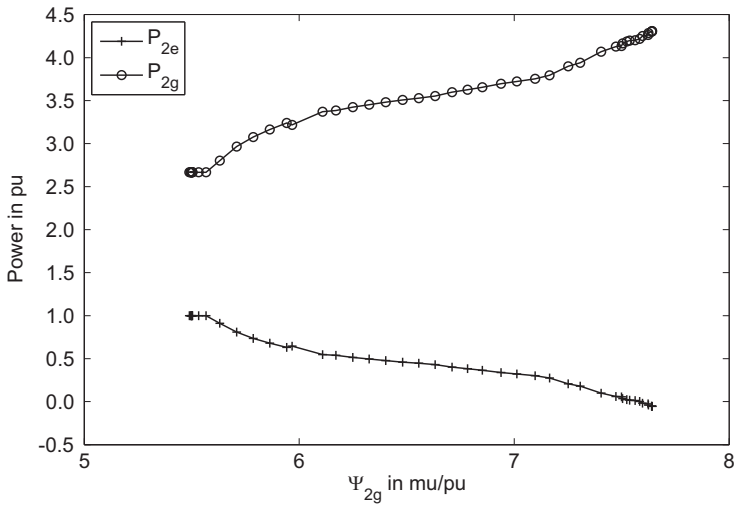


Figure 5.16: Electrical and natural gas power consumption P_{2e} and P_{2g} , respectively, versus gas LMC Ψ_{2g} at H2.

For higher LMC, elasticities differ from zero. The mean elasticities in the range $\Psi_{2e} = 10 \dots 11$ mu/pu, for example, result in:

$$\sigma_{2ee} (10 \leq \Psi_{2e} \leq 11) = -4.476 \quad (5.25)$$

$$\sigma_{2ge} (10 \leq \Psi_{2e} \leq 11) = +0.741 \quad (5.26)$$

Note that these values are relative measures; even if P_{2g} increases faster than P_{2e} decreases, $|\sigma_{2ge}(\cdot)| < |\sigma_{2ee}(\cdot)|$ because P_{2g} is generally higher than P_{2e} , i.e., its relative change is smaller.

From this example, it can be concluded that energy hubs can be considered elastic consumers, even if they supply inelastic loads. Hence, energy hubs can be used to increase load elasticity from the electrical point of view. In this regard, a counter-intuitive effect can be observed in the natural gas system. Contrary to the electrical sensitivity, the gas consumption P_{2g} increases with increasing LMC Ψ_{2g} . This can be seen in Figure 5.16, which plots the electricity and natural gas powers consumed from the grids versus the LMC of natural gas at node 2.

5.3 OPF-Based Investment Evaluation

In this section, an approach for evaluating investment in converter and storage technology is presented and applied in a simple example. The basic concept is adopted from [93], which develops a method for economic evaluation of transmission technology. A similar but simplified approach for economic evaluation of hub elements is presented in the following.

It has been demonstrated in several examples that with optimally operated energy hubs, energy cost can be reduced quite significantly. However, besides operational cost, investment in the converter and storage elements is important to consider when evaluating the economic performance of the system. In order to avoid critical assumptions such as investment cost of emerging technologies (e.g., fuel cells), an approach is developed that enables the determination of justifiable investment cost for converter and storage elements by comparing operational energy cost with and without the devices. For example, energy cost and CO₂ taxes can be compared for conventional, decoupled supply and CHP-coupled natural gas and electricity networks (as done in Section 5.2). The savings in energy cost can be determined for various load situations, for

example for a typical load profile. From this comparison, annual savings in energy cost can be accumulated and interpreted as a stream of annual energy cost savings, which can be transformed into future and present values. Referring to the CHP-coupled networks, the present value of the energy cost savings can then be understood as the reasonable amount of money to be paid for the CHP units, which establishes the stream of savings.

Besides multi-carrier optimal power flow computations, the economic value of the energy savings has to be determined. A proper measure for that can be found in [94], where the concept of “future value” and “present value” of cash flow streams is presented. Considering a number of time periods where a certain cash flow is generated in each period, the future value of this cash flow stream represents the sum of the compounded cash flows generated in each period. For a given cash flow stream z_0, z_1, \dots, z_n and a constant interest rate r (per period), the future value of the stream accumulates to:

$$\text{FV} = z_0 (1 + r)^n + z_1 (1 + r)^{n-1} + \dots + z_n \quad (5.27)$$

The present value of the stream can be determined by discounting the future value:

$$\text{PV} = \frac{\text{FV}}{(1 + r)^n} = \sum_{k=0}^n \frac{z_k}{(1 + r)^k} \quad (5.28)$$

As outlined in [94], “the present value of a cash flow stream can be regarded as the present payment amount that is equivalent to the entire stream.” Thus, the present value of energy cost savings due to operation of converter and/or storage elements represents their turn-over investment cost. Investment decisions can be based on a comparison of the present value of savings with expected investment cost of the devices.

The evaluation procedure can be summarized as follows:

1. Determine the total energy cost for the optimally operated system *without* the new element(s) for all time periods.
2. Determine the total energy cost for the optimally operated system *including* the new element(s) for all periods.
3. Calculate the differences (savings) in energy cost for all periods.
4. Calculate the present value of the stream of energy cost savings.

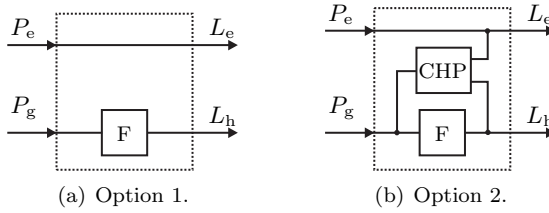


Figure 5.17: Energy hub options with furnace (F) and combined heat and power (CHP) units.

5. Compare the present value of savings with the expected investment cost of the new device(s).

From an economic point of view, the investment can be considered reasonable if the present value of savings is equal or higher than the expected investment cost. The following simple example demonstrates the application of this evaluation method.

Figure 5.17 sketches two possible hub layouts for the supply of electricity and heat loads L_e and L_h , respectively. The hubs are connected to electricity and natural gas networks, from which P_e and P_g are demanded, respectively. The first possible layout is shown in Figure 5.17(a). It contains only a gas furnace (F) which enables to convert natural gas into heat. The second option in Figure 5.17(b) includes a combined heat and power (CHP) unit as well, which enables to generate both heat and electricity from natural gas. The load can be met by both structures, but it can be expected that utilizing the CHP results in lower total energy cost. The question to be answered is: What is the reasonable amount of money to be invested into a CHP?

For the evaluation, the following situation is considered:

- The furnace operates with an efficiency of $\eta_{gh}^F = 0.75$; the CHP operates with efficiencies $\eta_{ge}^{CHP} = 0.30$ and $\eta_{gh}^{CHP} = 0.40$ (gas-electric and gas-thermal conversion, respectively).
- At the hub inputs, electricity and natural gas can be purchased for $a_e = 50 \text{ €/MWh}$ and $a_g = 25 \text{ €/MWh}$, respectively.
- The fixed costs for operating the CHP are $b_{on} = 5 \text{ €/h}$; standby costs are $b_{stb} = 2 \text{ €/h}$.

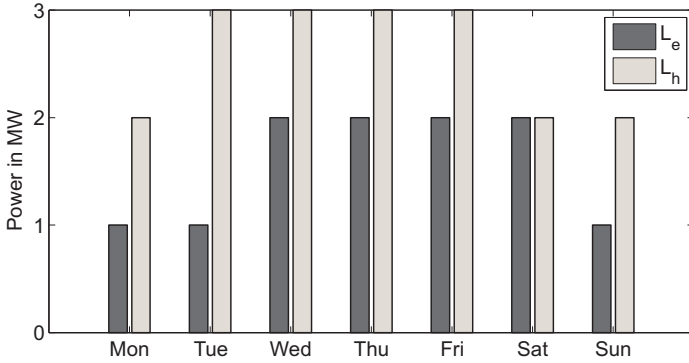


Figure 5.18: Assumed weekly load profile of industrial process. Electricity load L_e and heat load L_h , respectively, in MW. The loads are constant over the day.

- The hub is intended to supply an industrial process characterized by a weekly load profile as shown in Figure 5.18. The process runs 45 weeks per year.

The objective to be minimized is stated as the total energy cost plus the operation cost of the CHP:

$$TC = a_e P_e + a_g P_g + \delta \cdot b_{\text{on}} + (1 - \delta) \cdot b_{\text{stb}} \quad (5.29)$$

where δ keeps the information whether the CHP is in operation ($\delta = 1$) or in standby mode ($\delta = 0$ if zero power in-/output). Constraints are given by the hub equations (3.3), which include the coupling matrices:

$$\mathbf{C}_1 = \begin{bmatrix} 1 & 0 \\ 0 & \eta_{\text{gh}}^F \end{bmatrix}; \quad \mathbf{C}_2 = \begin{bmatrix} 1 & \nu \eta_{\text{ge}}^{\text{CHP}} \\ 0 & \nu \eta_{\text{gh}}^{\text{CHP}} + (1 - \nu) \eta_{\text{gh}}^F \end{bmatrix} \quad (5.30)$$

where \mathbf{C}_1 characterizes option 1, and \mathbf{C}_2 describes option 2. The problem is further constrained by limitations of the input powers. In both cases the hubs cannot to export power:

$$\begin{bmatrix} 0 \\ 0 \end{bmatrix} \leq \begin{bmatrix} P_e \\ P_g \end{bmatrix} \quad (5.31)$$

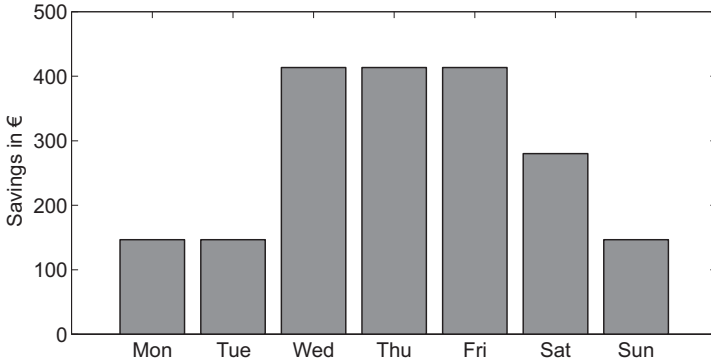


Figure 5.19: Energy cost savings due to optimal operation of the CHP plant. The savings are higher in high load periods (see Figure 5.18). Especially the electric load has a strong influence on the savings.

With these assumptions, optimal dispatch can be performed for both hub options and the resulting total cost can be compared. Figure 5.19 shows the total savings in energy cost during a week. The savings can be accumulated into yearly savings, which result in 156 k€. Considering a depreciation time of ten years ($n = 10$) and a fixed interest rate of 5% ($r = 0.05$, yearly compounding), future and present values can be calculated. The resulting present value of the savings due to CHP operation is $PV = 681$ k€. This value can now be compared with typical investment cost of state-of-the-art CHP technologies. Typically, investment cost for CHP plants in the few MW range are between 500 and 1000 k€ per MW electrical (MWe) output rating [8]. Relating the calculated present value to the maximal electrical output required in this example (2 MWe) yields a relative present value of 341 k€/MWe, which is significantly lower than typical investment cost. Thus, the conclusion is that in the given situation possible savings in energy cost do not justify installation of a CHP device.

Simple sensitivity analysis shows that the result of this investment evaluation is quite sensitive on the efficiencies of the CHP unit, since these values determine the savings in energy cost. Figure 5.20 shows the sensitivity of the present value with respect to the gas-electric efficiency of the CHP plant. The figure shows that the relative present value approaches realistic relative investment cost (between 500 and 1000 k€/MWe) if

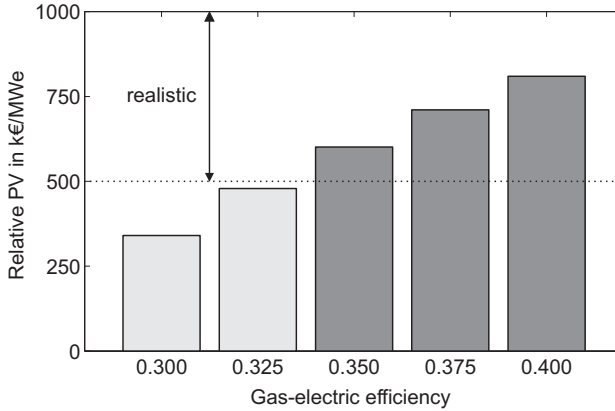


Figure 5.20: Present value of savings PV per rated MW electrical (MWe) output versus gas-electric efficiency of the CHP unit. The present value approaches realistic investment cost with increasing efficiency.

the CHP unit can be operated at gas-electric efficiencies above 33%. The purpose of this investigation is to show the requirements on the technology in order to fulfill economic criteria. The chart in Figure 5.20 relates the plant's technological characteristic (energy efficiency) to its economic performance.

The intention of this simple example is to show a possible application of multi-carrier OPF for economic evaluation of converter and storage technologies. The approach is based on a number of simplifying assumptions, which can be relieved for more advanced investigations. Uncertainty and other features could be included in an enhanced model, but this is beyond the scope of this thesis.

5.4 Optimal Hub Coupling

In this section, the determination of optimal hub couplings is demonstrated in two examples. First, a single energy hub is considered, then a system of interconnected hubs is investigated.

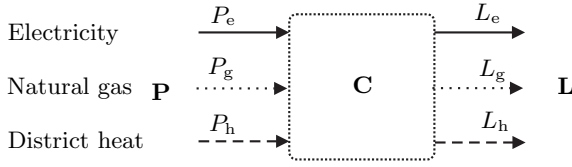


Figure 5.21: Example hub connected to electricity, natural gas, and district heating systems. Power input vector \mathbf{P} with elements P_e , P_g , and P_h ; power output vector \mathbf{L} with entries L_e , L_g , and L_h . The power coupling established by the hub is described by the coupling matrix \mathbf{C} .

Table 5.9: Penalty Function Coefficients.

Carrier (α)	a_α in mu/pu	b_α in mu/pu ²	c_α in mu/pu ³
Electricity (e)	2	0.05	0
Natural gas (g)	1	0	0.10
Distr. heat (h)	1	0	0.20

5.4.1 Single Hub

In the following, the approach for determining the optimal coupling matrix (presented in Section 4.7) is demonstrated for a single energy hub. Figure 5.21 shows an example hub connected to electricity, natural gas, and district heating networks at the input side. The same energy carriers are demanded by the loads at the output.

We will now determine the optimal coupling matrix \mathbf{C} and power input vector \mathbf{P} for a given output vector \mathbf{L} . The penalty to be minimized is defined as a polynomial function of the input powers:

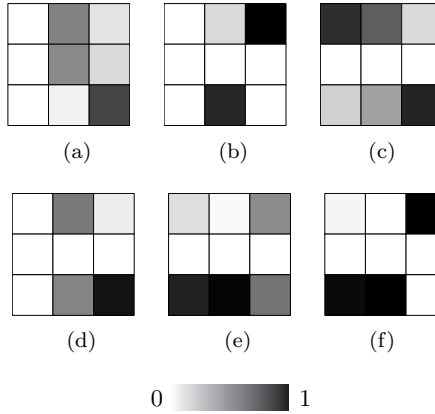
$$\text{TC} = \sum_{\alpha=e,g,h} (a_\alpha P_\alpha + b_\alpha P_\alpha^2 + c_\alpha P_\alpha^3) \quad (5.32)$$

Table 5.9 gives the parameters a_α , b_α , and c_α assumed for this example. The values are chosen based on common energy prices and loss behavior of the related carrier.

Table 5.10 shows the resulting optimal input vectors for different required loads. Figure 5.22 shows the corresponding optimal coupling

Table 5.10: Optimal Inputs for Different Loads.

Case	Required \mathbf{L}^T in pu	Optimal \mathbf{P}^T in pu
(a)	[1 1 1]	[0.00 1.76 1.24]
(b)	[1 0 1]	[0.00 1.17 0.83]
(c)	[2 0 2]	[0.77 1.89 1.34]
(d)	[1 0 2]	[0.00 1.76 1.24]
(e)	[1 0 5]	[2.51 2.04 1.45]
(f)	[2 0 10]	[7.84 2.44 1.72]

Figure 5.22: Color-mapped results for optimal \mathbf{C} .

matrices of the structure

$$\mathbf{C} = \begin{bmatrix} c_{ee} & c_{ge} & c_{he} \\ c_{eg} & c_{gg} & c_{hg} \\ c_{eh} & c_{gh} & c_{hh} \end{bmatrix} \quad (5.33)$$

In order to enhance interpretability and clearness of the results, the matrix entries are displayed according to a color map.

From the theoretical results of the optimization, a technological representation (i.e., hub layout) can be derived that establishes the desired optimal coupling. For case (b), (d), and (f), interpretation of the results

in terms of technological implementation can be carried out heuristically by comparing the matrix patterns with common technologies such as combined heat and power generation. However, interpretation of the results for case (a), (c), and (e) is not a straightforward task. Compared with (b), (d), and (f), the cases (a), (c), and (e) are characterized by more dense matrices, where the interrelations between efficiencies, dispatch factors, and coupling factors complicate an intuitive solution.

Consider for example case (d) in Figure 5.22. Natural gas and heat are demanded from the networks to meet the load. The optimal coupling matrix shows non-zero elements for conversions from gas to electricity ($c_{ge} = 0.52$), gas to heat ($c_{gh} = 0.48$), heat to electricity ($c_{he} = 0.07$), and heat to heat ($c_{hh} = 0.93$). A converter layout that has the potential to realize this coupling could be based on a combined heat and power plant (CHP), which converts natural gas into electricity and heat with efficiencies c_{ge} and c_{gh} , i.e., 52% and 48%, respectively. The factor c_{hh} could be realized by directly connecting the heat load (and the thermal CHP output) to the district heating network. Since the first column of \mathbf{C} does not contain non-zero elements, there is no need to connect to the electricity network.

5.4.2 Multiple Hubs

Consider the 3-bus electricity and natural gas networks in Figure 5.23 which have to supply electricity, natural gas, and heat loads located at nodes 2 and 3. The loads are connected to the output port of the corresponding hubs:

$$\mathbf{L}_2^T = \begin{bmatrix} 1 & 1 & 2 \end{bmatrix} \text{ pu}; \quad \mathbf{L}_3^T = \begin{bmatrix} 1 & 0 & 3 \end{bmatrix} \text{ pu} \quad (5.34)$$

The electricity network is supplied by the generators G_1 (slack) and G_2 , whose output is limited between 0.2 and 0.8 pu. The gas network is fed by a single source S . Besides the network infeeds, there are two smaller local sources of biomass at node 2 (B , max. 0.5 pu) and heat at node 3 (H , max. 1 pu).

Flows through the networks are described by a network flow model as discussed in Section 3.4.1. Link losses are considered according to (3.33), where quadratic and cubic functions of the flows are used to approximate electricity and gas losses, respectively:

$$\Delta F_{mn\alpha} = a_{mn\alpha} F_{mn\alpha}^i \quad (5.35)$$

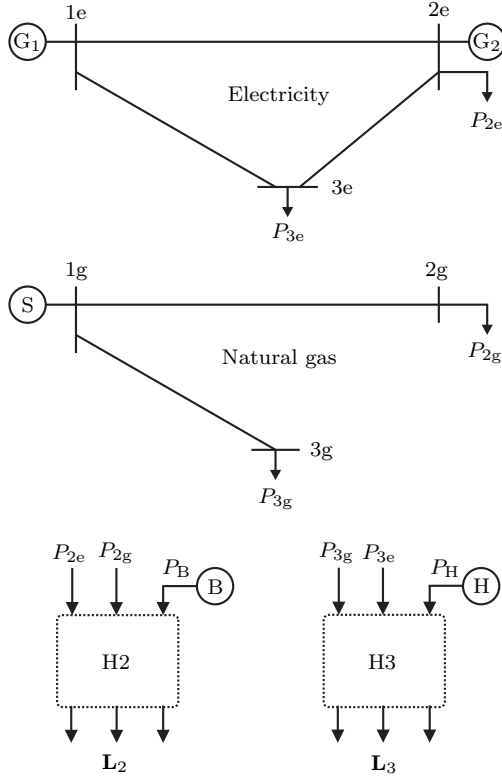


Figure 5.23: Example system with energy hubs at nodes 2 and 3. H2 is connected to nodes 2e and 2g, H3 is connects to 3e and 3g. The system is supplied by generators G_1 and G_2 , a natural gas source S , and two local sources B (biomass) and H (heat).

Table 5.11: Loss Coefficients.

Link $(m\alpha, n\alpha)$	Exponent i	Coefficient $a_{mn\alpha}$ in pu^{-i}
(1e,2e)	2	0.006
(1e,3e)	2	0.004
(2e,3e)	2	0.003
(1g,2g)	3	0.014
(1g,3g)	3	0.010

Table 5.12: Penalty Function Coefficients.

Source s	a_s in pu^{-1}	b_s in pu^{-2}	c_s in pu^{-3}
G_1	8	0.003	0
G_2	9	0.005	0
S	5	0	0.5
B	4	0	0
H	4	0	0

The corresponding loss coefficients are given in Table 5.11.

The objective to be minimized is basically stated as the cost of energy input (considering all sources). In order to achieve technically reasonable results and to avoid the problems mentioned in Section 5.4.1, we reduce the penalty by terms reflecting the sum of the diagonal elements (trace) of the coupling matrices:

$$\mathcal{F} = \sum_{s \in \mathcal{S}} (a_s P_s + b_s P_s^2 + c_s P_s^3) - \xi_2 \cdot \text{tr}(\mathbf{C}_2) - \xi_3 \cdot \text{tr}(\mathbf{C}_3) \quad (5.36)$$

Here $\mathcal{S} = \{G_1, G_2, S, B, H\}$ is the set of sources, and P_s is the power delivered by the source $s \in \mathcal{S}$. The values for a_s , b_s , and c_s used in this example are given in Table 5.12. The weighting coefficients ξ_2 and ξ_3 are set to $\xi_2 = \xi_3 = 1$ in this example.

Note that the formulation (5.36) intrinsically includes network losses, since the sources have to compensate for them. The optimal coupling matrices of hubs 2 and 3 (\mathbf{C}_2 and \mathbf{C}_3 , respectively) describing the cou-

plings established by these hubs can now be determined using the proposed optimization model.

As discussed in Section 4.7, this problem is characterized by a non-convex solution space. Again, the solver “fmincon.m” from the Matlab Optimization Toolbox [86] is used for implementation. Note that the solution obtained depends on the initial values, and there is no guarantee that the global optimum has been reached.

However, the following locally optimal solution has been found:

$$\mathbf{C}_2 = \begin{bmatrix} 0.383 & 0 & 0 \\ 0.042 & 1 & 0 \\ 0.575 & 0 & 1 \end{bmatrix}; \quad \mathbf{C}_3 = \begin{bmatrix} 1 & 0 & 0 \\ 0 & 0 & 0 \\ 0 & 1 & 1 \end{bmatrix} \quad (5.37)$$

Figure 5.24 gives a graphical illustration of \mathbf{C}_2 and \mathbf{C}_3 . From the results a technological realization (converter layout) for the hubs can be derived that approximately establishes the theoretically optimal coupling. To realize the coupling described by \mathbf{C}_2 , direct connections linking all inputs and outputs are necessary in hub 2, what means that biomass has to be converted into heat. Additionally, a conversion from electricity to heat has to be implemented, what is technically possible with high efficiencies close to 100%. About 58% of the electric input should be used for producing heat (what corresponds to a dispatch factor of 0.58). The comparably low entry representing conversions from electricity to gas can be neglected. Hub 3 should be equipped with direct connections for electricity and heat, and a device that converts gas into heat. Ideally, this device should operate with 100% efficiency; practical installations will of course show significantly lower efficiencies.

In Figure 5.25 the resulting hub input flows are shown. Note that both local sources (biomass and heat) are utilized at their limits. Power from these sources is not transported via networks, therefore no losses occur from their use. The remaining power comes from the network infeeds: $P_{G_1} = 3.44$ pu, $P_{G_2} = 0.2$ pu (lower limit), and $P_S = 3$ pu.

The results are optimal for the given specific load situation. For system design investigations, different load scenarios should be investigated. It is also possible to perform the optimization for a certain load profile.

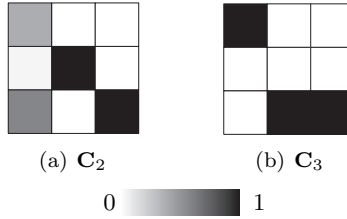


Figure 5.24: Color-mapped results for optimal coupling matrices.

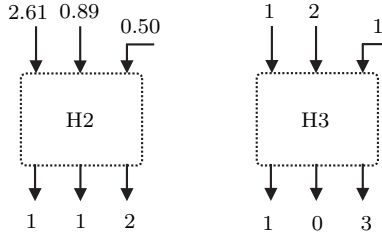


Figure 5.25: Given loads and resulting hub inputs (all values in pu).

5.5 Optimal Hub Layout

In this section, the optimal hub layout approach presented in Section 4.8 is exemplified.

Figure 5.26(a) shows an empty hub which is connected to electricity and natural gas networks at the input side. At the output, the hub has to deliver electricity and heat to a residential load. Figure 5.26(b) shows the set of elements available for the hub. All elements are characterized by different ratings, efficiencies, and installation cost, see Tables 5.13 and 5.14. The loads to be supplied at the output side and the energy prices at the input side of the hub are shown in Figure 5.27.

The first three potential hub elements A, B, and C are combined heat and power technologies. The corresponding data in Table 5.13 are taken from [8]. Compared with B and C, option A shows the highest efficiencies and lowest installation cost, but also the lowest rating. Option B has the highest rating, but most of the gas is converted into heat instead of more expensive electricity. Option C has the highest investment cost, but both rating and efficiencies are high as well. Elements D and E are electrical

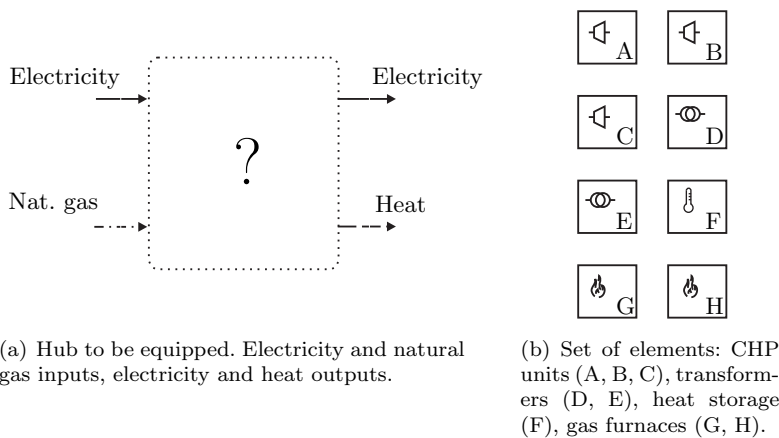


Figure 5.26: Hub layout problem. Which element(s) should be used?

Table 5.13: Data of Converter Elements.

Converter element k	Max. input power in pu	Efficiencies in %			Installation cost b_k in 1000 mu
		el.	th.	Σ	
A	5	43	43	86	100
B	20	25	55	80	250
C	15	32	53	85	300
D	7	97	–	97	30
E	10	98	–	98	40
G	7	–	85	85	40
H	10	–	80	80	40

Table 5.14: Data of Storage Element.

Storage element F	
Charge efficiency in %	90
Discharge efficiency in %	90
Min./max. power in pu	$-3/3$
Min./max. energy in pu	$0.5/3$
Standby losses in pu	0.3
Installation cost b_F in 1000 mu	20

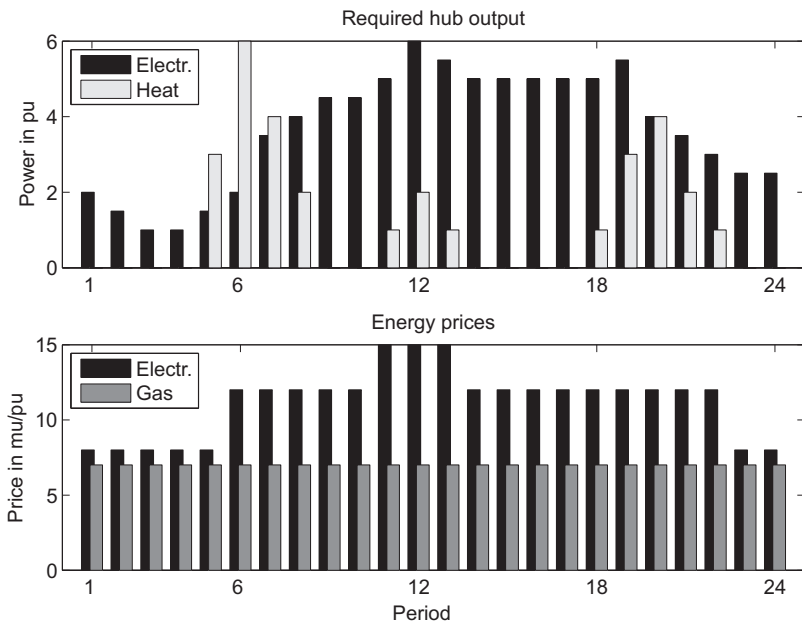


Figure 5.27: Required load powers and energy prices for 24 hours.

transformers. D is smaller than E, less efficient, but also cheaper. The converters G and H represent gas furnaces with different properties. Device G is smaller than H but more efficient, whereas installation costs are equal. Also a thermal storage element could be used for the hub.

The investment cost for the hub should be depreciated within 10 years. During this time, the hub is intended to meet the given 24×1 hour load cycle 365 days a year. Incorporating the installation cost of the devices into a 24-hour optimization requires to relate the installation cost to one 24-hour load cycle. This can be done by transforming the total installation cost:

$$b'_k = \frac{b_k}{T_d \cdot N_c} \quad (5.38)$$

where T_d is the depreciation time (in years) and N_c is the number of load cycles the hub has to perform within one year (in cycles per year). In this example we have $T_d = 10$ a and $N_c = 365$ a⁻¹. The total cost for one 24-hour load cycle are modeled as the cost for energy plus the transformed installation cost of the devices used for the hub:

$$\text{TC} = \sum_{t=1}^{24} (a_e^t P_e^t + a_g^t P_g^t) + \sum_{k \in \{\mathcal{C}, \mathcal{D}\}} b'_k \cdot I_k \quad (5.39)$$

where $\mathcal{C} = \{A, B, C, D, E, G, H\}$ and $\mathcal{D} = \{F\}$. According to (4.18), the decision variable I_k keeps the information whether the element k is used in the hub or not.

The question to be answered is: Which element(s) should be used in the hub in order to obtain minimum total cost TC? The problem is stated according to (4.20), with the additional constraint that only one element of each category can be used (max. one CHP, one transformer, one furnace). Implementation is done in Matlab [86] using the solver “minlpBB” from Tomlab [91]. Due to the nonconvex nature of the problem, it cannot be guaranteed that the global optimum is achieved using this numerical method.

Figure 5.28 shows the obtained optimal hub layout for two different cases:

- (a) All loads and energy prices are assumed as shown in Figure 5.27.
- (b) The gas prices from (a) are doubled, i.e., they are increased to 14 mu/pu for all 24 periods. Electricity prices and loads remain unchanged.

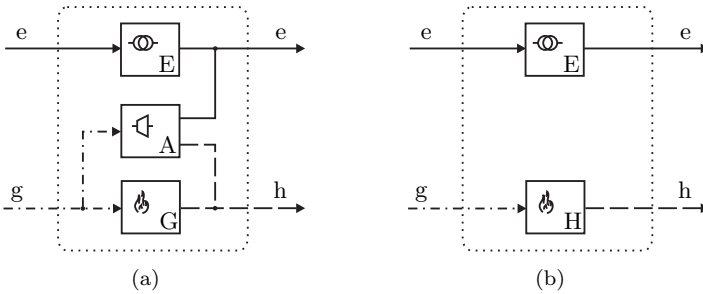


Figure 5.28: Optimal hub layouts.

For case (a) the total cost is minimized if the elements A, E, and G are used. The CHP unit A is selected due to its high power-to-heat ratio and low installation cost; the rating is sufficient for the given situation. Transformer E is selected instead of D due to higher efficiency and rating, although the installation costs are significantly higher. The furnace G performs better than H because it is more efficient and sufficiently rated, whereas installation costs are equal.

In case (b) minimal costs are achieved using the transformer E and the gas furnace H. In case (a) the furnace G was the choice, but without the support of a CHP element, G's rating is not sufficient to supply the heat load. Therefore the furnace H is used in this case. Generation of electricity via CHP is not reasonable since the gas price is too high.

In both situations (a) and (b) the storage device is not useful for improving the objective. In case (a) the gap between CHP heat production and heat load is covered by the furnace, which makes the storage unnecessary. In case (b) the heat is generated by the furnace anyway, and again there is no need for a heat storage.

However, a detailed explanation of the results is difficult due to the complexity of the problem. The utilization of an element can hardly be justified by its own properties only, because also the interactions with the other elements are influencing the objective.

Chapter 6

Closure

6.1 Summary

This dissertation presents a framework for combined steady-state modeling and optimization of multi-carrier energy systems. The models are based on the novel concept of energy hubs; the multi-carrier system is considered as one integrated system of interconnected energy hubs.

The general mathematical model explicitly includes the couplings of the different energy flows established by the energy hubs. Together with conventional network models, a complete system description is achieved which is used to formulate various optimization problems.

The operational optimization problems are stated according to the standard approaches known from electric power engineering—“optimal dispatch” and “optimal power flow”. Similar to the dispatch rule “equal incremental cost” in electric systems, a general condition for optimal dispatch of energy hubs is derived. A modification of the operational problem yields the problem of optimal hub coupling. Another structural optimization problem, the optimal hub layout, represents a combinatorial problem similar to “optimal plant layout” known from manufacturing science.

There are a number of potential applications for the presented method. In general, all applications of electricity optimal power flow in system

planning and operation are also potential applications of the multi-carrier approach, for example:

- integrated system planning;
- multi-carrier generation scheduling;
- security analysis of coupled energy systems.

6.2 Conclusions

The main conclusions that can be summarized are as follows:

- The presented energy hub model represents a general and comprehensive approach of modeling conversion and storage of multiple energy carriers.
- The matrix-based energy hub model is appropriate to be used in the formulation of optimization problems. The model allows the derivation of a general sufficient optimality condition for convex dispatch problems.
- Optimization problems related to energy hubs are generally constrained by nonlinear relations, thus characterized by a nonconvex solution space. Numerical methods can be used to solve nonconvex problems, but it cannot be ensured that the global optimum has been achieved.
- Case studies and examples have shown that the flexible combination of different energy carriers using conversion and storage technology keeps potential for system improvement, such as reduction of overall energy cost and emissions.
- In the presented examples, a number of simplifying assumptions are made that reduce the problem complexity, for example:
 - Converter and storage efficiencies are assumed to be constant (except in Section 5.1.2).
 - Only single snapshots of the loads are considered in most of the examples.

- Even if multiple time steps are considered, couplings between these time steps are kept low, and computationally expensive constraints such as minimum up-/downtimes etc. are not taken into account.
- The systems considered are mostly supplied by stiff adjacent systems and sources.

Resolution of these items is expected to significantly complicate the numerical solution of the problems. Advanced software tools and efficient implementation will be required to achieve reasonable computation times.

6.3 Future Work

The framework developed in this thesis has been tested in a number of examples and small-scaled case studies. More experience with realistically-sized problems should be gained by applying the models.

A promising practical application of the presented framework is the analysis of multi-source multi-product energy systems, such as co- and trigeneration plants. References [46] and [47] represent first steps in this direction. Another application is the investigation of power flow and marginal cost interactions among different energy infrastructures, e.g., natural gas and electricity systems. Also the combination of electricity and natural gas markets and their integrated clearing could be studied.

Besides applying recent developments to real problems, future work could include the following subjects:

- Dynamic phenomena and stability of multi-carrier systems.
- Hub communication, information exchange, ancillary services, and consumer services. Inspiring ideas in this field are presented in [95].
- Optimal control of multi-carrier systems, which can be considered “systems integrating logic, dynamics, and constraints” [96, 97].

Appendix A

Flow Constant

The constant k_{mn} in the general flow equation (3.36) includes properties of the pipe and the fluid [63]:

$$k_{mn} = \frac{\text{GHV}}{24} \cdot 1.1494 \cdot 10^{-3} \cdot \frac{T_b}{p_b} \cdot \sqrt{\frac{D_{mn}^5}{T \cdot G \cdot K \cdot L_{mn} \cdot f_{mn}}} \quad (\text{A.1})$$

where

- GHV is the gross heating value of the fluid in MWh/m³;
- T_b is the base temperature in K;
- p_b is the base pressure in kPa;
- D_{mn} is the inside diameter of pipe section (m, n) in mm;
- T is the average gas flowing temperature in K;
- G is the gas gravity relative to air;
- K is the dimensionless gas compressibility factor at flowing temperature;
- L_{mn} is the length of the pipe segment (m, n) in km;
- f_{mn} is the dimensionless friction factor of the pipe segment (m, n) .

With up- and downstream pressures p_m and p_n in kPa, the power flow F_{mn} results in MW.

Appendix B

Optimality Conditions

For convex nonlinear constrained optimization problems of the form (4.2), optimality conditions due to Karush, Kuhn and Tucker (KKT) apply, which are both necessary and sufficient for a globally optimal solution [65, 68, 78]. These conditions are based on the Lagrange function of the problem. For problems of the structure (4.2), the Lagrange function can be stated as

$$\mathcal{L} = \mathcal{F}(\mathbf{x}) + \mathbf{\Lambda} \mathbf{g}(\mathbf{x}) + \mathbf{\Phi} \mathbf{h}(\mathbf{x}) \quad (\text{B.1})$$

where $\mathbf{\Lambda}$ and $\mathbf{\Phi}$ are vectors of Lagrange multipliers. For an optimal solution point, the KKT conditions require to fulfill the following set of equations [65]:

$$\frac{\partial \mathcal{L}}{\partial \mathbf{x}} = \mathbf{0} \quad (\text{B.2a})$$

$$\mathbf{g}(\mathbf{x}) = \mathbf{0} \quad (\text{B.2b})$$

$$\mathbf{h}(\mathbf{x}) \leq \mathbf{0} \quad (\text{B.2c})$$

$$\mathbf{\Phi} \mathbf{h}(\mathbf{x}) = \mathbf{0} \quad (\text{B.2d})$$

$$\mathbf{\Phi} \geq \mathbf{0} \quad (\text{B.2e})$$

These conditions are interesting since they provide certain information about the optimal solution, in particular about the marginal objectives.

B.1 Multi-Carrier Optimal Dispatch

Consider a problem defined by (4.5a), (4.5b), and (4.5c), where the objective function (4.5a) is convex and the constraint (4.5b) is linear. Using (4.6), the Lagrange function of this problem can be stated as

$$\mathcal{L} = \mathcal{F}(\mathbf{P}) + \mathbf{\Lambda} \begin{bmatrix} \mathbf{L} - \mathbf{C}\mathbf{P} \end{bmatrix} + \begin{bmatrix} \underline{\Phi} & \overline{\Phi} \end{bmatrix} \begin{bmatrix} \mathbf{P} - \mathbf{P} \\ \mathbf{P} - \overline{\mathbf{P}} \end{bmatrix} \quad (\text{B.3})$$

The first KKT optimality condition (B.2a) requires

$$\frac{\partial \mathcal{L}}{\partial \mathbf{P}} = \frac{\partial \mathcal{F}}{\partial \mathbf{P}} - \mathbf{\Lambda} \mathbf{C} \underbrace{-\underline{\Phi} + \overline{\Phi}}_{\mathbf{\Phi}} = \mathbf{0} \quad (\text{B.4})$$

which can be written as

$$\mathbf{\Psi} = \frac{\partial \mathcal{F}}{\partial \mathbf{P}} + \mathbf{\Phi} = \mathbf{\Lambda} \mathbf{C} \quad (\text{B.5})$$

The vector $\mathbf{\Psi}$ includes marginal objectives related to the input side of the hub, $\mathbf{\Lambda}$ contains marginal objectives at the outputs. The total marginal objectives at the input $\mathbf{\Psi}$ are sums of a production- or generation-related component $\partial \mathcal{F} / \partial \mathbf{P}$ and a congestion-related component $\mathbf{\Phi}$ reflecting the objective increase due to input limitations [69].

Conditions (B.2b) and (B.2c) correspond to the constraint equations (4.5b) and (4.5c), respectively. The remaining conditions (B.2d) and (B.2e) ensure complementary slackness of binding and nonbinding inequalities.

B.2 Multi-Carrier Optimal Power Flow

Consider a problem defined by (4.9a)–(4.9e), where (4.9b) and (4.9c) are linear and the objective function (4.9a) is convex. The Lagrange function for this problem can be stated as

$$\begin{aligned} \mathcal{L} = & \mathcal{F}(\mathbf{P}_i, \mathbf{F}_\alpha) + \sum_{i \in \mathcal{H}} \mathbf{\Lambda}_i \begin{bmatrix} \mathbf{L}_i - \mathbf{C}_i \mathbf{P}_i \end{bmatrix} + \sum_{\alpha \in \mathcal{E}} \mathbf{\Gamma}_\alpha \mathbf{G}_\alpha \\ & + \sum_{i \in \mathcal{H}} \begin{bmatrix} \underline{\Phi}_i & \overline{\Phi}_i \end{bmatrix} \begin{bmatrix} \mathbf{P}_i - \mathbf{P}_i \\ \mathbf{P}_i - \overline{\mathbf{P}}_i \end{bmatrix} + \sum_{\alpha \in \mathcal{E}} \begin{bmatrix} \underline{\Omega}_\alpha & \overline{\Omega}_\alpha \end{bmatrix} \begin{bmatrix} \mathbf{F}_\alpha - \mathbf{F}_\alpha \\ \mathbf{F}_\alpha - \overline{\mathbf{F}}_\alpha \end{bmatrix} \end{aligned} \quad (\text{B.6})$$

The first KKT condition (B.2a) requires

$$\begin{aligned} \frac{\partial \mathcal{L}}{\partial \mathbf{P}_i} &= \frac{\partial \mathcal{F}}{\partial \mathbf{P}_i} - \mathbf{\Lambda}_i \mathbf{C}_i + \underbrace{\sum_{\alpha \in \mathcal{E}} \frac{\partial}{\partial \mathbf{P}_i} \left[\mathbf{\Gamma}_\alpha \mathbf{G}_\alpha \right]}_{\mathbf{\Theta}_i} \underbrace{\left[-\mathbf{\Phi}_i + \overline{\mathbf{\Phi}}_i \right]}_{\mathbf{\Phi}_i} \\ &+ \underbrace{\sum_{\alpha \in \mathcal{E}} \left[-\underline{\mathbf{\Omega}}_\alpha + \overline{\mathbf{\Omega}}_\alpha \right]}_{\mathbf{\Upsilon}_i} \frac{\partial \mathbf{F}_\alpha}{\partial \mathbf{P}_i} = \mathbf{0} \quad \forall i \in \mathcal{H} \end{aligned} \quad (\text{B.7})$$

This can be rewritten as

$$\mathbf{\Psi}_i = \frac{\partial \mathcal{F}}{\partial \mathbf{P}_i} + \mathbf{\Theta}_i + \mathbf{\Phi}_i + \mathbf{\Upsilon}_i = \mathbf{\Lambda}_i \mathbf{C}_i \quad \forall i \in \mathcal{H} \quad (\text{B.8})$$

This is basically the same condition as (B.5), but the vector of input marginal objectives $\mathbf{\Psi}_i$ includes additional components:

- $\partial \mathcal{F} / \partial \mathbf{P}_i$ is the production/generation-related component;
- $\mathbf{\Theta}_i$ accounts for network effects (losses);
- $\mathbf{\Phi}_i$ accounts for limitations of the hub inputs;
- $\mathbf{\Upsilon}_i$ accounts for network congestion.

The remaining KKT conditions do not deliver information relevant for this work, and they are therefore not further discussed.

Bibliography

- [1] M. Ilic, F. Galiana, and L. Fink, editors. *Power System Restructuring: Engineering and Economics*. Kluwer Academic Publishers, Boston, 2000. ISBN 0-7923-8163-7.
- [2] A.-M. Borbely and J. F. Kreider, editors. *Distributed Generation: The Power Paradigm for the New Millennium*. CRC Press, Boca Raton, 2001. ISBN 0-8493-0074-6.
- [3] International Energy Agency. Key world energy statistics 2006.
- [4] M. Shahidehpour. Our aging power systems: Infrastructure and life extension issues. *IEEE Power and Energy Magazine*, 4(3):22–76, 2006.
- [5] J. Depledge and R. Lamb, editors. *Caring for Climate: A Guide to the Climate Change Convention and the Kyoto Protocol*. Climate Change Secretariat (UNFCCC), Bonn, 2003. ISBN 92-9219-000-8.
- [6] D. Hinrichs. Cogeneration. In *Encyclopedia of Energy*, volume 1, pages 581–594. Elsevier, New York, 2004.
- [7] J. Hernandez-Santoyo and A. Sanchez-Cifuentes. Trigeneration: An alternative for energy savings. *Applied Energy*, 76(1–3):219–227, 2003.
- [8] P. A. Pilavachi, C. P. Roumpeas, S. Minett, and N. H. Afgan. Multi-criteria evaluation for CHP system options. *Energy Conversion and Management*, 47(20):3519–3529, 2006.
- [9] H. I. Onovwiona and V. I. Ugursal. Residential cogeneration systems: Review of the current technology. *Renewable and Sustainable Energy Reviews*, 10(5):389–431, 2006.

- [10] S. C. Sciacca and W. R. Block. Advanced SCADA concepts. *IEEE Computer Applications in Power*, 8(1):23–28, 1995.
- [11] M. G. Adamiak, A. P. Apostolov, M. M. Begovic, C. F. Henville, K. E. Martin, G. L. Michel, A. G. Phadke, and J. S. Thorp. Wide area protection—technology and infrastructures. *IEEE Transactions on Power Delivery*, 21(2):601–609, 2006.
- [12] L. K. Kirchmayer. *Economic Operation of Power Systems*. Wiley, New York, 1958. ISBN 0-471-48180-7.
- [13] H. W. Dommel and W. F. Tinney. Optimal power flow solutions. *IEEE Transactions on Power Apparatus and Systems*, PAS-87(10):1866–1876, 1968.
- [14] J. Carpentier. Optimal power flows. *International Journal of Electrical Power & Energy Systems*, 1(1):3–15, 1979.
- [15] J. Carpentier and A. Merlin. Optimization methods in planning and operation. *International Journal of Electrical Power & Energy Systems*, 4(1):11–18, 1982.
- [16] P. J. Wong and R. E. Larson. Optimization of natural-gas pipeline systems via dynamic programming. *IEEE Transactions on Automatic Control*, 13(5):475–481, 1968.
- [17] O. Flanigan. Constrained derivatives in natural gas pipeline system optimization. *Journal of Petroleum Technology*, pages 549–556, 1972.
- [18] K. F. Pratt and J. G. Wilson. Optimization of the operation of gas transmission systems. *Transactions of the Institute of Measurement and Control*, 6(5):261–269, 1984.
- [19] A. Benonysson, B. Bøhm, and H. F. Ravn. Operational optimization in a district heating system. *Energy Conversion and Management*, 36(5):297–314, 1995.
- [20] H. Zhao, B. Bøhm, and H. F. Ravn. On optimum operation of a CHP type district heating system by mathematical modeling. *Euroheat & Power (Fernwärme International)*, 11:618–622, 1995.
- [21] D. K. Baker and S. A. Sherif. Heat transfer optimization of a district heating system using search methods. *International Journal of Energy Research*, 21(3):233–252, 1997.

- [22] K. Moslehi, M. Khadem, R. Bernal, and G. Hernandez. Optimization of multipplant cogeneration system operation including electric and steam networks. *IEEE Transactions on Power Systems*, 6(2):484–490, 1991.
- [23] H. M. Groscurth, T. Bruckner, and R. Kümmel. Modeling of energy-services supply systems. *Energy*, 20(9):941–958, 1995.
- [24] B. Bakken, A. Haugstad, K. S. Hornnes, and S. Vist. Simulation and optimization of systems with multiple energy carriers. In *Proc. of Scandinavian Conference on Simulation and Modeling*, Linköping, Sweden, 1999.
- [25] B. Bakken, M. M. Belsnes, and J. Røystrand. Energy distribution systems with multiple energy carriers. In *Proc. of Symposium Gas and Electricity Networks*, Brasilia, Brasil, 2002.
- [26] I. Bouwmans and K. Hemmes. Optimising energy systems—hydrogen and distributed generation. In *Proc. of 2nd International Symposium on Distributed Generation*, Stockholm, Sweden, 2002.
- [27] J. Korhonen. A material and energy flow model for co-production of heat and power. *Journal of Cleaner Production*, 10(6):537–544, 2002.
- [28] S. An, Q. Li, and T. W. Gedra. Natural gas and electricity optimal power flow. In *Proc. of IEEE PES Transmission and Distribution Conference*, Dallas, USA, 2003.
- [29] E. M. Gil, A. M. Quelhas, J. D. McCalley, and T. V. Voorhis. Modeling integrated energy transportation networks for analysis of economic efficiency and network interdependencies. In *Proc. of North American Power Symposium*, Rolla, USA, 2003.
- [30] A. M. Quelhas, E. M. Gil, and J. D. McCalley. Nodal prices in an integrated energy system. *International Journal of Critical Infrastructures*, 2(1):50–68, 2006.
- [31] O. D. de Mello and T. Ohishi. Natural gas transmission for thermoelectric generation problem. In *Proc. of IX Symposium of Specialists in Electric Operational and Expansion Planning*, Rio de Janeiro, Brasil, 2004.

- [32] O. D. de Mello and T. Ohishi. An integrated dispatch model of gas supply and thermoelectric systems. In *Proc. of 15th Power Systems Computation Conference*, Liege, Belgium, 2005.
- [33] J. Söderman and F. Pettersson. Structural and operational optimisation of distributed energy systems. *Applied Thermal Engineering*, 26(13):1400–1408, 2006.
- [34] S. Hecq, Y. Bouffoulx, P. Doulliez, and P. Saintes. The integrated planning of the natural gas and electricity systems under market conditions. In *Proc. of IEEE PowerTech*, Porto, Portugal, 2001.
- [35] M. S. Morais and J. W. M. Lima. Natural gas network pricing and its influence on electricity and gas markets. In *Proc. of IEEE PowerTech*, Bologna, Italy, 2003.
- [36] B. Bakken and A. T. Holen. Energy service systems: Integrated planning case studies. In *Proc. of IEEE PES General Meeting*, Denver, USA, 2004.
- [37] M. Shahidehpour, Y. Fu, and T. Wiedman. Impact of natural gas infrastructure on electric power systems. *Proceedings of the IEEE*, 93(5):1042–1056, 2005.
- [38] IEEE PES Energy Development and Power Generation Committee Panel Session: Integrated natural gas-electricity resource adequacy planning in Latin America. In *Proc. of IEEE PES General Meeting*, San Francisco, USA, 2005.
- [39] A. Hugo, P. Rutter, S. Pistikopoulos, A. Amorelli, and G. Zoia. Hydrogen infrastructure strategic planning using multi-objective optimization. *International Journal of Hydrogen Energy*, 30(15):1523–1534, 2005.
- [40] J. F. Manwell. Hybrid energy systems. In *Encyclopedia of Energy*, volume 3, pages 215–229. Elsevier, New York, 2004.
- [41] R. H. Lasseter. Microgrids. In *Proc. of IEEE PES Winter Meeting*, New York, USA, 2002.
- [42] R. Frik and P. Favre-Perrod. *Proposal for a multifunctional energy bus and its interlink with generation and consumption*. Diploma thesis, High Voltage Laboratory, ETH Zurich, 2004.

- [43] T. R. Weymouth. Problems in natural gas engineering. *Transactions of the ASME*, 64(34):185–234, 1942.
- [44] P. Favre-Perrod, M. Geidl, B. Klöckl, and G. Koepfel. A vision of future energy networks. In *Proc. of Inaugural IEEE PES Conference and Exposition in Africa*, Durban, South Africa, 2005.
- [45] M. Geidl, P. Favre-Perrod, B. Klöckl, and G. Koepfel. A green-field approach for future power systems. In *Proc. of Cigre General Session 41*, Paris, France, 2006.
- [46] G. Chicco and P. Mancarella. A comprehensive approach to the characterization of trigeneration systems. In *Proc. of 6th World Energy System Conference*, Turin, Italy, 2006.
- [47] K. Hemmes, J. L. Zachariah-Wolff, M. Geidl, and G. Andersson. Towards multi-source multi-product energy systems. *International Journal of Hydrogen Energy*, to appear.
- [48] B. Marti. *Integrated Analysis of Energy and Transportation Systems*. Master thesis, Power Systems Laboratory, ETH Zurich, 2006.
- [49] M. Geidl, G. Koepfel, P. Favre-Perrod, B. Klöckl, G. Andersson, and K. Fröhlich. Energy hubs for the future. *IEEE Power and Energy Magazine*, 5(1):24–30, 2007.
- [50] G. Koepfel and G. Andersson. The influence of combined power, gas, and thermal networks on the reliability of supply. In *Proc. of 6th World Energy System Conference*, Turin, Italy, 2006.
- [51] G. Koepfel. *Reliability Considerations of Future Energy Systems: Multi-Carrier Systems and the Effect of Energy Storage*. PhD thesis, Power Systems Laboratory, ETH Zurich, 2007.
- [52] P. M. Grant. The supercable: Dual delivery of chemical and electric power. *IEEE Transactions on Applied Superconductivity*, 15(2):1810–1813, 2005.
- [53] P. Favre-Perrod and A. Bitschi. A concept for dual gaseous and electric energy transmission. In *Proc. of IEEE PES General Meeting*, Montreal, Canada, 2006.
- [54] M. Geidl and G. Andersson. Optimal power dispatch and conversion in systems with multiple energy carriers. In *Proc. of 15th Power Systems Computation Conference*, Liege, Belgium, 2005.

- [55] B. Klöckl and P. Favre-Perrod. On the influence of demanded power upon the performance of energy storage devices. In *Proc. of 11th International Power Electronics and Motion Control Conference*, Riga, Latvia, 2004.
- [56] M. Geidl and G. Andersson. A modeling and optimization approach for multiple energy carrier power flow. In *Proc. of IEEE PES PowerTech*, St. Petersburg, Russian Federation, 2005.
- [57] M. Geidl and G. Andersson. Operational and structural optimization of multi-carrier energy systems. *European Transactions on Electrical Power*, 16(5):463–477, 2006.
- [58] M. Geidl and G. Andersson. Optimal power flow of multiple energy carriers. *IEEE Transactions on Power Systems*, 22(1):145–155, 2007.
- [59] F. Glover, D. Klingman, and N. V. Phillips. *Network Models in Optimization and Their Applications in Practice*. Wiley, New York, 1992. ISBN 0-471-57138-5.
- [60] A. R. Bergen and V. Vittal. *Power Systems Analysis*. Prentice Hall, Upper Saddle River, 2nd edition, 2000. ISBN 0-13-691990-1.
- [61] A. J. Osiadacz. *Simulation and Analysis of Gas Networks*. E. & F. N. Spon, London, 1987. ISBN 0-419-12480-2.
- [62] E. S. Menon. *Liquid Pipeline Hydraulics*. Marcel Dekker, New York, 2004. ISBN 0-8247-5317-8.
- [63] E. S. Menon. *Gas Pipeline Hydraulics*. Taylor & Francis, Boca Raton, 2005. ISBN 0-8493-2785-7.
- [64] Q. Li, S. An, and T. W. Gedra. Solving natural gas loadflow problems using electric loadflow techniques. In *Proc. of North American Power Symposium*, Rolla, USA, 2003.
- [65] A. J. Wood and B. F. Wollenberg. *Power Generation, Operation, and Control*. Wiley, New York, 2nd edition, 1996. ISBN 0-471-58699-4.
- [66] P. M. Pardalos and M. G. C. Resende, editors. *Handbook of Applied Optimization*. Oxford University Press, Oxford, 2002. ISBN 0-19-512594-0.

- [67] M. Khoshnevisan and S. Bhattacharya. Optimal plant layout design based on MASS algorithm. In *Proc. of 6th International Conference on Information Fusion*, Cairns, Australia, 2003.
- [68] R. Fletcher. *Practical Methods of Optimization*. Wiley, Chichester, 2nd edition, 1987. ISBN 0-471-91547-5.
- [69] L. Chen, H. Suzuki, T. Wachi, and Y. Shimura. Components of nodal prices for electric power systems. *IEEE Transactions on Power Systems*, 17(1):41–49, 2002.
- [70] M. R. Gent and J. W. Lamont. Minimum emission dispatch. *IEEE Transactions on Power Apparatus and Systems*, PAS-90:2650–2660, 1971.
- [71] J. H. Talaq, F. El-Hawary, and M. E. El-Hawary. Minimum emissions power flow. *IEEE Transactions on Power Systems*, 9(1):429–435, 1994.
- [72] J. W. Lamont and E. V. Obessis. Emission dispatch models and algorithms for the 1990s. *IEEE Transactions on Power Systems*, 10(2):941–947, 1995.
- [73] B. Marti. *Emissions of Power Delivery Systems*. Semester thesis, Power Systems Laboratory, ETH Zurich, 2005.
- [74] T. Gjengedal, S. Johansen, and O. Hansen. A qualitative approach to economic-environmental dispatch—treatment of multiple pollutants. *IEEE Transactions on Energy Conversion*, 7(3):367–373, 1992.
- [75] S. D. Pohekar and M. Ramachandran. Application of multi-criteria decision making to sustainable energy planning—a review. *Renewable and Sustainable Energy Reviews*, 8(4):365–381, 2004.
- [76] F. C. Schweppe. *Spot Pricing of Electricity*. Kluwer Academic Publishers, Boston, 1988. ISBN 0-89838-260-2.
- [77] S. Stoft. *Power System Economics: Designing Markets for Electricity*. IEEE Press, Wiley, Piscataway, 2002. ISBN 0-471-15040-1.
- [78] H. W. Kuhn and A. W. Tucker. Nonlinear programming. In *Proc. of 2nd Berkeley Symposium on Mathematical Statistics and Probability*, Berkeley, USA, 1951.

- [79] J. M. Arroyo and A. J. Conejo. Modeling of start-up and shut-down power trajectories of thermal units. *IEEE Transactions on Power Systems*, 19(3):1562–1568, 2004.
- [80] E. Gallestey, A. Stothert, M. Antoine, and S. Morton. Model predictive control and the optimization of power plant load while considering lifetime consumption. *IEEE Transactions on Power Systems*, 17(1):186–191, 2002.
- [81] J. M. Arroyo and A. J. Conejo. Multiperiod auction for a pool-based electricity market. *IEEE Transactions on Power Systems*, 17(4):1225–1231, 2002.
- [82] F. J. Rooijers and R. A. M. van Amerongen. Static economic dispatch for co-generation systems. *IEEE Transactions on Power Systems*, 9(3):1392–1398, 1994.
- [83] I. A. Hiskens and R. J. Davy. Exploring the power flow solution space boundary. *IEEE Transactions on Power Systems*, 16(3):389–395, 2001.
- [84] M. Geidl and G. Andersson. Optimal coupling of energy infrastructures. In *Proc. of IEEE PES PowerTech*, Lausanne, Switzerland, 2007.
- [85] H. Wilk. Betriebsweisen und Systemeinbindung von Brennstoffzellen-Heizgeräten aus Sicht eines EVU. In *Proc. of Workshop “Brennstoffzellen-Systeme für stationäre Anwendungen”*, E.V.A./BMVIT, Vienna, Austria, 2001 (in German).
- [86] The Mathworks Inc. Website, available at <http://www.mathworks.com/>, last accessed at November 23, 2006.
- [87] V. Pareto. *Manuale di Economia Politica*. Società Editrice Libreria, Milano, 1906 (in Italian).
- [88] R. E. Steuer. *Multiple Criteria Optimization: Theory, Computation, and Application*. Wiley, New York, 1986. ISBN 0-471-88846-X.
- [89] I. Y. Kim and O. L. de Weck. Adaptive weighted-sum method for bi-objective optimization: Pareto front generation. *Structural and Multidisciplinary Optimization*, 29(2):149–158, 2005.

-
- [90] Ziena Optimization Inc. Website, available at <http://www.ziena.com/>, last accessed at December 13, 2006.
 - [91] Tomlab Optimization Inc. Website, available at <http://tomopt.com/tomlab/>, last accessed at November 23, 2006.
 - [92] R. F. Kahn. The elasticity of substitution and the relative share of a factor. *Review of Economic Studies*, 1(1):72–78, 1933.
 - [93] C. Schaffner. *Valuation of Controllable Devices in Liberalized Electricity Markets*. PhD thesis, Power Systems Laboratory, ETH Zurich, 2004.
 - [94] D. G. Luenberger. *Investment Science*. Oxford University Press, New York, 1998. ISBN 0-19-510809-4.
 - [95] C. W. Gellings. A consumer portal at the junction of electricity, communications, and consumer energy services. *The Electricity Journal*, 17(9):78–84, 2004.
 - [96] A. Bemporad and M. Morari. Control of systems integrating logic, dynamics, and constraints. *Automatica*, 35(3):407–427, 1999.
 - [97] G. Ferrari-Trecate, E. Gallestey, P. Letizia, M. Spedicato, M. Morari, and M. Antoine. Modeling and control of co-generation power plants: A hybrid system approach. *IEEE Transactions on Control Systems Technology*, 12(5):694–705, 2002.

Curriculum Vitae

June 28, 1977	Born in Wels, Austria
1991 – 1996	HTL for Electrical Engineering in Wels, Austria
1996 – 2003	Study of Electrical Engineering at TU Graz, Austria
2003 – 2007	Assistant at the Power Systems Laboratory of ETH Zurich, Switzerland; doctoral thesis supervised by Prof. Göran Andersson
2003 – 2007	Study of Pedagogics and Didactics at ETH Zurich, Switzerland